ABSTRACT

Title of Dissertation: DYNAMIC SPECTRUM ALLOCATION AND SHARING IN COGNITIVE COOPERATIVE NETWORKS

Beibei Wang, Doctor of Philosophy, 2009

Dissertation directed by: Professor K. J. Ray Liu
Department of Electrical and Computer Engineering

The dramatic increase of service quality and channel capacity in wireless networks is severely limited by the scarcity of energy and bandwidth, which are the two fundamental resources for communications. New communications and networking paradigms such as cooperative communication and cognitive radio networks emerged in recent years that can intelligently and efficiently utilize these scarce resources. With the development of these new techniques, how to design efficient spectrum allocation and sharing schemes becomes very important, due to the challenges brought by the new techniques. In this dissertation we have investigated several critical issues in spectrum allocation and sharing and address these challenges.

Due to limited network resources in a multiuser radio environment, a particular user may try to exploit the resources for self-enrichment, which in turn may

prompt other users to behave the same way. In addition, cognitive users are able to make intelligent decisions on spectrum usage and communication parameters based on the sensed spectrum dynamics and other users' decisions. Thus, it is important to analyze the intelligent behavior and complicated interactions of cognitive users via game-theoretic approaches. Moreover, the radio environment is highly dynamic, subject to shadowing/fading, user mobility in space/frequency domains, traffic variations, and etc. Such dynamics brings a lot of overhead when users try to optimize system performance through information exchange in real-time. Hence, statistical modeling of spectrum variations becomes essential in order to achieve near-optimal solutions on average.

In this dissertation, we first study a stochastic modeling approach for dynamic spectrum access. Since the radio spectrum environment is highly dynamic, we model the traffic variations in dynamic spectrum access using continuous-time Markov chains that characterizes future traffic patterns, and optimize access probabilities to reduce performance degradation due to co-channel interference. Second, we propose an evolutionary game framework for cooperative spectrum sensing with selfish users, and develop the optimal collaboration strategy that has better performance than fully cooperating strategy. Further, we study user cooperation enforcement for cooperative networks with selfish users. We model the optimal relay selection and power control problem as a Stackelberg game, and consider the joint benefits of source nodes as buyers and relay nodes as sellers. The proposed scheme achieves the same performance compared to traditional centralized optimization while reducing the signaling overhead. Finally, we investigate possible attacks on cooperative

spectrum sensing under the evolutionary sensing game framework, and analyze their damage both theoretically and by simulations.

DYNAMIC SPECTRUM ALLOCATION AND SHARING IN COGNITIVE COOPERATIVE NETWORKS

by

Beibei Wang

Dissertation submitted to the Faculty of the Graduate School of the
University of Maryland, College Park in partial fulfillment
of the requirements for the degree of
Doctor of Philosophy
2009

Advisory Committee:

Professor K. J. Ray Liu, Chairman
Professor Mark Shayman
Professor Richard J. La
Professor T. Charles Clancy
Professor Lawrence C. Washington

DEDICATION

To my parents.

ACKNOWLEDGEMENTS

First of all, I would like to express my sincere gratitude to my advisor, Professor K. J. Ray Liu. With his enthusiasm, his inspiration, his confidence on me, he has put so many efforts to help me find good directions and conduct high quality research. During my Ph.D. studies, his unwavering support and constant encouragement for my research endeavors make this thesis possible. I also value his influences for my vision, attitude, energy and desire of my professional and personal developments.

Meanwhile, I would also like to explicitly thank the following people. I would like to thank Dr. Zhu Han, Dr. Zhu Ji, Dr. Wei Yu, Yongle Wu, Yan Chen, and Mahmoud Abdulrehen for their invaluable collaboration during the last five years. Thanks are due to Professor Mark Shayman, Professor Richard J. La, Professor T. Charles Clancy, and Professor Lawrence C. Washington for agreeing to serve on my thesis committee and for sparing their invaluable time reviewing the manuscript. I am also grateful to Professor Michael Fu, Professor Min Wu, Professor Gang Qu, and Professor Peter Cramton, for their kind assistance with writing letters, giving wise advice, helping with various applications, and so on. I would also like to thank all the members of SIG and other friends throughput the University of Maryland for giving me such happy five years.

Lastly, and most importantly, I wish to thank my parents. They born me, raised me, supported me, taught me, and loved me. To them I dedicate this thesis.

TABLE OF CONTENTS

LIST OF TABLES

LIST OF FIGURES

Chapter 1

Introduction

1.1 Motivation

The dramatic increase of service quality and channel capacity in wireless networks is severely limited by the scarcity of energy and bandwidth, which are the two fundamental resources for communications. Therefore, researchers are currently focusing their attention on new communications and networking paradigms that can intelligently and efficiently utilize these scarce resources. For instance, cooperative communications [LTW04] can take advantage of the broadcasting nature of wireless networks and exploit the inherent spatial and multiuser diversities, where relay nodes act as a virtual antenna array to help source nodes forward information to the destination nodes to achieve higher data throughput and more reliable transmission. Moreover, with the development of cognitive radio technology [III00], future wireless communication devices are envisioned to be able to sense and analyze their surrounding environment, learn from the environment variations, and adapt their

operating parameters accordingly in order for a better performance and more efficient spectrum utilization. For instance, when cognitive network users share a licensed spectrum, they can detect spectrum white space, select the best frequency bands, coordinate spectrum access with other users and vacate the frequency when a primary user appears.

In traditional military and emergency applications, users in a wireless network usually belong to the same authority and have the same objective. However, in emerging networks, such as cooperative and cognitive communication networks envisioned in civilian applications, different network users typically belong to different operators and may pursue different goals. Fully cooperative behaviors such as forwarding data for other users or contributing to a common task unconditionally cannot be pre-assumed. Due to limited network resources in a multiuser radio environment, a particular user may try to exploit the resources for self-enrichment, which in turn may prompt other users to behave the same way. Moreover, the radio environment is highly dynamic, subject to shadowing/fading, user mobility in space/frequency domains, traffic variations, and etc. Such dynamics brings a lot of overhead when users try to optimize system performance through information exchange in real-time.

Since these emerging communication paradigms are usually deployed in a highly dynamic spectrum environment where network users tend to be selfish, before they can be successfully exploited in order to achieve efficient spectrum utilization, the following two critical issues must be resolved first: *user cooperation* and *dynamic spectrum sharing*. Since selfish network users only aim at maximizing their

own benefits, without a properly designed cooperation enforcement mechanism, they may be unwilling to help other users at the expense of their own resources, such as forward data for other users or spend their own time detecting spectrum white space. Furthermore, dynamics caused by different user activities, e.g., primary users re-occupying/vacating their licensed bands and secondary users starting/ceasing a communication session, pose even greater challenges for the design of dynamic spectrum sharing schemes.

In recent years, efficient spectrum allocation and sharing in cooperative and cognitive communication networks has drawn extensive attentions [CZ05, ZC05, EPT07, JL07, JL06, RYM05, SA06]. The performance in cooperative communication networks depends on careful resource allocations such as relay placement, relay selection, bandwidth allocation, and transmission power control. Transmission power allocation is optimized to minimize the outage probability and maximize network lifetime [HA03, SSL08]. Relay selection and assignment schemes are proposed to fully utilize the cooperative diversity, minimize the outage probability, extend coverage area, and maximize throughput [LBG+04, BLR05, SHL06]. In addition, there have been several previous efforts addressing how to efficiently and fairly share the spectrum resources in cognitive communication networks, on a negotiation/pricing basis [CZ05, ZC05, EPT07, JL07, JL06, RYM05] or an opportunistic basis [XCMS06, KC06]. In negotiation/pricing-based spectrum allocation, the unused spectrum resources from legacy spectrum holders (primary users) can be shared among unlicensed users through auction-based pricing approaches. In opportunistic spectrum sharing, unlicensed/secondary users can access the licensed spectrum

when the spectrum is sensed as idle. Furthermore, in order to protect primary users from the interference due to secondary spectrum usage, various spectrum detection schemes have been proposed to improve the detection performance and minimize the conflict/interference with the primary user. Recent study has shown that cooperative spectrum sensing with multiple secondary users can further improve the efficiency of primary user detection.

Although the existing spectrum allocation and sharing schemes can enhance system performance in cooperative and cognitive communication networks, there are still some fundamental issues that require further treatment.

First, the radio spectrum environment is constantly changing. In conventional power control to manage mutual interference for a fixed number of secondary users, after each change of the number of contending secondary users, the network needs to re-optimize the power allocation for all users completely. This results in high complexity and much overhead. If a primary user appears in some specific portion of the spectrum, secondary users in that band also need to adapt their transmission parameters to avoid interfering with the primary user. Therefore, efficient dynamic spectrum sharing scheme must include a traffic model based on traffic statistics to predict the future traffic patterns in the shared spectrum.

Second, in order to improve the detection performance of a primary user, most cooperative spectrum sensing schemes assume a fully cooperative scenario, meaning all secondary user will voluntarily fuse their sensing outcomes to a common controller such as a secondary base station. But this assumption does not hold in a decentralized network. Moreover, due to users' specific channel conditions, it is even

not optimal to have all secondary users cooperate in every sensing effort. In addition, sensing takes energy/time which may be diverted to useful data transmission. In self-organizing networks where secondary users exchange sensory data to make a final decision, selfish users tend to take advantage of the others so as to reserve more time for their own data transmission. Therefore, how to collaborate with selfish users in cooperative spectrum sensing is another very important issue.

Third, most existing works on spectrum sharing in cooperative communication networks mainly focus on resource allocation by means of a centralized fashion. Such schemes require that complete and precise channel state information (CSI) be available in order to optimize the system performance, which are generally neither scalable nor robust to channel estimation errors. Moreover, users in decentralized self-organizing cooperative communication networks belong to different authorities. Therefore, a mechanism of reimbursement to relay nodes is needed such that relay nodes can earn benefits from spending their own transmission power in helping the source node forward information.

1.2 Contributions and Thesis Organization

This dissertation has investigated how to efficiently utilize the limited network resources in cognitive cooperative networks with selfish users under a time-varying spectrum radio environment. Specifically, two important issues have been addressed: 1) how to collaborate with selfish users in forwarding information and cooperative spectrum sensing, and 2) how to design dynamic spectrum access strategy by uti-

lizing the traffic statistics to predict future traffic patterns and reduce information exchange. The contributions lie in the following three aspects.

Evolution of behavior dynamics in cooperative spectrum sensing: In order to study the time evolution of selfish users' cooperation behavior, we have proposed an evolutionary cooperative sensing game, derived users' behavior dynamics, and proved their convergence to the evolutionarily stable strategy (ESS). The proposed approach not only reveals the underlying behavior dynamics involved in establishing robust equilibrium, but also helps to develop a distributed learning algorithm that guides secondary users to approach the ESS only with their own throughput observation. More important, it opens a new avenue for future research on studying behavior dynamics in cognitive radio networks using evolutionary game theory.

Statistical modelling for dynamic spectrum access: Another contribution of this dissertation is the traffic modelling of primary and secondary users in cognitive radio networks. Specifically, we have modelled the traffic variations of the radio environment as continuous-time Markov chains (CTMC). Since the model can characterize the traffic dynamics of different users occupying the licensed spectrum, the proposed approach provides a means for predicting future traffic patterns in the shared spectrum. As mutual interference will impair spectrum efficiency when multiple secondary users transmit in the same frequency, in order to compensate throughput degradation due to mutual interference, we have further introduced optimal access probabilities for secondary users so that the chance of spectrum sharing is controlled and spectrum resources are shared in a more efficient way without con-

flicting with primary users.

User cooperation enforcement in cooperative networks: In this dissertation, we have also proposed a two-level Stackelberg game which considers the joint benefits of source nodes as buyers and relay nodes as sellers. With the proposed approach, not only can source nodes and relays at relatively better locations and buy an optimal amount of power, but also competing relays can maximize their profits by asking optimal prices. Furthermore, we have designed a distributed price updating function by which relay nodes can iteratively approach their optimal prices and system performance is gradually optimized. Compared to most existing works, the proposed approach does not require CSI, and therefore greatly reduces overhead and signaling. Moreover, the distributed nature of the proposed scheme makes it a building block in large-scale wireless ad hoc networks for the cooperation simulation among nodes.

The reminder of this dissertation is organized as follows. Chapter 2 introduces the related works, game-theoretic models, and basic concepts of Markov chain for spectrum allocation and sharing in cognitive cooperative networks. In Chapter 3, a primary-prioritized Markov approach is described for dynamic spectrum access in licensed bands [WJLC09]. In Chapter 4, an evolutionary game framework for cooperative spectrum sensing with selfish users is discussed [WLC09]. The user collaboration enforcement in cooperative wireless networks using Stackelberg game [WHL09] is presented in Chapter 5. Malicious attacks on cooperative spectrum sensing are studied in Chapter 6. Finally, Chapter 7 concludes this dissertation and discusses the future work.

Chapter 2

Background

2.1 Related Works

2.1.1 Spectrum Sharing and Management in Cognitive Radios

The usage of radio spectrum resources and the regulation of radio emissions are coordinated by national regulatory bodies like the Federal Communications Commission (FCC). The FCC assigns spectrum to license holders or services on a long-term basis for large geographical regions; however, a large portion of the assigned spectrum remains unutilized. The inefficient usage of the limited spectrum resources necessitates the development of dynamic spectrum access techniques. Recently, the FCC began considering more flexible and comprehensive uses of the available spectrum [FCC02, FCC03b], through the use of *cognitive radio* technology [III00]. By exploiting the spectrum in an opportunistic fashion, dynamic spectrum access en-

ables secondary users to sense which portions of the spectrum are available, select the best channel, coordinate access to spectrum channels with other users, and vacate the channel when a primary user appears.

In order to fully utilize the limited spectrum resources, how to efficiently and fairly share the spectrum among secondary users becomes an important issue, especially when multiple dissimilar secondary users coexist in the same portion of the spectrum band. There have been several previous efforts addressing this issue on a negotiated/pricing basis [CZ05, ZC05, EPT07, JL07, JL06, RYM05] or an opportunistic basis [XCMS06, KC06]. A local bargaining mechanism was proposed in [CZ05] to distributively optimize the efficiency of spectrum allocation and maintain bargaining fairness among secondary users. In [HBH06], auction mechanisms were proposed for sharing spectrum among multiple users such that the interference was controlled below a certain level. Rule-based approaches were proposed in [ZC05] that regulated users' spectrum access in order to trade-off fairness and utilization with communication costs and algorithmic complexity. In [EPT07], the authors proposed a repeated game approach, in which the spectrum sharing strategy could be enforced using the Nash Equilibrium of dynamic games. In [JL07, JL06], belief-assisted dynamic pricing was used to optimize the overall spectrum efficiency while basing the participating incentives of the selfish users on double auction rules. A centralized spectrum server was considered in [RYM05] to coordinate the transmissions of a group of wireless links sharing a common spectrum. Recently, attention is being drawn to opportunistic spectrum sharing. In [XCMS06], a distributed random access protocol was proposed to achieve airtime fairness between dissimilar secondary

users in open spectrum wireless networks without considering primary users' activities. The work in [KC06] examined the impact of secondary user access patterns on blocking probability and achievable improvement in spectrum utilization with statistical multiplexing, and proposed a feasible spectrum sharing scheme.

2.1.2 Cooperative Spectrum Sensing for Primary Detection

In order to identify the spectrum hole when the primary is inactive, an important requirement of secondary users is the capability to sense their surrounding radio spectrum environment. Further, since primary users should be carefully protected from interference due to secondary users' operation, secondary users also need to sense the licensed spectrum before each transmission and can only transmit when the spectrum is idle. One efficient way of spectrum detection is the primary transmitter detection based on local observations of secondary users. If the information of the primary user signal is known to secondary users, they can use matched filter detection to maximize the received signal-to-noise ratio (SNR) under stationary Gaussian noise [SC05]. Another detection approach is the cyclostationary feature detection which analyzes the spectral correlation function of modulated signals [FGR05]. Although these two types of detection schemes can achieve precise detection, they either require priori knowledge of the primary user signal, or have high complexity. A good alternative is energy detection.

Energy detection is suitable to the scenario when secondary users cannot gather sufficient information about the primary user signal. An energy detector

collects locally observed signal samples within a certain time, measures the signal energy, and compare the energy with a threshold to determine whether a primary user is present or not [SC05]. However, energy detection is heavily affected by noise uncertainty.

Recently, cooperative spectrum sensing with relay nodes' help and multi-user collaborative sensing has been shown to greatly improve the sensing performance [GS05, MSB06, GL07, PL07, LYZH07, VJP08, GLBL08]. In [GS05], the authors proposed collaborative spectrum sensing to combat shadowing/fading effects. The work in [MSB06] proposed light-weight cooperation in sensing based on hard decisions to reduce the sensitivity requirements. The authors of [GL07] showed that cooperative sensing can reduce the detection time of the primary user and increase the overall agility. How to choose proper secondary users for cooperation was investigated in [PL07]. The authors of [LYZH07] studied the design of sensing slot duration to maximize secondary users' throughput under certain constraints. Two energy-based cooperative detection methods using weighted combining were analyzed in [VJP08]. Spatial diversity in multiuser networks to improve spectrum sensing capabilities of centralized cognitive radio networks were exploited in [GLBL08].

2.1.3 Relay Selection and Power Control in Cooperative Networks

The performance in cooperative communication networks depends on careful resource allocation, such as relay placement, relay selection, and power con-

trol [HA03, SSL08, MY04, LBG+04, BLR05, SHL06, HHSL05, ISSL08, ZAL06, NY07, SS07, HSHL07, ACM07, LHXS07]. In [HA03], the power allocation was optimized to satisfy the outage probability criterion. The authors in [SSL08] provided the analysis on symbol error rates and optimum power allocations for the decode-and-forward cooperation protocol in wireless networks. The energy-efficient broadcast problem in wireless networks was considered in [MY04]. The work in [LBG+04] evaluated the cooperative diversity performance when the best relay was chosen according to the average SNR, and the outage probability of relay selection based on instantaneous SNRs. In [BLR05], the authors proposed a distributed relay selection scheme that required limited network knowledge with instantaneous SNRs. In [SHL06], the relay assignment problem was solved for the multiuser cooperative communications. In [HHSL05], the cooperative resource allocation for OFDM was studied. The authors of [ISSL08] investigated the relay selection problem with focus on when to cooperate and which relay to cooperate with, which required channel state information (CSI). In [ZAL06], centralized power allocation schemes were presented by assuming all the relay nodes should help. In order to further minimize the system outage behaviors and improve the average throughput, a selection forward protocol was proposed to choose only one "best" relay node to assist transmission. A centralized resource allocation algorithm for power control, bandwidth allocation, relay selection and relay strategy choice in an OFDMA-based relay network was proposed in [NY07]. The work in [SS07] developed distributed power control strategies for multi-hop cooperative transmission schemes. Lifetime extension for wireless sensor networks with the aid of relay selection and power management schemes was

investigated in [HSHL07]. The authors of [ACM07] studied the optimal power allocation problem in the high SNR regime for different relaying protocols. Relay station placement and relay time allocation in IEEE 802.16j networks was investigated in [LHXS07].

In recent years, some efforts have been made towards mathematical analysis of cooperation in wireless networking using game theory, since game theory is a natural and flexible tool that studies how the autonomous network users interact and cooperate with each other. In game-theoretic literature of wireless networking, in [MW01], the behaviors of selfish nodes in the case of random access and power control were examined. In [DPA00], static pricing policies for multiple-service networks were proposed. Such policies can offer incentives for each node to choose the service that best matches its needs, so as to discourage over-allocation of resources and improve social welfare. The work in [SMG02] presented a power control solution for wireless data in the analytical setting of a game-theoretic framework. Pricing of transmit powers was introduced to improve user utilities that reflected the quality of service a wireless terminal received. A pricing game that stimulated cooperation via reimbursements to the relay was proposed in [SA06], but there was no detailed analysis on how to select the best relays and how to achieve the equilibrium distributively. In [HJL05], the authors employed a cooperative game for the single-cell OFDMA resource allocation.

2.2 Game-Theoretic Models

In self-organized wireless networks, users may belong to different operators and compete for limited network resources, In other words, users are selfish and only aim at maximizing their own profits by utilizing more resources. With the rapid development of cognitive radio technique, network users can further make intelligent decisions on spectrum usage and communication parameters based on the sensed spectrum dynamics and other users' decisions. Moreover, many fundamental network functionalities, such as packet forwarding, relaying information, and spectrum sharing, cannot be performed without relying on cooperation among the selfish users. In such scenarios, it is no longer feasible to optimize the network performance by assuming there is a central authority and every user will obey the resource allocation rule. Therefore, it is natural to study the intelligent behaviors and interactions of selfish network users from the game-theoretic perspective.

Game theory [FL91, FT93] is a mathematical tool that analyzes the strategic interactions among rational decision makers. Three major components in a strategic-form game model are the set of *players*, the *strategy space* of each player, and the *payoff/utility function*, which measures the outcome of the game for each player.

In cooperative communication networks, source nodes may need to provide relay nodes with incentives for relaying their data and relay nodes need to select the best pricing strategy, which can be modeled as a buyer/seller game [WHL07, WHL09, SA06, HL08]. In cognitive radio networks, the competition and cooperation among the cognitive network users can also be well modeled as a spectrum sharing

game [WWLC09, EPT07, JL07, HBH06, Y. 09, WWJ+08]. Specifically, in open spectrum sharing (e.g., [WWLC09, EPT07]), the players are all the secondary users that compete for unlicensed spectrum; in licensed spectrum sharing, where primary users lease their unused bands to secondary users, the players include both the primary and secondary users (e.g., [HBH06, Y. 09, JL06]).

The strategy space for each player may vary according to the specific spectrum sharing scenario. For instance, in cooperative communication networks, the strategy space of the source nodes includes which relay to choose for help and the relay power levels, while the strategy space of the relay nodes are the prices for relaying data. In open spectrum sharing, the strategy space of secondary users may include the transmission parameters they want to adopt, such as the transmission powers, access rates, time duration, etc.; while in licensed spectrum trading, their strategy space includes which licensed bands they want to rent, and how much they would pay for leasing those licensed bands. For the primary users, the strategy space may include which secondary users they would lease each of their unused bands to, and how much they will charge for each band.

The payoff functions for different users are defined to characterize various performance criteria accordingly. For instance, in open spectrum sharing, the payoff function for the secondary users is often defined as a non-decreasing function of the Quality of Service (QoS) they receive by utilizing the unlicensed band; in licensed spectrum trading, the payoff function for the users often represents the monetary gains (e.g., revenue minus cost) by leasing the licensed bands.

In a noncooperative spectrum sharing game with selfish network users, each

user only targets for maximizing his/her own payoff by choosing an optimal strategy. And the outcome of the noncooperative game is often measured by the *Nash Equilibrium* (NE). The NE is defined as the set of strategies for all the users such that no user can improve his/her payoff by unilaterally deviating from the equilibrium strategy, given that the other users adopt the equilibrium strategies. So the NE indicates that no individual user would have the incentive to choose a different strategy.

2.2.1 Stackelberg Game

If players choose their strategies simultaneously, the game can be described using a strategic-form representation [FT93]. In order to model a game with a dynamic structure, game theorists use the concept of a *game in extensive form*, which explicitly states the order in which players move, and what each player knows when making each of his decisions [FT93]. An example of an extensive-form game is the *Stackelberg game* [FT93]. In a Stackelberg game, one player must commit to a strategy before other players choose their own strategies. Specifically, the players of a Stackelberg game include a leader and a follower/followers. A leader commits to a strategy first, and then a follower selfishly optimizes his own reward, considering the strategy selected by the leader. Compared to Nash games, where all players take their moves simultaneously, Stackelberg games can better model the scenario with heterogeneous players that take sequential moves. For example in cooperative communication networks with self-organized nodes/users, after a source

node broadcasts his data to a destination node and several relay nodes, the relay nodes will signal their optimal prices for relaying data to the source node, and the source node then optimizes the service he purchases from the relay nodes. Thus, we can use Stackelberg game to model such cooperation, where the source node is the leader and the relay nodes are the followers. Stackelberg game have been used to model congestion control [BS02], attacker-defender scenarios in security domains [PPM+08], network routing [KLO97] and scheduling strategies [Rou01].

2.2.2 Evolutionary Game

There can be more than one NE in a game. When there exist several different NE, how should a rational player decide which of them is the "right one"? Game theorists have proposed different refinement criteria [FT93]; however, each equilibrium could be justified by some refinement. The problem becomes even more complicated if the players are uncertain about the game being played and the game involves a dynamic process. Therefore, *evolutionary game theory* (EGT) was proposed [Smi82] to reveal the underlying dynamics and find a robust equilibrium.

The idea of EGT was inspired by the study of ecological biology, and it differs from classic game theory by focusing on the dynamics of strategy change more than the properties of strategy equilibrium. EGT was first used to study the adjustment of population fractions by evolution, which states that the genes whose strategies are more successful will have higher reproductive fitness. Therefore, the population fractions of strategies whose payoff against the current distribution of opponents'

play is relatively high will tend to grow at a faster rate. Since strategies with lower payoff values are eliminated during the dynamic process, the stable steady states after the evolution converges must be an NE. But not all NE are locally stable and robust to mutations. In EGT, the equilibrium strategy is defined as the **Evolutionary Stable Strategy** (ESS) [Smi82], which is a strategy such that if all members of the population adopt it, then no mutant strategy could invade the population under the influence of natural selection. Even if a small part of players may not be rational and take out-of-equilibrium strategies, ESS is still a locally stable state.

2.3 Markov Chain

Markov chains are popular models in many application areas, including economic systems, queuing theory, and networking. In this section, we focus our attention on the Markov chain in discrete-time domain, and continuous-time Markov chain can be similarly defined.

A Markov chain is a stochastic process where the probability of the next state given the current state and the entire past depends only on the current state. Suppose that $S = \{X_n; n = 1, 2, \cdots\}$ is a stochastic process, then $\{X_n\}$ is a Markov chain if and only if

$$\Pr(X_{n+1} = x | X_n = x_n, \cdots, X_1 = x_1) = \Pr(X_{n+1} = x | X_n = x_n), \qquad (2.1)$$

where the countable set of $\{X_n\}$ represents the state space of the chain. In other words, the description of the present state fully captures all the information that

could influence the future evolution of the stochastic process.

Future states will be reached through a probabilistic process instead of a deterministic one. At each step the system may change its state from the current state to another state, or remain in the same state, according to a certain probability distribution. The changes of state are called transitions, and the probabilities associated with various state-changes are called transition probabilities. If the transition probability only depends on the current and the next states and not on the time index of the states, i.e.,

$$\Pr(X_{n+1} = j | X_n = i) = \Pr(X_n = j | X_{n-1} = i), \tag{2.2}$$

then the Markov chain is called time-homogeneous.

Denote $p_{ij} = \Pr(X_{n+1} = j | X_n = i)$ as the single-step time-independent transition probability. For a time-homogeneous Markov chain, it can be described by a transition matrix $[p_{ij}]$ (i.e., $[p_{ij}]$ is the $(i, j)th$ element), and the *stationary distribution* $\mathbf{\Pi}$ of state $i \in S$ is defined as a set of probabilities that satisfies

$$\Pi_j = \sum_{i \in S} \Pi_i p_{ij}, \tag{2.3}$$

and

$$\sum_{j \in S} \Pi_j = 1, \tag{2.4}$$

where (2.3) is usually called the *flow-balance* equation.

Chapter 3

Primary-Prioritized Markov Approach for Dynamic Spectrum Allocation

Dynamic spectrum access has become a promising approach to fully utilize the scarce spectrum resources. It enhances service quality by utilizing others' spectrum resources. Dynamic spectrum access has shown its great potential in efficient spectrum utilization by opening white space in under-used licensed spectrum to unlicensed users (a.k.a. secondary users), meaning secondary users can opportunistically utilize the licensed spectrum when primary users are not operating in the licensed spectrum.

Several prior works as discussed in Chapter 2 have proposed efficient spectrum management approaches, but most of them only focus on spectrum allocation among

secondary users in a static spectrum environment. Therefore, several fundamental challenges still remain unanswered. First, the radio spectrum environment is constantly changing. In conventional power control to manage mutual interference for a fixed number of secondary users, after each change of the number of contending secondary users, the network needs to re-optimize the power allocation for all users completely. This results in high complexity and much overhead. Second, if a primary user appears in some specific portion of the spectrum, secondary users in that band need to adapt their transmission parameters to avoid interfering with the primary user. Furthermore, in addition to maximizing the overall spectrum utilization, a good spectrum sharing scheme should also achieve fairness among dissimilar users. If multiple secondary users are allowed to access the licensed spectrum, dynamically coordinating their access to alleviate mutual interference and avoid conflict with primary users should be carefully considered.

In this chapter we propose a primary-prioritized Markov approach for dynamic spectrum access. Specifically, we propose to model the interactions between the primary users and the secondary users as continuous-time Markov chains (CTMC), by which we can capture the system evolution dynamics, especially the effect of the primary user's activities on the secondary users. It has been shown in [Cla07a], [Cla07b] that when unlicensed devices coexist with licensed devices in the same frequency and time simultaneously, the capacity achieved by unlicensed devices with reduced power is very low, while they still cause harmful interference to the licensed users. Therefore, in this chapter, we assume that when primary users exist in some spectrum band, secondary users cannot operate in the same band simultaneously.

Further, in order to coordinate secondary spectrum access in a fair and efficient manner, dynamic spectrum access under different criteria is proposed based on the CTMC models. In the proposed approach, the spectrum access of different users is optimally coordinated through the modeling of secondary spectrum access statistics to alleviate mutual interference.

The contributions of the proposed primary-prioritized Markov approach for dynamic spectrum access are as follows. First, the dynamics of the radio system, including the primary user's activities, is thoroughly captured through CTMC modeling. Second, we consider various policies of spectrum access by employing different optimality criteria, among which we focus on the proportional-fair (PF) spectrum access approach to achieve the optimal tradeoff between spectrum utilization efficiency and fairness. Third, the proposed PF spectrum access approach can achieve better performance than the CSMA-based scheme, and can be generalized to spectrum sharing among multiple secondary users.

The remainder of this chapter is organized as follows: Dynamic spectrum access system model is described in Section 3.1. The primary-prioritized Markov models are derived in Section 3.2, and dynamic spectrum access approaches based on these models are developed in Section 3.3. The simulation studies are provided in Section 3.4. Finally, Section 3.5 provides the summary.

3.1 System Model

We consider dynamic spectrum access networks where multiple secondary users are allowed to access the temporarily-unused licensed spectrum bands on an opportunistic basis, without conflicting or interfering the primary spectrum holders' usage. Such scenarios can be envisioned in many applications. Considering the fact [FCC02] that heavy spectrum utilization often takes place in unlicensed bands while licensed bands often experience low (e.g., TV bands) or medium (e.g., some cellular bands) utilization, IEEE 802.22 [IEE] proposes to reuse the fallow TV spectrum without causing any harmful interference to incumbents (e.g., the TV receivers). Moreover, with regard to more efficient utilization of some cellular bands, [Ofc] proposes to share the spectrum between a cellular communication system and wireless local area network (WLAN) systems. In rural areas where there is little demand on the cellular communication system, the WLAN users can efficiently increase their data rates by sharing the spectrum.

In order to take advantage of the temporally unused spectrum holes in the licensed band, without loss of generality we consider a snapshot of the above spectrum access networks shown in Figure 3.1, where two secondary users and one primary user coexist, and the secondary users opportunistically utilize the spectrum holes in the licensed band. Note that the system diagram shown here serves only as an example model to gain more insight and the scenario with multiple secondary users will be studied in details in the following section.

The primary user is denoted by P, which has a license to operate in the

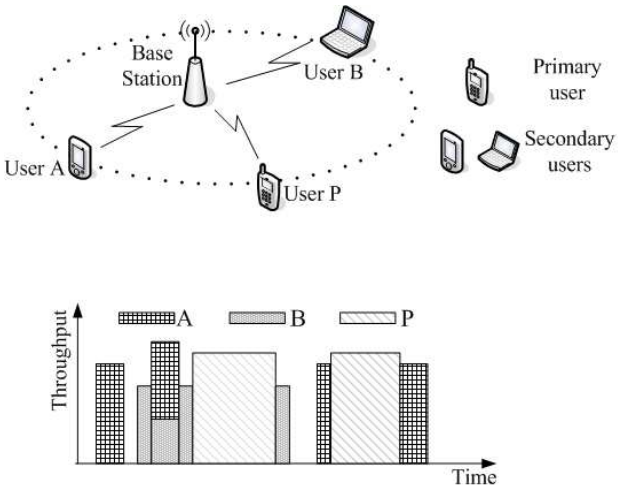

Figure 3.1: System model (upper: system diagram; lower: throughput vs. time).

spectrum band. The offered traffic for primary user P is modeled with two random processes[1]. The service request is modeled as a Poisson process with rate λ_P s^{-1}. The service duration (holding time) is negative-exponentially distributed with mean time $1/\mu_P$ s, so the departure of user P's traffic is another Poisson process with rate μ_P s^{-1}.

The secondary users are denoted by A and B, and set S is defined as $\mathrm{S} = \{A, B\}$. For each secondary user γ, where $\gamma \in \mathrm{S}$, its service session is similarly characterized by two independent Poisson processes, with arrival rate λ_γ s^{-1} and departure rate μ_γ s^{-1}. They contend to access the spectrum when primary user P is not using the spectrum band.

Since the primary user has a license to operate in the spectrum band, its access

[1]Identical assumptions that the service requests and departures are Poisson processes can be found in [XCMS06], [HHLW00] and references therein.

should not be affected by the operation of any other secondary user, and priority to access the spectrum is given to primary user P. We assume that the secondary users equipped with cognitive radios are capable of detecting the primary user's activities, i.e., the appearance of the primary user in the spectrum band and its departure from the spectrum. Furthermore, the secondary users' access is assumed to be controlled by a secondary management point so that they can distinguish whether the spectrum is occupied by the primary user or secondary users. Therefore, when primary user P appears, the secondary users should adjust their transmission parameters, for instance reduce the transmit power or vacate the channels and try to transfer their communications to other available bands. The *interference temperature* model [FCC03a] is proposed by FCC that allows secondary users to transmit in licensed bands with carefully adjusted power, provided that secondary users' transmission does not raise the interference temperature for that frequency band over the interference temperature limit. Although it can provide better service continuity for the secondary users to remain operating in the band with reduced power, the capacity they can achieve is very low [Cla07a], [Cla07b]. Therefore, in this chapter, we assume that when primary user P appears, any secondary user should vacate and the traffic currently being served is cut off. In the duration of primary user P being served, any entry of the secondary user's traffic into the spectrum is denied until primary user P finishes its service.

In the bottom of Figure 3.1, we show an example of the system throughput versus time for the dynamic spectrum access. First, user A accesses the spectrum band, followed by user B. During B's service, user A accesses the band again and

shares the spectrum band with user B, which may result in less throughput to both user A and B due to their mutual interference. After user A has finished its service for a while, primary user P accesses the band, and user B's service is interrupted. After user P vacates the band, user B continues its service until its service duration ends. Afterwards, user A accesses the band, and its service is ceased when primary user P appears and resumed when P finishes its service in the way as user B.

For any secondary user γ that operates in the spectrum band alone, its maximal data rate [CT90] can be represented by

$$r_1^\gamma = W \log_2(1 + \frac{p_\gamma G_{\gamma\gamma}}{n_0}), \tag{3.1}$$

where W is the communication bandwidth, n_0 is power of the additive white Gaussian noise (AWGN), p_γ is the transmission power for user γ, and $G_{\gamma\gamma}$ is the channel gain for user γ. The secondary users A and B are allowed to share the spectrum band. We assume that the transmitter of a secondary user can vary its data rate through a combination of adaptive modulation and coding, so the transmitter and receiver can employ the highest rate that permits reliable communication, given the signal-to-interference-plus-noise ratio (SINR). We assume that the secondary users use random Gaussian codebooks, so their transmitted signals can be treated as white Gaussian processes and the transmission of other secondary users are treated as Gaussian noise. Then, the maximal rate of user γ when secondary users share the spectrum can be represented by

$$r_2^\gamma = W \log_2(1 + \frac{p_\gamma G_{\gamma\gamma}}{n_0 + \sum_{\alpha\neq\gamma} p_\alpha G_{\alpha\gamma}}), \tag{3.2}$$

where $\alpha \neq \gamma$, $\alpha \in$ S, and $G_{\alpha\gamma}$ is the channel gain from user α's transmitter to user

γ's receiver.

3.2 Primary-Prioritized Markov Models

In this section, we derive primary-prioritized Markov models to capture the dynamics of spectrum access statistics for the primary user and the secondary users.

3.2.1 CTMC without Queuing

In dynamic spectrum access, where the secondary users opportunistically access the unused licensed spectrum, priority should be given to the primary user. That is, secondary users cannot operate in the same spectrum band with the primary user at the same time; when the primary user appears in the spectrum band, all secondary users in the same band should stop operating in the spectrum. Moreover, the arrival and departure of different users' traffic are assumed to be independent Poisson processes. Therefore, we model the interactions between the secondary users and the primary user as a primary-prioritized CTMC.

In the CTMC, when the secondary users contend to access the idle spectrum using CSMA, collisions only occur when their service requests arrive exactly at the same time. This case rarely happens for independent Poisson processes. Therefore, in the CTMC model we omit the collision state of the secondary users, and assume their service durations always start from different time instances.

If we assume that when the primary user appears, there is no queuing of the interrupted service for the secondary users, then we can model the spectrum

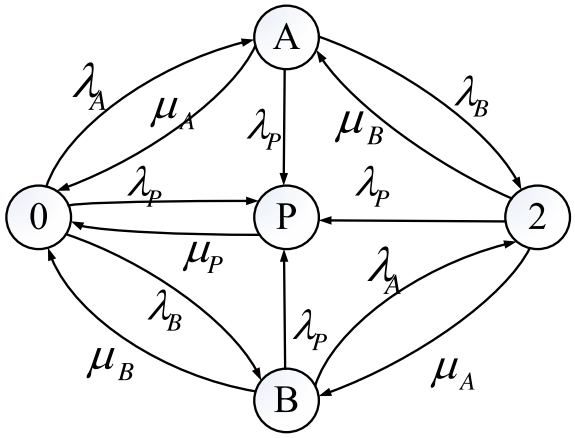

Figure 3.2: The rate diagram of CTMC with no queuing.

access process as a five-state CTMC shown in Figure 3.2. We denote this five-state Markov chain by "CTMC-5" for short, where state 0 means no user operates in the spectrum, state γ means user γ operates in the spectrum with $\gamma \in \{A, B, P\}$, and state 2 means both user A and user B operate in the spectrum.

Assume at first the spectrum band is idle, i.e., CTMC-5 is in state 0. Secondary users contend to operate in the spectrum. Upon the first access attempt of some user, say user A, CTMC-5 enters state A with transition rate λ_A s^{-1}. If user A's service completes before any other user requests spectrum access, CTMC-5 then transits to state 0 with rate μ_A s^{-1}. If user B's service request arrives before A completes its service, CTMC-5 transits to state 2 with rate λ_B s^{-1}, where both secondary users share the spectrum. Once user B (or A)'s service is completed, CTMC-5 transits from state 2 to state A (or B), with rate μ_B (or μ_A) s^{-1}. However, primary user P may, once in a while, appear during the service duration of the secondary users, i.e., when CTMC-5 is in state A, B or 2. At that time, the secondary user's traffic is dropped to avoid conflict with the primary user, and CTMC-5 transits to state

P with rate λ_P s^{-1}. During the primary user operating in the spectrum band, no secondary user is given access to the spectrum. CTMC-5 transits to state 0 with rate μ_P s^{-1} only if P completes its service.

The "flow-balance" (the rate at which transitions take place out of state s_i equals to the rate at which transitions take place into state s_i) and the normalization [Kul95] equations governing the above system are given by

$$\mu_A\Pi_A + \mu_P\Pi_P + \mu_B\Pi_B = (\lambda_A + \lambda_B + \lambda_P)\Pi_0, \tag{3.3}$$

$$\lambda_A\Pi_0 + \mu_B\Pi_2 = (\mu_A + \lambda_P + \lambda_B)\Pi_A, \tag{3.4}$$

$$\lambda_P(\Pi_0 + \Pi_A + \Pi_2 + \Pi_B) = \mu_P\Pi_P, \tag{3.5}$$

$$\lambda_B\Pi_0 + \mu_A\Pi_2 = (\mu_B + \lambda_P + \lambda_A)\Pi_B, \tag{3.6}$$

$$\lambda_B\Pi_A + \lambda_A\Pi_B = (\mu_B + \lambda_P + \mu_A)\Pi_2, \tag{3.7}$$

$$\Pi_0 + \Pi_A + \Pi_B + \Pi_P + \Pi_2 = 1, \tag{3.8}$$

where Π_{s_i} represents the stationary probability of being in state s_i, $s_i \in \mathcal{S} \triangleq \{0, A, B, P, 2\}$.

The solutions to the above equations, i.e., the probabilities when the spectrum is occupied by either primary user P or the secondary users, are given by

$$\Pi_P = \lambda_P/(\lambda_P + \mu_P), \tag{3.9}$$

$$\Pi_A = C_1\lambda_A[\lambda_B\mu_B + (\lambda_P + \mu_B)(\lambda_A + \lambda_P + \mu_A + \mu_B)], \tag{3.10}$$

$$\Pi_B = C_1\lambda_B[\lambda_A\mu_A + (\lambda_P + \mu_A)(\lambda_B + \lambda_P + \mu_A + \mu_B)], \tag{3.11}$$

$$\Pi_2 = C_1\lambda_A\lambda_B(\lambda_A + \lambda_B + 2\lambda_P + \mu_A + \mu_B), \tag{3.12}$$

where, for simplicity, the coefficient C_1 is defined as

$$\begin{aligned} C_1 =&(1-\Pi_P)[(\lambda_A+\mu_A+\lambda_P)(\lambda_B+\mu_B+\lambda_P) \\ &(\lambda_A+\mu_A+\lambda_B+\mu_B+\lambda_P)]^{-1}. \end{aligned} \tag{3.13}$$

One of the most important goals in spectrum sharing is efficient spectrum utilization, i.e., high throughput achieved by each secondary user through successful acquisition of a spectrum band. From a statistical point of view, the secondary users want to maximize their average throughput. Given the solutions of the steady state probabilities, we know that Π_{s_i} is the stationary probability that the system is in state s_i, so it can be thought of as the expected long-run fraction of the time that the CTMC spends in state s_i [Kul95]:

$$\Pi_{s_i} = \lim_{T\to\infty} \frac{1}{T} \int_0^T \Pr\{\mathcal{S}(t) = s_i\} dt, \tag{3.14}$$

where $\mathcal{S}(t)$ is the state of the CTMC at time t. If we define

$$U_\gamma = \lim_{T\to\infty} \frac{1}{T} E\left(\int_0^T R_\gamma(\mathcal{S}(t)) dt \right) \tag{3.15}$$

as the long-run expected average throughput for user γ, where $R_\gamma(\mathcal{S}(t))$ is the throughput of user γ achieved in state $\mathcal{S}(t)$, we have

$$\begin{aligned} U_\gamma &= \lim_{T\to\infty} \frac{1}{T} \int_0^T E(R_\gamma(\mathcal{S}(t))) dt \\ &= \lim_{T\to\infty} \frac{1}{T} \int_0^T \sum_{s_i\in\mathcal{S}} R_\gamma(s_i) \Pr\{\mathcal{S}(t) = s_i\} dt \\ &= \sum_{s_i\in\mathcal{S}} R_\gamma(s_i) \lim_{T\to\infty} \frac{1}{T} \int_0^T \Pr\{\mathcal{S}(t) = s_i\} dt \\ &= \sum_{s_i\in\mathcal{S}} R_\gamma(s_i) \Pi_{s_i}. \end{aligned} \tag{3.16}$$

The interchanges of limits, integrals, sums, etc. are permitted as long as $\sum_{s_i \in \mathcal{S}} |R_\gamma(s_i)| \Pi_{s_i} < \infty$. Thus, from CTMC-5, we can express the total average throughput for user γ as follows,

$$U_\gamma = \Pi_\gamma r_1^\gamma + \Pi_2 r_2^\gamma, \tag{3.17}$$

where Π_γ and Π_2 are as solved in (3.10)-(3.12), and r_1^γ and r_2^γ are defined in (3.1) and (3.2), respectively. The first term on the right-hand side of (3.17) represents the throughput when user γ occupies the spectrum alone, and the second term represents the throughput when two secondary users share the spectrum.

Therefore, by using CTMC-5, we not only can capture the dynamic utilization of the unused licensed spectrum for secondary users without conflicting with the primary user, but also can study their stationary behaviors and quantify their spectrum utilization from a statistical point of view.

The CTMC can also be generalized to model the scenario with more than two secondary users. Suppose the set of N secondary users is denoted by $\mathbf{S} = \{1, \cdots, N\}$, then the state space $\mathcal{A}$ consists of $2^N + 1$ combinations of the status of primary user P and the secondary users:

$$\begin{aligned} (\Phi_P, \Phi_{\mathbf{S}}) \in \mathcal{A} \triangleq \{(1, [0, \cdots, 0])\} \bigcup \\ \{(0, \phi_{\mathbf{S}}) : \phi_{\mathbf{S}} \triangleq [n_N, \cdots, n_1] \in \{0, 1\}^N\}, \end{aligned} \tag{3.18}$$

where state $(1, [0, \cdots, 0])$ represents the case where the primary user is in service in the spectrum band alone, and $\{(0, \phi_{\mathbf{S}})\}$ represents all 2^N states where primary user P is not in service and zero up to N secondary users are in service.

For this generalized Markov model, the rate diagram can be drawn as an N-

dimensional hypercube. Each vertex of the hypercube represents a state in $\{(0, \phi_{\mathbf{S}})\}$; each edge connecting two vertices is bi-directional, and it represents the transition that some secondary user begins or completes its service. The center of the hypercube represents state $(1, [0, \cdots, 0])$; a straight line from each vertex to the center represents the transition when primary user P begins its service, and another line from the center to state $(0, [0, \cdots, 0])$ represents the transition when user P completes its service.

The stationary probabilities can be obtained as follows.

- Notation: Let S_i denote state $(0, [n_N, \cdots, n_1])$, where $n_k \in \{0, 1\}, k = 1, \cdots, N$, and $i = \sum_{j=1}^{N} 2^{j-1} n_j$, S_{2^N} denote state $(1, [0, \cdots, 0])$, and $q_{ij} \stackrel{\triangle}{=} q\{S_i \to S_j\}$ denote the transition rate from state S_i to S_j;

- Construct the generator matrix $\mathbf{Q} = [q_{ij}]$:

  1. for $S_i = (0, [n_N, \cdots, n_j, \cdots, n_1])$, where $i = 0, \cdots, 2^N - 1$, and $j = 1, \cdots, N$,

     $q\{(0, [n_N, \cdots, n_j, \cdots, n_1]) \to (0, [n_N, \cdots, 1 - n_j, \cdots, n_1])\} = \mu_j(n_j = 1)$, or $\lambda_j(n_j = 0)$; $q\{S_i \to S_{2^N}\} = \lambda_P$; $q_{ii} = -\sum_{j \neq i} q_{ij}$;

  2. $q\{S_{2^N} \to S_0\} = \mu_P$, $q\{S_{2^N} \to S_{2^N}\} = -\mu_P$;

- Solve the stationary probability $\mathbf{\Pi} = [\Pi_{S_0}, \cdots, \Pi_{S_{2^N-1}}, \Pi_{S_{2^N}}]$ from

$$\mathbf{Q}_{aug} \mathbf{\Pi}^T = \mathbf{b}, \tag{3.19}$$

where $\mathbf{Q}_{aug} = \begin{bmatrix} \mathbf{Q}^T \\ \mathbf{1}_{1 \times (2^N+1)} \end{bmatrix}$, and $\mathbf{b} = \begin{bmatrix} \mathbf{0}_{(2^N+1) \times 1} \\ 1 \end{bmatrix}$.

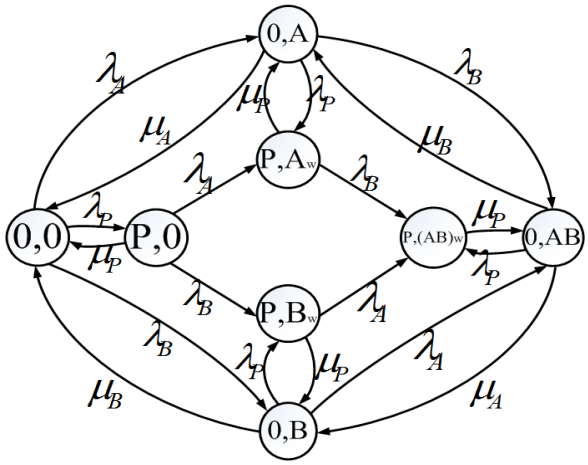

Figure 3.3: The rate diagram of CTMC with queuing.

For each secondary user γ, $\gamma \in \mathbf{S} = \{1, \cdots, N\}$, its average throughput consists of 2^{N-1} components, each of which represents the average throughput when user γ, together with zero up to all the other $N-1$ secondary users, are in service. Since more secondary users contend the spectrum access, the contention in the generalized Markov model becomes heavier than CTMC-5. As a result, each secondary user shares less spectrum access on average. Moreover, the interference also increases by introducing more secondary users. Therefore, as the number of secondary users increases, the average throughput for each of them is reduced.

3.2.2 CTMC with Queuing

In CTMC-5 presented in Section 3.2.1, the service of the secondary users is forced to stop and be dropped when primary user P appears in the spectrum band. After primary user P completes its service, CTMC-5 will transit to the idle state.

However, there may be some time interval wasted between when the system is in the idle state and the next secondary user accesses the spectrum. In order to further increase the spectrum utilization, queuing of the secondary users' service requests due to the primary user's presence is considered. More specifically, when the spectrum is being occupied by secondary users, upon the appearance of primary user, the secondary users should stop transmission, buffer their interrupted service session, and continue scanning the licensed band until the licensed band becomes available again. Also, if the primary user begins to operate in the previously idle spectrum, new service requests of secondary users are also queued. In this chapter, we assume that there is one waiting room for the secondary user, i.e., each user can only buffer a single service request; and if a service request already exists in the queue, the secondary user will direct the following service requests to other available licensed bands to avoid potential delay, and that scenario is beyond the scope of this chapter.

By considering the above factors, we model the spectrum access with queuing as an eight-state CTMC, denoted by "CTMC-8". The rate diagram of CTMC-8 is shown in Figure 3.3. Compared to CTMC-5 and its dynamics, in CTMC-8 three additional states are introduced: (P, A_w), (P, B_w) and $(P, (AB)_w)$. State (P, γ_w) means primary user P is in service and secondary user γ is waiting, and state $(P, (AB)_w)$ means P is in service and both secondary users are waiting. The transitions in CTMC-8 are briefed as follows. When the spectrum band is occupied by secondary user A, if A detects that primary user P needs to acquire the spectrum band, it buffers the unfinished service session, sensing the licensed band until the

end of the primary user's service session, and CTMC-8 transits from state $(0, A)$ to state (P, A_w) with rate λ_P s^{-1}. If primary user P finishes its service before B's access, CTMC-8 transits from state (P, A_w) to $(0, A)$ with rate μ_P s^{-1}. In contrast, if secondary user B requests access to the licensed spectrum before primary user P completes its service duration, B also buffers its service session, and CTMC-8 transits to state $(P, (AB)_w)$ with rate λ_B s^{-1}. In state $(P, (AB)_w)$, both A and B keep sensing the spectrum. Once P vacates, CTMC-8 transits to state $(0, AB)$ with rate μ_P s^{-1}, where A and B share the spectrum band. Also, when CTMC-8 is in state $(P, 0)$, if secondary users attempt to access the spectrum, they will keep sensing the licensed band until the primary user vacates, and CTMC-8 transits to state (P, A_w) or state (P, B_w), with rate λ_A s^{-1} or λ_B s^{-1}, respectively.

The equations governing the above system and the corresponding solutions can be obtained in a similar way as in Section 3.2.1.

CTMC with queuing can also be generalized to model the scenario with more than two secondary users. For the Markov chain with a set $\mathbf{S} = \{1, \cdots, N\}$ of secondary users, the state space $\mathcal{B}$ consists of all possible 2^{N+1} combinations of the status for primary user P and the secondary users:

$$\begin{aligned}(\Psi_P, \Psi_{\mathbf{S}}) \in \mathcal{B} \triangleq \{&(1, \psi_{\mathbf{S}}^w) \bigcup \\ &(0, \psi_{\mathbf{S}}) : \psi_{\mathbf{S}} \triangleq [n_N, \cdots, n_1] \in \{0, 1\}^N\},\end{aligned} \tag{3.20}$$

where $\{(1, \psi_{\mathbf{S}}^w)\}$ represents all 2^N states in which the primary user is in service and zero up to N secondary users are waiting, and $\{(0, \psi_{\mathbf{S}})\}$ represents all 2^N states where primary user P is not in service and a subset of the N secondary users are in service. The rate diagram for this model can be similarly drawn as in Section 3.2.1,

and the stationary probabilities can be obtained as follows.

- Notation: Let S_i denote state $(0, [n_N, \cdots, n_1])$, and S_i^w denote state $(1, [n_N, \cdots, n_1]^w)$.
- Construct the generator matrix $\mathbf{Q} = [q_{ij}]$:
  1. for $S_i = (0, [n_N, \cdots, n_j, \cdots, n_1])$, where $i = 0, \cdots, 2^N - 1$, and $j = 1, \cdots, N$,

     $q\{(0, [n_N, \cdots, n_j, \cdots, n_1]) \rightarrow (0, [n_N, \cdots, 1 - n_j, \cdots, n_1])\} = \mu_j(n_j = 1)$, or $\lambda_j(n_j = 0)$;

     $q\{(1, [n_N, \cdots, n_j, \cdots, n_1]^w) \rightarrow (1, [n_N, \cdots, 1 - n_j, \cdots, n_1]^w)\} = \lambda_j(n_j = 0)$;
  2. $q\{S_i \rightarrow S_i^w\} = \lambda_P$; $q\{S_i^w \rightarrow S_i\} = \mu_P$; $q_{ii} = -\sum_{j \neq i} q_{ij}$;
- Solve the equation array similar to (3.19).

As more secondary users contend the spectrum, in addition to increased interference, more waiting time is also introduced; therefore, the average throughput for each secondary user will be reduced.

3.3 Proposed Dynamic Spectrum Access

In this section, we will first analyze the effect of secondary users' behavior on the system performance. Then, we propose primary-prioritized dynamic spectrum access with different optimality criteria and compare them to CSMA-based random access approaches.

In order to develop primary-prioritized dynamic spectrum access, it is important to first analyze the behavior of the secondary users. Since the secondary users contend for the spectrum, if they access the spectrum in a greedy manner such that all of their injected traffic is admitted, then the Markov chain is more likely to be in the state where more than one user shares the spectrum. Hence, the secondary users may suffer a throughput degradation due to interference, if there is no control on very high arrival rates. On the other hand, if the secondary users reduce their arrival rates too much so as to avoid interference, the average throughput may be unnecessarily low. Therefore, secondary user spectrum access should be carefully controlled.

In the proposed dynamic spectrum access scheme, we introduce the state-dependent spectrum access probabilities for user A and user B, and the resulting random access process can be approximated by slightly modifying the original CTMCs. Without loss of generality, we take CTMC-5 as an example, and the modified Markov chain is shown in Figure 3.4. It is seen from the figure that when one secondary user, e.g. user B, already occupies the spectrum and the system is in state B, user A's spectrum access requests are admitted with probability $a_{A,1}$, where $0 \leq a_{A,1} \leq 1$. Since on average one out of $\frac{1}{a_{A,1}}$ user A's access requests are allowed when user B is in service, the chance of coexistence of the secondary users and mutual interference can be reduced. Due to the *decomposition property* of Poisson random process [Kul95], if each access request of user A has a probability $a_{A,1}$ of being admitted, then the number of actual admitted access requests is also a Poisson process with parameter $a_{A,1}\lambda_A$ s^{-1}. Hence, the transition rate from state

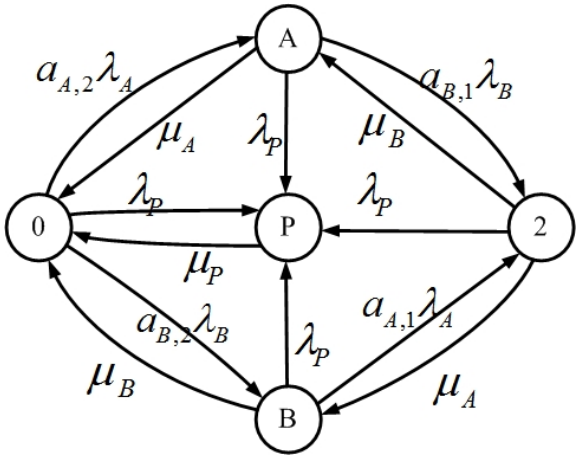

Figure 3.4: Modified CTMC with access control (no queuing).

B to state 2 now becomes $a_{A,1}\lambda_A$ s^{-1}. It is also seen that user A's access requests are admitted with probability $a_{A,2}$ when the spectrum is idle (i.e., the transition from state 0 to state A). However, there is no interference in state A. In order to obtain a high throughput, we assume that when the spectrum is sensed idle, user A is allowed to access the spectrum with probability one, i.e., $a_{A,2} = 1$. In addition, it is expected that if the mutual interference between the secondary users is high, $a_{A,1}$ should be close to 0; if there is little mutual interference, $a_{A,1}$ should be close to 1. User B's spectrum access is controlled in a similar way as user A, because the CTMC is symmetric.

Denote the access probability for user A and user B as vectors $\mathbf{a}_A = [a_{A,1}, a_{A,2}]$, and $\mathbf{a}_B = [a_{B,1}, a_{B,2}]$, respectively. Then, the optimization goal is to determine $\mathbf{a}_A$ and $\mathbf{a}_B$, such that the system performance can be maximized, i.e.,

$$\{\mathbf{a}_\gamma\} = \underset{0 \le \mathbf{a}_\gamma \le 1}{\operatorname{argmax}} \quad U(\{\mathbf{a}_\gamma\}), \tag{3.21}$$

where $\forall\gamma \in \{A, B\}$.

Since a good spectrum sharing scheme not only can efficiently utilize the spectrum resources, but also can provide fairness among different users, we first propose to maximize the average throughput based on PF criterion [Kel97] [HJL05]. Thus, in (3.21), $U(\mathbf{a}_A, \mathbf{a}_B)$ can be written as

$$U_{PF}(\mathbf{a}_A, \mathbf{a}_B) = \prod_{\gamma \in \mathrm{S}} U_\gamma(\mathbf{a}_A, \mathbf{a}_B). \tag{3.22}$$

We also consider other criteria to compare with PF, expressed by the following maximal-throughput criterion

$$U(\mathbf{a}_A, \mathbf{a}_B) = \sum_{\gamma \in \mathrm{S}} U_\gamma(\mathbf{a}_A, \mathbf{a}_B), \tag{3.23}$$

and max-min fairness criterion

$$U(\mathbf{a}_A, \mathbf{a}_B) = \min_{\gamma \in \mathrm{S}} U_\gamma(\mathbf{a}_A, \mathbf{a}_B). \tag{3.24}$$

For the maximal-throughput optimization, the overall system throughput is maximized, but the users with the worse channel conditions may starve. For the max-min fairness optimization, the performance of the secondary user with the worst channel condition is optimized, while resulting in inferior overall system performance. In this chapter, we will demonstrate that the PF dynamic spectrum access is preferred because it can ensure more fairness than the maximal-throughput optimization, while achieve better performance than the max-min fairness optimization. Specifically, the definition of PF is expressed as follows.

Definition: The throughput distribution is proportionally fair if any change in the distribution of throughput pairs results in the sum of the proportional changes

of the throughput being non-positive [Kel97], i.e.,

$$\sum_{\gamma \in \mathrm{S}} \frac{U_\gamma(\mathbf{a}_A, \mathbf{a}_B) - U^*_\gamma(\mathbf{a}_A, \mathbf{a}_B)}{U^*_\gamma(\mathbf{a}_A, \mathbf{a}_B)} \leq 0, \tag{3.25}$$

where $U^*_\gamma(\mathbf{a}_A, \mathbf{a}_B)$ is the proportionally fair throughput distribution, and $U_\gamma(\mathbf{a}_A, \mathbf{a}_B)$ is any other feasible throughput distribution for user γ.

The optimal solution $U^*_\gamma(\mathbf{a}_A, \mathbf{a}_B)$ defined in (3.25) can be obtained by solving (3.21), with $U(\mathbf{a}_A, \mathbf{a}_B)$ defined in (3.22). We sketch the proof as follows.

Since the function of ln is monotonic, the PF-based utility defined in (3.22) is equivalent to

$$\sum_{\gamma \in \mathrm{S}} \ln U_\gamma(\mathbf{a}_A, \mathbf{a}_B). \tag{3.26}$$

Define $\tilde{U}_\gamma = \ln U_\gamma$, then the gradient of $\tilde{U}_\gamma$ at the PF utility U^*_γ is $\frac{\partial \tilde{U}_\gamma}{\partial U_\gamma}\Big|_{U^*_\gamma} = \frac{1}{U^*_\gamma}$.

As the PF utility U^*_γ optimizes (3.26), for a small feasible perturbation from the PF utility, we can omit the high-order polynomials in the Taylor series, apply first-order Taylor approximation, and obtain the following condition:

$$\sum_{\gamma} \frac{\partial \tilde{U}_\gamma}{\partial U_\gamma}\Big|_{U^*_\gamma} (U_\gamma - U^*_\gamma) = \sum_{\gamma} \frac{U_\gamma - U^*_\gamma}{U^*_\gamma} \leq 0, \tag{3.27}$$

Since the feasible region for U_γ is a convex set and the logarithm function (3.26) is strictly concave, (3.27) holds for any point deviating from the PF utility. Therefore, the definition of the PF criterion in (3.22) and (3.25) is equivalent.

As mentioned earlier in this section, we assume $a_{A,2} = a_{B,2} = 1$, then the two access probabilities to be optimized are $a_{A,1}$ and $a_{B,1}$. We denote them by a_A and a_B for simplicity, and can write U_γ as

$$U_\gamma(a_A, a_B) = \Pi_\gamma(a_A, a_B) r_1^\gamma + \Pi_2(a_A, a_B) r_2^\gamma \quad , \tag{3.28}$$

where

$$\begin{aligned}
\Pi_A(a_A, a_B) &= C_1\lambda_A[(\lambda_P+\mu_B)(a_A\lambda_A+\lambda_P+\mu_A+\mu_B)+a_A\lambda_B\mu_B] \\
\Pi_B(a_A, a_B) &= C_1\lambda_B[(\lambda_P+\mu_A)(a_B\lambda_B+\lambda_P+\mu_A+\mu_B)+a_B\lambda_A\mu_A] \quad , \\
\Pi_2(a_A, a_B) &= C_1\lambda_A\lambda_B[a_A(a_B(\lambda_A+\lambda_B)+\lambda_P+\mu_A)+a_B(\lambda_P+\mu_B)]
\end{aligned} \tag{3.29}$$

with

$$\begin{aligned}
C_1 =&(1-\Pi_P)\Big\{a_A\lambda_A[a_B\lambda_B(\lambda_A+\lambda_B+\lambda_P)+(\lambda_B+\lambda_P)(\lambda_P+\mu_A) \\
&+(\lambda_B+\lambda_P+\mu_A)\mu_B+\lambda_A(\lambda_P+\mu_B)] \\
&+(\lambda_P+\mu_A+\mu_B)[\lambda_A(\lambda_P+\mu_B)+(\lambda_P+\mu_A)(\lambda_B+\lambda_P+\mu_B)] \\
&+a_B\lambda_B[(\lambda_P+\mu_A)(\lambda_B+\lambda_P+\mu_B)+\lambda_A(\lambda_P+\mu_A+\mu_B)]\Big\}^{-1},
\end{aligned} \tag{3.30}$$

When $0 \le a_\gamma \le 1$, we have $\Pi_A(a_A, a_B) \ge 0$, $\Pi_B(a_A, a_B) \ge 0$, $\Pi_2(a_A, a_B) \ge 0$, and $U_\gamma(a_A, a_B) \ge 0$. Taking derivative of $U_\gamma(a_A, a_B)$ with respect to a_A, we can show that

$$\frac{\partial U_A(a_A, a_B)}{\partial a_A} > 0, \quad \frac{\partial U_B(a_A, a_B)}{\partial a_A} < 0. \tag{3.31}$$

So when secondary user A is given more chance to access the frequency band, i.e., when a_A increases, $U_A(a_A, a_B)$ becomes larger while $U_B(a_A, a_B)$ shrinks, indicating that there is a possible tradeoff to choose the optimal a_A that maximizes $U_{PF}(a_A, a_B) = U_A(a_A, a_B)U_B(a_A, a_B)$. However, it can be seen that there are a lot of variables in $U_\gamma(a_A, a_B)$ and hence the objective function $U_{PF}(a_A, a_B)$. In addition, the utility of each secondary user U_γ is a complicated function of the $\{\lambda_\gamma, \mu_\gamma, a_\gamma\}$'s and the data rates $\{r_1^\gamma, r_2^\gamma\}$'s. Therefore, it is analytically difficult to justify the concavity for arbitrary parameters. Nevertheless, given a specific set of parameters $\{\lambda_\gamma, \mu_\gamma\}$'s and $\{r_1^\gamma, r_2^\gamma\}$'s, we can substitute their values in (3.29) and determine

Table 3.1: Primary-prioritized dynamic spectrum access

1. Initially primary user P is operating in the spectrum band;
2. Secondary access point obtains optimal access probabilities defined in (3.32) for secondary users (Other optimality criteria can also be implemented);
3. Once primary user P is sensed to have completed its service, secondary users start to access the spectrum band with the probabilities solved in Step 2 depending on various states;
4. When primary user P re-appears in the band, secondary users currently operating in the band vacate;
5. If secondary users still have service not completed, go back to Step 3; If the statistics of secondary users' services or their locations change, go to Step 2.

the concavity of $U_{PF}(a_A, a_B)$ by observing the Hessian matrix $\nabla^2 U_{PF}(a_A, a_B)$, for $0 \leq a_A, a_B \leq 1$. When the two eigenvalues of $\nabla^2 U_{PF}(a_A, a_B)$ are not greater than zero, i.e., the Hessian matrix is negative semidefinite, we can determine that $U_{PF}(a_A, a_B)$ is concave with respect to a_A and a_B, and the optimal access probabilities can be expressed as

$$a_{\gamma,i}^{opt} = \min\{\max(a_{\gamma,i}^{*}, 0), 1\}, \tag{3.32}$$

where $a_{\gamma,i}^{*}$ is the solution to the following equations

$$\frac{\partial U_{PF}(a_A, a_B)}{\partial a_{\gamma,i}} = 0, \quad \forall \gamma, i \in \mathrm{S}. \tag{3.33}$$

However, for some value of $\lambda_\gamma, \mu_\gamma$, if $r_1^\gamma \gg r_2^\gamma$, indicating heavy mutual interference, function $U_{PF}(a_A, a_B)$ may not be concave, and the optimal solution of a_γ is 0 to avoid interference. Another instance where $U_{PF}(a_A, a_B)$ is not concave happens when $\lambda_\gamma \ll \mu_\gamma$, and the optimal solution is $a_\gamma = 1$.

We assume that there exists a secondary base station (BS) that can control the medium access for all the secondary users. The secondary users send periodic reports to the BS informing it about their service statistics and date rates. Using the information gathered from all secondary users, the BS evaluates the spectrum utilization, computes the optimal access probability in different states (i.e., when different set of secondary users are in service), and sends the access probability to the secondary users. Based on the above discussions, we illustrate our primary-prioritized Markov approach for dynamic spectrum access in Table 3.1.

The proposed primary-prioritized dynamic spectrum access shares some characteristic with conventional medium access control (MAC) protocols, since they

all target appropriate coordination of different users' access to the medium. For instance, in IEEE 802.11 [IEE99], a CSMA/CA mechanism is employed. If the medium is sensed idle, a user transmits its packet; if the medium is sensed busy, then the user may re-schedule the retransmission of the packet according to some random back-off time distribution. These kinds of protocols are effective when the medium is not heavily loaded, since they allow users to transmit with minimum delay. However, under heavy traffic load, there is always a chance that users' attempts conflict with each other. If the conflicted users are kept waiting for an idle medium, their packets suffer significant delay and may expire.

In the proposed primary-prioritized dynamic spectrum access, different secondary users are allowed to share the spectrum band simultaneously. This will increase the spectrum utilization because of the following reasons. First, for independent Poisson processes, the service durations of different secondary users are generally not the same. For instance, in CTMC-5, even though user B begins operating in the spectrum band right after user A, it is possible that user A completes its service much earlier than user B. After user B is admitted to occupy the spectrum band, the two secondary users share the spectrum only for a very short time. Once A finishes its service, the Markov chain transits to the state where B operates in the spectrum alone and no interference exists. Using CSMA protocols, however, user B is forced to re-transmit its packet after a random back-off time, which may not be short. Therefore, using the proposed approaches, the spectrum can be more efficiently utilized. Furthermore, in the proposed schemes, optimal access probabilities are employed to carefully control the coexistence of the secondary users. In this

way, the interference is maintained at a low level.

Also, in a mobile network, the radio spectrum environment is dynamic. When using global optimization approaches specific to a fixed environment, for instance conventional power control to manage mutual interference between a fixed number of secondary users, after each change in the number of contending secondary users, the network needs to re-optimize the power allocation for all users completely. This results in high complexity and much overhead, especially when there are frequent service requests and the service duration is short. In the proposed approach, by controlling the access probabilities for secondary users, there is no need to perform delicate power control to manage the interference, and computational complexity is reduced while the average throughput is maximized in the long-run.

In order to achieve optimal dynamic spectrum access, a certain overhead is needed. More specifically, the overhead mainly comes from access controlling and sensing primary users. To optimally coordinate the access of the secondary users, necessary measurements needs to be taken, such as the throughput and arrival/departure rates for different secondary users. On the other hand, detecting a primary user's presence relies mainly on the observations from the secondary users and the necessary spectral analysis.

3.4 Simulation Studies

In this section, we first compare the performance of CTMC-8 with different optimization goals (maximal-throughput, max-min, and PF). Then we compare the

performance of CTMC-8, CTMC-5, and the nonpersistent CSMA-based random access. Finally we show the throughput gain of spectrum sharing among more than two secondary users against the case without access control.

The parameters in the simulations are chosen as follows. We set the bandwidth of the licensed spectrum as $W = 200$ KHz, the transmission power of each secondary user $p_\gamma = 2$ mW, the noise power $n_0 = 10^{-15}$ W, and the propagation loss exponent factor as 3.6. The departure rates μ_A, μ_B, μ_P are set to be 100 s^{-1}. According to [M. 05], in the spectrum band allocated to cellular phone and Specialized Mobile Radio (SMR), the fraction of time that the spectrum is being used by primary users in an urban environment is measured as approximately 45%. Thus, when μ_P is 100 s^{-1}, we set the arrival rate of the primary user $\lambda_P = 85$ s^{-1}. The arrival rate of secondary user B is $\lambda_B = 85$ s^{-1}, and we vary λ_A from 70 to 100 s^{-1}. In the simulation results, we use "Max-Thr" to denote the maximal-throughput criterion, "Max-Min" to denote the max-min fairness criterion, and "A" and "B" to denote secondary users A and B, respectively.

3.4.1 CTMC-8 for the Symmetric-Interference Case

In the first set of simulations, we test the case where two secondary users experience symmetric interference. The transmitter of user A is at $(0\text{m}, 0\text{m})$, and its receiver is at $(200\text{m}, 0\text{m})$. The transmitter of user B is at $(200\text{m}, 460\text{m})$, and its receiver is at $(0\text{m}, 460\text{m})$. According to their symmetric locations, we know that $r_1^B = r_1^A > r_2^B = r_2^A$ from (3.1) and (3.2). In Figure 3.5, we show the optimal

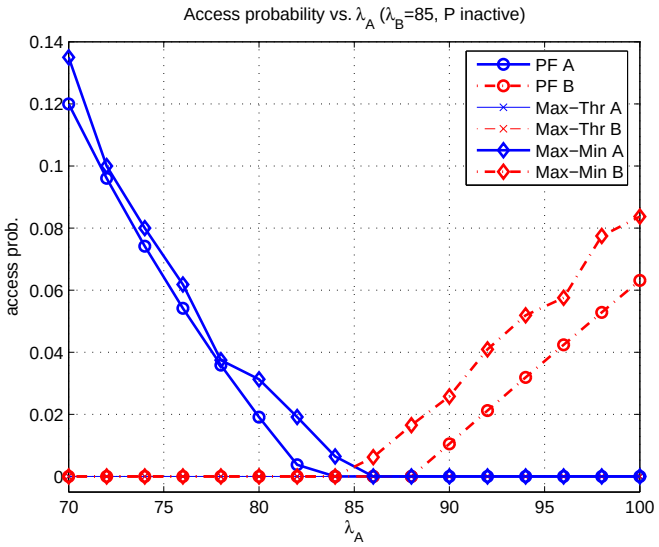

Figure 3.5: Access probability vs. λ_A (symmetric-interference, $\lambda_B = 85$ s^{-1}).

access probability versus λ_A for each secondary user when the other secondary user is transmitting, i.e., the access probability associated with the transition from state $(0, \gamma)$ to $(0, AB)$ in CTMC-8 (see Figure 3.3).

Since CTMC-8 is symmetric for the two users, when $\lambda_A < \lambda_B = 85$ s^{-1}, user A will have a smaller time share than user B if there is no access probability control. Further because we have $r_1^B = r_1^A > r_2^B = r_2^A$, from the definition of the average throughput in (3.17), user A will experience a lower average throughput than B. In order to provide more fairness, PF and max-min optimization assigns user B a zero access probability and assigns user A a higher access probability than user B when $\lambda_A < \lambda_B = 85$ s^{-1}. With the increase of λ_A, the difference between the two users' time share becomes smaller, so the access probability of user A decreases and is equal to B's access probability when $\lambda_A = \lambda_B$. When $\lambda_A > \lambda_B$, user B is assigned a higher access probability due to a smaller time share, while user A's access requests

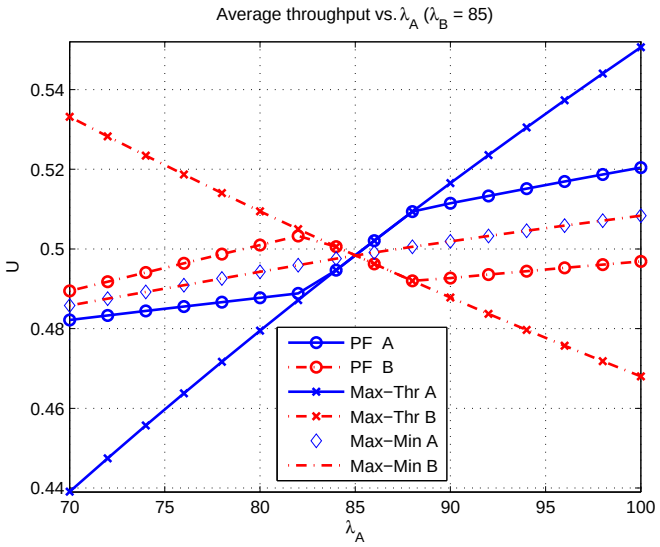

Figure 3.6: Average throughput vs. λ_A (symmetric-interference, $\lambda_B = 85$ s^{-1}).

are denied. However, when $\lambda_A > \lambda_B = 85$ s^{-1}, λ_A is much higher and the probability of State A is also higher, in order to reduce the mutual interference, the growth of B's access probability is not symmetric to the decrease of A's. Due to the mutual interference, the maximal-throughput optimization assigns zero access probability to both users when the other user is in service.

In Figure 3.6, we show the throughput U_γ for each user. Max-min fairness optimization provides absolute fairness to both users: the two U_γ's are identical and increase as λ_A goes up. In the PF optimization, when $\lambda_A < \lambda_B$, we have $U_A < U_B$. As λ_A becomes higher, U_A increases; however, as shown in Figure 3.5, user A's access probability decreases as λ_A increases until $\lambda_A = \lambda_B = 85$ s^{-1}, so the mutual interference is managed and U_B also increases. When $\lambda_A = \lambda_B = 85$ s^{-1}, $U_A = U_B$, since the secondary users are identical in terms of both channel conditions and service requests. As λ_A further increases, $U_A > U_B$ and U_A keeps increasing;

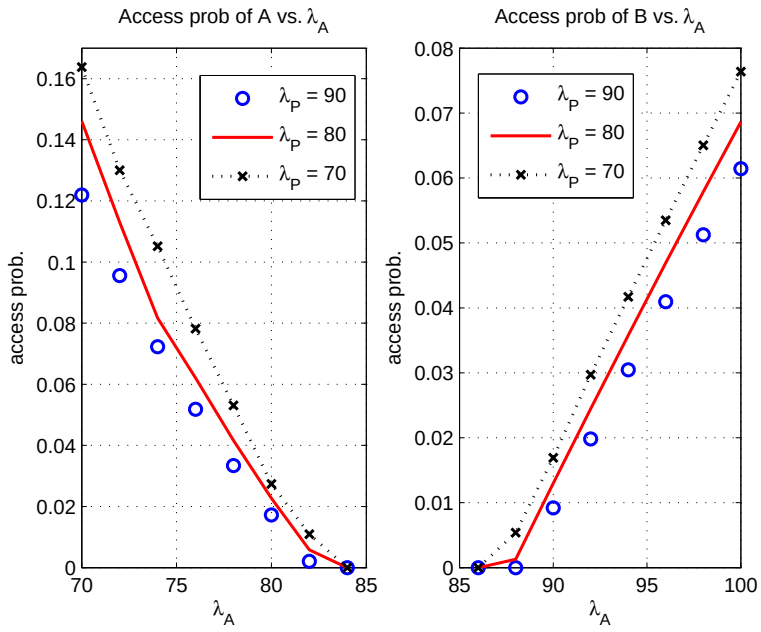

Figure 3.7: Access probability for different λ_P ($\lambda_B = 85$ s^{-1}).

since user B's access probability increases as $\lambda_A > \lambda_B = 85$ s^{-1} (see Figure 3.5), U_B also increases. For the maximal-throughput optimization, as seen from Figure 3.5, the access probabilities of the two users are both zero, indicating that they are not allowed to transmit simultaneously, so U_A keeps increasing as λ_A increases, while U_B drops quickly, which is unfair.

In Figure 3.7, we show the effect of λ_P on the average access probability. In this set of simulations, λ_B is still set as 85 s^{-1} and we vary λ_A from 70 to 100 s^{-1}. We know from Figure 3.5 that the user with the higher access rate has a zero access probability when the other user is in service. Therefore, we only demonstrate the nonzero access probability of the user with a lower access rate, i.e., we show user A's access probability when $\lambda_A < \lambda_B = 85$ s^{-1} and user B's access probability when $\lambda_A > \lambda_B = 85$ s^{-1}. In Figure 3.7, we compare the average

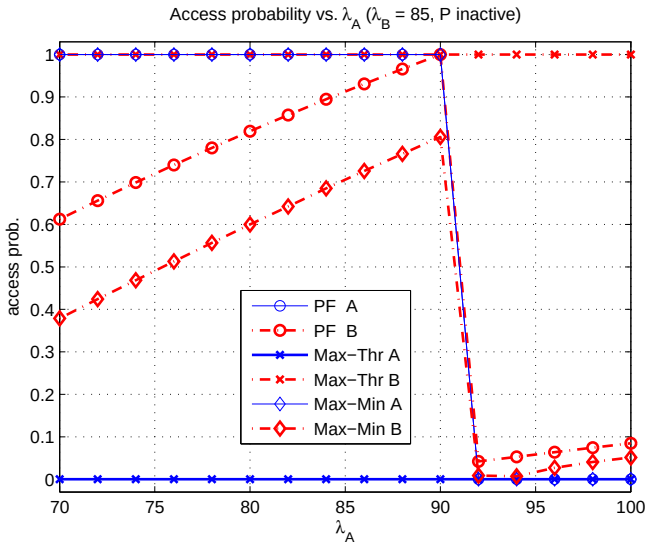

Figure 3.8: Access probability vs. λ_A (asymmetric-interference, $\lambda_B = 85$ s^{-1}).

access probability when λ_P is chosen from $\{90, 80, 70\}$ s^{-1}. We know that as λ_P increases, the competition between the secondary users becomes more severe. In order to reduce mutual interference, when λ_A is a fixed value, both users' access probabilities decrease as λ_P becomes larger.

3.4.2 CTMC-8 for the Asymmetric-Interference Case

In the second set of simulations, the transmitter of user A is at $(0\text{m}, 0\text{m})$, and its receiver is at $(200\text{m}, 0\text{m})$. The transmitter of user B is at $(185\text{m}, 460\text{m})$, and its receiver is at $(15\text{m}, 460\text{m})$. Under these settings, we have $r_1^B > r_1^A > r_2^B > r_2^A$ from (3.1) and (3.2), so the interference is asymmetric. In Figure 3.8, we show the optimal access probabilities versus λ_A for each secondary user when the other is transmitting. Since user A has a worse channel condition than user B, for the maximal-throughput optimization, user A's access probability is 0 (e.g., user A's

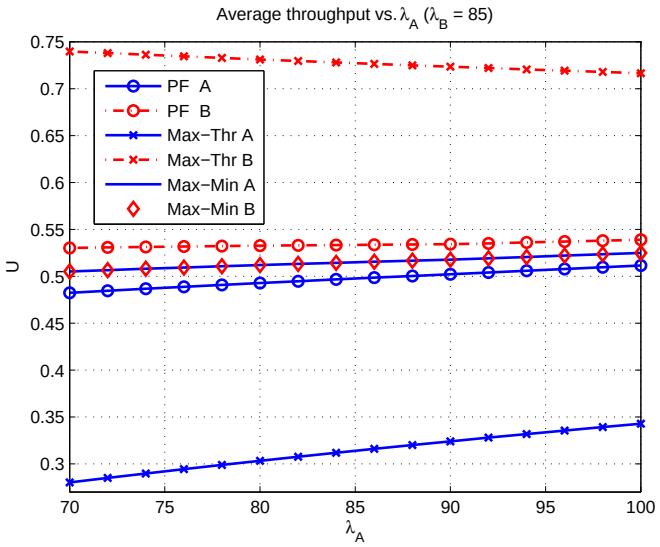

Figure 3.9: Average throughput vs. λ_A (asymmetric-interference, $\lambda_B = 85$ s^{-1}).

requests are always rejected) when user B is in service, which is unfair. For the PF or max-min fairness optimization, when $\lambda_A < \lambda_B = 85$ s^{-1}, user A's access probability is 1 (e.g., user A's requests are always admitted), while only a part of B's requests are admitted, due to fairness concerns. When λ_A is a little greater than λ_B, unlike the symmetric-interference case, user A's probability is still 1 and higher than B's access probability, because user A has a worse channel condition than B. When λ_A exceeds 90 s^{-1}, the chance of co-existence is so high that the access probabilities for both users drop to avoid interference.

In Figure 3.9, we show the average throughput for each secondary user. We know from Figure 3.8 that in the maximal-throughput optimization, user A's access probability is 0 and user B's access probability is 1; therefore, U_B is much greater than U_A. The PF optimization greatly reduces the throughput difference between the two users, with only a small loss of total throughput.

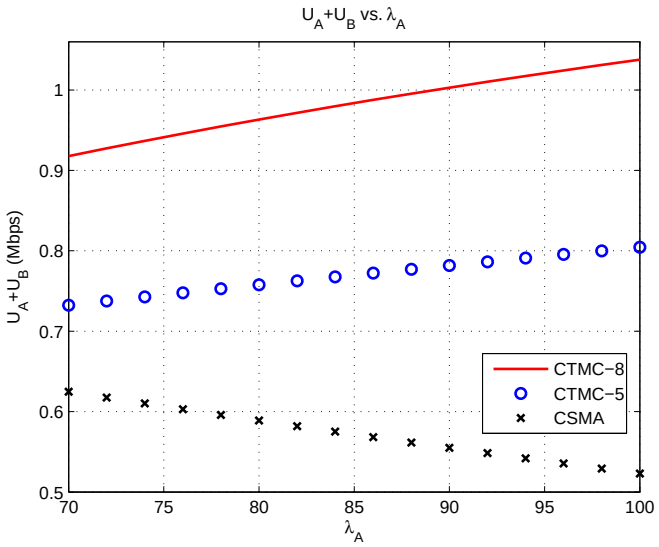

Figure 3.10: Overall throughput for CTMC-5, CTMC-8 and CSMA.

3.4.3 Comparison with a CSMA-based Scheme

In Figure 3.10, we show the overall throughput of the PF dynamic spectrum access for CTMC-8, CTMC-5, and the overall throughput for a CSMA-based scheme [KT75]. The transmitters for both secondary users are uniformly located in a 200m $\times$ 200m square area, the distance between each transmitter-receiver pair is uniformly distributed in $[100\text{m}, 200\text{m}]$, and the other parameters are the same as in the previous setting. We choose the slotted version of the nonpersistent CSMA to avoid frequent collisions assuming the secondary users experience severe contention for the licensed spectrum, and the slot size is 0.005. So when primary user P is absent and one secondary user γ is transmitting, the later-coming secondary user senses the spectrum in every $0.005/\mu_\gamma$ s until the licensed spectrum is available again.

We can see that the PF access for both CTMCs have better performance than

CSMA-based scheme as λ_A increases. This is because in CSMA, the secondary users cannot utilize the spectrum at the same time. Thus, even though interference exists when secondary users share the spectrum, by allowing spectrum sharing between them and optimally controlling their access probabilities, performance gain can still be achieved.

As λ_A increases, the overall throughput of the PF access for both CTMCs increases, while the throughput of CSMA-based scheme decreases. When $\lambda_A = 100$ s^{-1}, CTMC-5 can achieve about 50% throughput gain over CSMA, and CTMC-8 can achieve more than 95% throughput gain. This shows that the proposed PF access approach has a larger capability than CSMA to accommodate more traffic. Moreover, the spectrum efficiency of CTMC-8 is higher than that of CTMC-5, due to queuing of the interrupted service.

3.4.4 Comparison with a Uniform-Access-Probability Scheme

In [WJL07], we have proposed a uniform access probability for each secondary user no matter what state the CTMC is in. However, when the licensed spectrum is idle, the access probability may restrain full spectrum utilization. Moreover, the interference condition for one secondary user is varying when different subsets of secondary users share the spectrum. Only optimizing one single access probability may result in a sub-optimal solution. In this subsection, we conduct simulations to compare the scheme proposed in this chapter with the one in [WJL07]. In the comparison, we adopt the PF method, while the transmission power, request/service

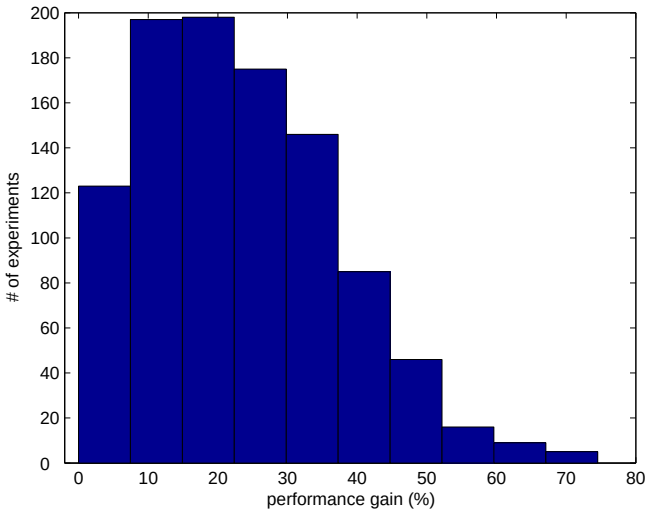

Figure 3.11: The histogram of throughput improvement (U_{PF})

rates, and the locations of the secondary users are all uniformly distributed in a proper interval, and we test 1000 independent experiments to get the average. The histogram of the performance gain (U_{PF}) is shown in Figure 3.11. We see that the proposed scheme in this chapter with state-dependent access probability achieves on average a 24% higher system throughput than the scheme using a uniform access probability in [WJL07].

3.4.5 Spectrum Sharing Among Multiple Secondary Users

Spectrum access with multiple secondary users can also be optimally controlled using a method where the access probabilities are obtained with numerical search algorithms. The transmitter-receiver pair of each user is randomly distributed in a 200m $\times$ 200m square area, and the transmission power is randomly chosen between 1mW and 3mW. In Figure 3.12, we compare the total throughput of the proposed

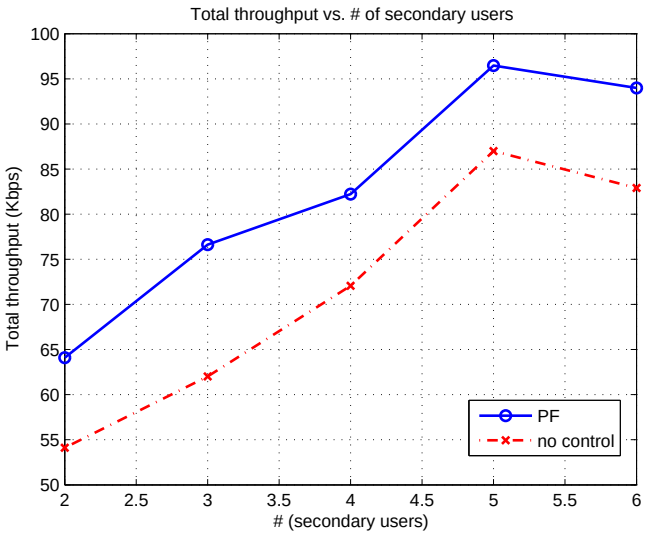

Figure 3.12: Comparison of overall throughput for multiple secondary users.

PF spectrum access to that without access control (i.e., all service requests are admitted with probability one). By optimizing the access probabilities, the proposed scheme achieves 17% higher throughput on average, since the interference is successfully alleviated. We also see that as the number of competing secondary user increases, the average throughput for each user is greatly reduced, since the spectrum competition becomes much heavier and each user has a smaller spectrum share.

3.5 Summary

In this chapter, we propose a primary-prioritized Markov approach for dynamic spectrum access. We model the interactions between the primary users and the secondary users as continuous-time Markov chains, and optimize the state-dependent access probabilities for secondary users so that the spectrum resources can be ef-

ficiently and fairly shared by the secondary users in an opportunistic way without interrupting the primary usage. The simulation results show that the proposed spectrum access with PF criterion can achieve up to 95% performance gain over a CSMA-based random access approach, and also achieves the optimal tradeoff between efficient spectrum utilization and fairness.

Chapter 4

Evolutionary Game for Cooperative Spectrum Sensing

Good dynamic spectrum sharing schemes require precise spectrum sensing, which is an essential functionality that prevents primary users from being interfered by secondary users. Recent study has shown that cooperative spectrum sensing with multiple secondary users can further improve the efficiency of primary user detection.

However, in most of the existing cooperative spectrum sensing schemes as we discuss in Chapter 2, a fully cooperative scenario is assumed: all secondary users voluntarily contribute to sensing and fuse their detection results in every time slot to a central controller (e.g., secondary base station), which makes a final decision. However, sensing the primary band consumes a certain amount of energy and time which may alternatively be diverted to data transmissions, and it may not be optimal to have all users participate in sensing in every time slot, in order to guarantee a

certain system performance. Moreover, with the emerging applications of mobile ad hoc networks envisioned in civilian usage, the secondary users may be selfish and not serve a common goal. If multiple secondary users occupy different sub-bands of one primary user and can overhear the others' sensing outcomes, they tend to take advantage of the others and wait for the others to sense so as to reserve more time for their own data transmission. Therefore, it is of great importance to study the dynamic cooperative behaviors of selfish users in a competing environment while boosting the system performance simultaneously.

In this chapter, we model cooperative spectrum sensing as an evolutionary game, where the payoff is defined as the throughput of a secondary user. Evolutionary games have been previously applied to modeling networking problems, such as resource sharing mechanism in P2P networks [AH07] and congestion control [WMdSeSa08] using behavioral experiments. In this chapter, we incorporate practical multiuser effect and constraints into the spectrum sensing game. The secondary users want to fulfill a common task, i.e., given a required detection probability to protect the primary user from interference, sense the primary band collaboratively for the sake of getting a high throughput by sharing the sensing cost. The users who do not take part in cooperative sensing can overhear the sensing results and have more time for their own data transmission. However, if no user spends time in sensing the primary user, all of them may get a very low throughput. Therefore, secondary users need to try different strategies at each time slot and learn the best strategy from their strategic interactions using the methodology of understanding-by-building.

In order to study the evolution of secondary users' strategies and answer the question that how to cooperate in the evolutionary spectrum sensing game, we propose to analyze the process of secondary users updating their strategy profile with replicator dynamics equations [FL98], since a rational player should choose a strategy more often if that strategy brings a relatively higher payoff. We derive the evolutionarily stable strategy (ESS) of the game, and prove the convergence to the ESS through analyzing the users' behavior dynamics. Then we extend our observation to a more general game with heterogeneous users, analyze the properties of the ESSs, and develop a distributed learning algorithm so that the secondary users approach the ESS only with their own payoff history. Simulation results show that as the number of secondary users and the cost of sensing increases, the users tend to have less incentive to contribute to cooperative sensing. However, in general they can still achieve a higher average throughput in the spectrum sensing game than that of the single-user sensing. Furthermore, using the proposed game can achieve a higher total throughput than that of asking all users to contribute to sensing at every time slot.

The remainder of this chapter is organized as follows. In Section 4.1, we present the system model and formulate the multiuser cooperative spectrum sensing as a game. In Section 4.2, we introduce the background on evolutionary game theory, analyze the behavior dynamics and the ESS of the proposed game, and develop a distributed learning algorithm for ESS. Simulation results are shown in Section 4.3. Finally, we summarize the chapter in Section 4.4.

4.1 System Model and Spectrum Sensing Game

4.1.1 Hypothesis of Channel Sensing

When a secondary user is sensing the licensed spectrum channel in a cognitive radio network, the received signal $r(t)$ from the detection has two hypotheses when the primary user is present or absent, denoted by H_1 and H_0, respectively. Then, $r(t)$ can be written as

$$r(t) = \begin{cases} hs(t) + w(t), & \text{if } H_1; \\ w(t), & \text{if } H_0. \end{cases} \tag{4.1}$$

In (4.1), h is the gain of the channel from the primary user's transmitter to the secondary user's receiver, which is assumed to be slow flat fading; $s(t)$ is the signal of the primary user, which is assumed to be an i.i.d. random process with mean zero and variance σ_s^2; and $w(t)$ is an additive white Gaussian noise (AWGN) with mean zero and variance σ_w^2. Here $s(t)$ and $w(t)$ are assumed to be mutually independent.

Assume we use an energy detector to sense the licensed spectrum, then the test statistics $T(r)$ is defined as

$$T(r) = \frac{1}{N} \sum_{t=1}^{N} |r(t)|^2, \tag{4.2}$$

where N is the number of collected samples.

The performance of licensed spectrum sensing is characterized by two probabilities. The probability of detection, P_D, represents the probability of detecting the presence of primary user under hypothesis H_1. The probability of false alarm, P_F,

represents the probability of detecting the primary user's presence under hypothesis H_0. The higher the P_D, the better protection the primary user will receive; the lower the P_F, the more spectrum access the secondary user will obtain.

If the noise term $w(t)$ is assumed to be circularly symmetric complex Gaussian (CSCG), using central limit theorem the probability density function (PDF) of the test statistics $T(r)$ under H_0 can be approximated by a Gaussian distribution $\mathcal{N}(\sigma_w^2, \frac{1}{N}\sigma_w^4)$. Then, the probability of false alarm P_F is given by [Poo94]

$$P_F(\lambda) = \mathcal{Q}\left(\left(\frac{\lambda}{\sigma_w^2} - 1\right)\sqrt{N}\right), \tag{4.3}$$

where λ is the threshold of the energy detector, and $\mathcal{Q}(\cdot)$ denotes the complementary distribution function of the standard Gaussian, i.e.,

$$\mathcal{Q}(x) = \frac{1}{\sqrt{2\pi}}\int_x^\infty \exp\left(-\frac{t^2}{2}\right) dt.$$

Similarly, if we assume the primary signal is a complex PSK signal, then under hypothesis H_1, the PDF of $T(r)$ can be approximated by a Gaussian distribution $\mathcal{N}((\gamma+1)\sigma_w^2, \frac{1}{N}(2\gamma+1)\sigma_w^4)$, where $\gamma = \frac{|h|^2\sigma_s^2}{\sigma_w^2}$ denotes the received signal-to-noise ratio (SNR) of the primary user under H_1. Then, the probability of detection P_D can be approximated by [Poo94]

$$P_D(\lambda) = \mathcal{Q}\left(\left(\frac{\lambda}{\sigma_w^2} - \gamma - 1\right)\sqrt{\frac{N}{2\gamma+1}}\right). \tag{4.4}$$

Given a target detection probability $\bar{P}_D$, the threshold λ can be derived, and the probability of false alarm P_F can be further rewritten as

$$P_F(\bar{P}_D, N, \gamma) \triangleq \mathcal{Q}\left(\sqrt{2\gamma+1}\,\mathcal{Q}^{-1}(\bar{P}_D) + \sqrt{N}\gamma\right), \tag{4.5}$$

where $\mathcal{Q}^{-1}(\cdot)$ denotes the inverse function of $\mathcal{Q}(\cdot)$.

4.1.2 Throughput of a Secondary User

When sensing the primary user's activity, a secondary user cannot simultaneously perform data transmission. If we denote the sampling frequency by f_s and the frame duration by T, then the time duration for data transmission is given by $T - \delta(N)$, where $\delta(N) = \frac{N}{f_s}$ represents the time spent in sensing.

When the primary user is absent and no false alarm is generated, the average throughput of a secondary user is

$$R_{H_0}(N) = \frac{T - \delta(N)}{T}(1 - P_F)C_{H_0}, \tag{4.6}$$

where C_{H_0} represents the data rate of the secondary user under H_0. When the primary user is present, and not detected by the secondary user, the average throughput of a secondary user is

$$R_{H_1}(N) = \frac{T - \delta(N)}{T}(1 - P_D)C_{H_1}, \tag{4.7}$$

where C_{H_1} represents the data rate of the secondary user under H_1.

If we denote P_{H_0} as the probability that the primary user is absent, then the total throughput of a secondary user is

$$R(N) = P_{H_0}R_{H_0}(N) + (1 - P_{H_0})R_{H_1}(N). \tag{4.8}$$

In dynamic spectrum access, it is required that the secondary users' operation should not conflict or interfere with the primary users, and P_D should be one in the ideal case. According to (4.5), however, P_F is then also equal to one, and the total throughput of a secondary user (4.8) is zero, which is impractical. Hence, a

primary user who allows secondary spectrum access usually predetermines a target detection probability $\bar{P}_D$ very close to one [LYZH07], under which we assume the secondary spectrum access will be prohibited as a punishment. Then, from the secondary user's perspective, he/she wants to maximize his/her total throughput (4.8), given that $P_D \geq \bar{P}_D$. Since the target detection probability $\bar{P}_D$ is required by the primary user to be very close to 1, and we usually have $C_{H_1} < C_{H_0}$ due to the interference from the primary user to the secondary user, the second term in (4.8) is much smaller than the first term and can be omitted. Therefore, (4.8) can be approximated by

$$\tilde{R}(N) = P_{H_0} R_{H_0}(N) = P_{H_0} \frac{T - \delta(N)}{T} (1 - P_F) C_{H_0}. \tag{4.9}$$

We know from (4.5) that given a target detection probability $\bar{P}_D$, P_F is a decreasing function of N. As a secondary user reduces N (or $\delta(N)$) in the hope of having more time for data transmission, P_F will increase. This indicates a tradeoff for the secondary user to choose an optimal N that maximizes the throughput $\tilde{R}(N)$. In order to reduce both P_F and N, i.e., keep low false alarm P_F with a smaller N, a good choice for a secondary user is to cooperatively sense the spectrum with the other secondary users in the same licensed band.

4.1.3 Spectrum Sensing Game

A diagram of a cognitive radio network where multiple secondary users are allowed to access one licensed spectrum band is shown in Figure 4.1, where we assume that the secondary users within each others' transmission range can exchange

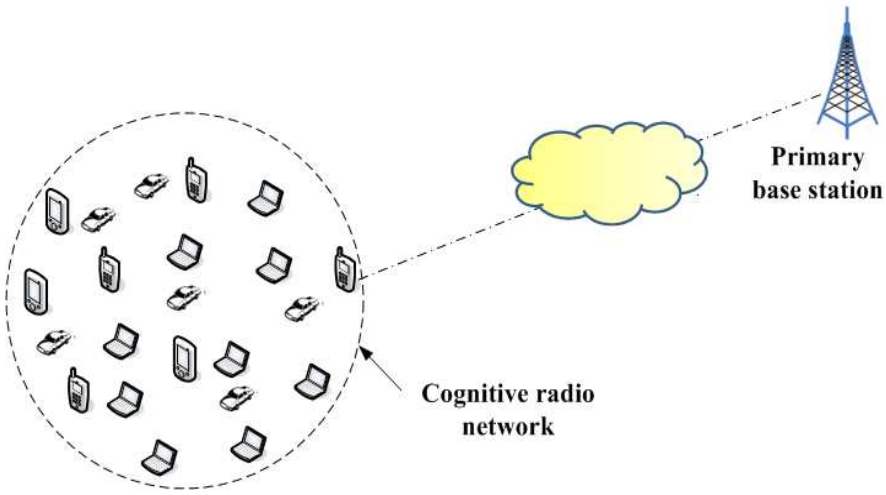

Figure 4.1: System model

their sensory data about primary user detection. The cooperative spectrum sensing scheme is illustrated in Figure 4.2. We assume that the entire licensed band is divided into K sub-bands, and each secondary user operates exclusively in one of the K sub-bands when the primary user is absent. Transmission time is slotted into intervals of length T. Before each data transmission, the secondary users need to sense the primary user's activity. Since the primary user will operate in all the sub-bands once becoming active, the secondary users within each other's transmission range can jointly sense the primary user's presence, and exchange their sensing results via a narrow-band signalling channel, as shown in Fig 4.2. In this way, each of them can spend less time detecting while enjoying a low false alarm probability P_F via some decision fusion rule [CV86], and the spectrum sensing cost ($\delta(N)$) can be shared by whoever is willing to contribute (C).

However, according to their locations and quality of the received primary sig-

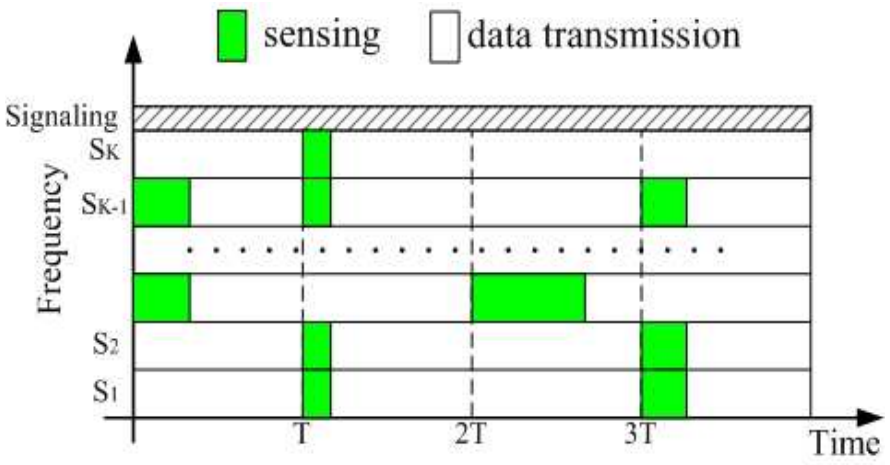

Figure 4.2: Cooperative spectrum sensing

nal, it may not be optimal to have all secondary users participate in spectrum sensing at every time slot, in order to guarantee certain system performance. Moreover, all secondary users cooperating in sensing may be difficult, if the users do not serve a common authority, and instead act selfishly to maximize their own throughput. In this case, once a secondary user is able to overhear the detection results from the other users, he/she can take advantage of that by refusing to take part in spectrum sensing, called denying (D). Although each secondary user in the cognitive radio network still achieves the same false alarm probability P_F, the users who refuse to join in cooperative sensing have more time for their own data transmission. The secondary users get a very low throughput if no one senses the spectrum, in the hope that someone else does the job.

Therefore, we can model the spectrum sensing as a noncooperative game. The players of the game are the secondary users, denoted by $\mathcal{S} = \{s_1, \cdots, s_K\}$.

Each player s_k has the same action/strategy space, denoted by $\mathcal{A} = \{\text{C,D}\}$, where "C" represents pure strategy *contribute* and "D" represents pure strategy *refuse to contribute (denying)*. The payoff function is defined as the throughput of the secondary user. Assume that secondary users contributing to cooperative sensing forms a set, denoted by $\mathcal{S}_c = \{s_1, \cdots, s_J\}$. Denote the false alarm probability of the cooperative sensing among set $\mathcal{S}_c$ with fusion rule "RULE" and a target detection probability $\bar{P}_D$ by $P_F^{\mathcal{S}_c} \triangleq P_F(\bar{P}_D, N, \{\gamma_i\}_{i\in\mathcal{S}_c}, \text{RULE})$. Then the payoff for a contributor $s_j \in \mathcal{S}_c$, can be defined as

$$\tilde{U}_{C,s_j} = P_{H_0}\left(1 - \frac{\delta(N)}{|\mathcal{S}_c|T}\right)(1 - P_F^{\mathcal{S}_c})C_{s_j}, \quad \text{if } |\mathcal{S}_c| \in [1, K], \tag{4.10}$$

where $|\mathcal{S}_c|$, i.e., the cardinality of set $\mathcal{S}_c$, represents the number of contributors, and C_{s_j} is the data rate for user s_j under hypothesis H_0. The payoff for a user $s_i \notin \mathcal{S}_c$, who selects strategy D, is then given by

$$\tilde{U}_{D,s_i} = P_{H_0}(1 - P_F^{\mathcal{S}_c})C_{s_i}, \quad \text{if } |\mathcal{S}_c| \in [1, K-1], \tag{4.11}$$

since s_i will not spend time sensing. If no secondary user contributes to sensing and waits for the others to sense, i.e., $|\mathcal{S}_c| = 0$, from (4.5), we know that $\lim_{N\to 0} P_F = 1$, especially for the low received SNR regime and high $\bar{P}_D$ requirement. In this case, the payoff for a denier becomes

$$\tilde{U}_{D,s_i} = 0, \quad \text{if } |\mathcal{S}_c| = 0. \tag{4.12}$$

The decision fusion rule can be selected as the logical-OR rule, logical-AND rule, or majority rule [LYZH07]. In this chapter, we use the majority rule to derive the $P_F^{\mathcal{S}_c}$, though the other fusion rules could be similarly analyzed. Denote the

detection and false alarm probability for a contributor $s_j \in \mathcal{S}_c$ by P_{D,s_j} and P_{F,s_j}, respectively. Then, under the majority rule we have the following

$$P_D = \Pr[\text{at least half users in } \mathcal{S}_c \text{ report } H_1 | H_1], \tag{4.13}$$

and

$$P_F = \Pr[\text{at least half users in } \mathcal{S}_c \text{ report } H_1 | H_0], \tag{4.14}$$

Hence, given a $\bar{P}_D$ for set $\mathcal{S}_c$, each individual user's target detection probability $\bar{P}_{D,s_j}$ can be obtained by solving the following equation

$$\bar{P}_D = \sum_{k=\lceil \frac{1+|\mathcal{S}_c|}{2} \rceil}^{|\mathcal{S}_c|} \binom{|\mathcal{S}_c|}{k} \bar{P}_{D,s_j}^k (1 - \bar{P}_{D,s_j})^{|\mathcal{S}_c|-k}, \tag{4.15}$$

where we assume each contributor $s_j \in \mathcal{S}_c$ takes equal responsibility in making the final decision for fairness concern and therefore $\bar{P}_{D,s_j}$ is identical for all s_j's. Then, from (4.5) we can write P_{F,s_j} as

$$P_{F,s_j} = \mathcal{Q}\left(\sqrt{2\gamma_{s_j}+1}\mathcal{Q}^{-1}(\bar{P}_{D,s_j}) + \sqrt{N/|\mathcal{S}_c|}\gamma_{s_j}\right), \tag{4.16}$$

and can further obtain $P_F^{\mathcal{S}_c}$ by substituting (4.16) in (4.14).

4.2 Evolutionary Sensing Game and Strategy Analysis

In this section, we first introduce the concept of ESS, and then use *replicator dynamics* to model and analyze the behavior dynamics of the secondary users in the sensing game.

4.2.1 Evolutionarily Stable Strategy

Evolutionary game theory provides a good means to address the strategic uncertainty that a player faces in a game by taking out-of-equilibrium behavior, learning during the strategic interactions, and approaching a robust equilibrium strategy. Such an equilibrium strategy concept widely adopted in evolutionary game theory is the *Evolutionarily Stable Strategy (ESS)* [Smi82], which is "a strategy such that, if all members of the population adopt it, then no mutant strategy could invade the population under the influence of natural selection". Let us define the expected payoff as the individual fitness, and use $\pi(p, \hat{p})$ to denote the payoff of an individual using strategy p against another individual using strategy $\hat{p}$. Then, we have the following formal definition of an ESS [Smi82].

Definition 1 *A strategy p^* is an ESS if and only if, for all $p \neq p^*$,*

1. $\pi(p, p^*) \leq \pi(p^*, p^*)$, *(equilibrium condition)*

2. *if* $\pi(p, p^*) = \pi(p^*, p^*)$, $\pi(p, p) < \pi(p^*, p)$ *(stability condition).*

Condition 1) states that p^* is the best response strategy to itself, and is hence a Nash equilibrium (NE). Condition 2) is interpreted as a stability condition. Suppose that the incumbents play p^*, and a collection of mutants play p. Then conditions 1) and 2) ensure that as long as the fraction of mutants playing p is not too large, the average payoff to p will fall short of that to p^*. Since strategies with a higher fitness value are expected to propagate faster in a population through strategic interactions, evolution will cause the population using mutation strategy p to decrease until the entire population uses strategy p^*.

Since data transmission for each secondary user is continuous, the spectrum sensing game is played repeatedly and evolves over time. Moreover, new secondary users may join in the spectrum sensing game from time to time, and the existing secondary users may even be unaware of their appearance and strategies. Hence, a stable strategy which is robust to mutants using different strategies is especially preferred. Therefore, we propose to use evolutionary game theory [Wei95] to analyze the behavior dynamics of the players and further derive the ESS.

4.2.2 Evolution Dynamics of the Sensing Game

When a set of rational players are uncertain of each other's actions and utilities, they will try different strategies in every play and learn from the strategic interactions using the methodology of understanding-by-building. During the process, the percentage (or population share) of players using a certain pure strategy may change. Such a population evolution is characterized by *replicator dynamics* in evolutionary game theory. Specifically, consider a population of homogeneous individuals with identical data rate C_{s_i} and received primary SNR γ_i. The players adopt the same set of pure strategies $\mathcal{A}$. Since all players have the same C_{s_i} and γ_i, payoffs for playing a particular strategy depend only on the other strategies employed, not on who is playing them. Therefore, all players have the same payoff function U. At time t, let $p_{a_i}(t) \geq 0$ be the *number* of individuals who are currently using pure strategy $a_i \in \mathcal{A}$, and let $p(t) = \sum_{a_i \in \mathcal{A}} p_{a_i}(t) > 0$ be the total population. Then the associated *population state* is defined as the vector $x(t) = \{x_{a_1}(t), \cdots, x_{|\mathcal{A}|}(t)\}$,

where $x_{a_i}(t)$ is defined as the population share $x_{a_i}(t) = p_{a_i}(t)/p(t)$. By replicator dynamics, at time t the evolution dynamics of $x_{a_i}(t)$ is given by the following differential equation [Wei95]

$$\dot{x}_{a_i} = \epsilon[\bar{U}(a_i, x_{-a_i}) - \bar{U}(x)]x_{a_i}, \tag{4.17}$$

where $\bar{U}(a_i, x_{-a_i})$ is the average payoff of the individuals using pure strategy a_i, x_{-a_i} is the set of population shares who use pure strategies other than a_i, $\bar{U}(x)$ is the average payoff of the whole population, and ϵ is some positive number representing the time scale. The intuition behind (4.17) is as follows: if strategy a_i results in a higher payoff than the average level, the population share using a_i will grow, and the *growth rate* $\dot{x}_{a_i}/x_{a_i}$ is proportional to the difference between strategy a_i's current payoff and the current average payoff in the entire population. By analogy, we can view $x_{a_i}(t)$ as the probability that one player adopts pure strategy a_i, and $x(t)$ can be equivalently viewed as a mixed strategy for that player.

For the spectrum sensing game with heterogeneous players, whose γ_i and/or C_{s_i} are different from each other, denote the probability that user s_j adopts strategy $h \in \mathcal{A}$ at time t by $x_{h,s_j}(t)$, then the time evolution of $x_{h,s_j}(t)$ is governed by the following dynamics equation [Wei95]

$$\dot{x}_{h,s_j} = \left[\bar{U}_{s_j}(h, x_{-s_j}) - \bar{U}_{s_j}(x)\right] x_{h,s_j}, \tag{4.18}$$

where $\bar{U}_{s_j}(h, x_{-s_j})$ is the average payoff for player s_j using pure strategy h, and $\bar{U}_{s_j}(x)$ is s_j's average payoff using mixed strategy x_{s_j}.

4.2.3 Sensing Game with Homogeneous Players

A strategy is ESS if and only if it is asymptotically stable to the replicator dynamics [Wei95] [Sam98]. Therefore, we can derive the ESS of the proposed spectrum sensing game by proving its asymptotical stability. In this subsection, we study the ESS of games with homogeneous players, and will discuss the heterogeneous case in the next.

As shown in Figure 4.1, players of the sensing game are secondary users within each other's transmission range. If the transmission range is small, we can approximately view that all the received γ_{s_j}'s are very similar to each other. As the γ_{s_j}'s are usually very low, in order to guarantee a low P_F given a target $\bar{P}_D$, the number of sampled signals N should be large. Under these assumptions, we can approximately view $P_F^{\mathcal{S}_c}$ as the same for different $\mathcal{S}_c$'s, denoted by $\hat{P}_F$. Further assume that all users have the same data rate, i.e. $C_{s_i} = C$, for all $s_i \in \mathcal{S}$. Then, the payoff functions defined in (4.10)-(4.12) become

$$U_C(J) = U_0 \left(1 - \frac{\tau}{J}\right), \quad \text{if } J \in [1, K], \tag{4.19}$$

and

$$U_D(J) = \begin{cases} U_0, & \text{if } J \in [1, K-1]; \\ 0, & \text{if } J = 0, \end{cases} \tag{4.20}$$

where $U_0 = P_{H_0}(1 - \hat{P}_F)C$, $J = |\mathcal{S}_c|$, and $\tau = \frac{\delta(N)}{T}$.

As the secondary users are homogeneous players, (4.17) can be applied to the special case as all players have the same evolution dynamics and equilibrium strategy. Denote x as the probability that one secondary user contributes to spectrum sensing,

then the average payoff for pure strategy C can be obtained as

$$\bar{U}_C(x) = \sum_{j=0}^{K-1} \binom{K-1}{j} x^j (1-x)^{K-1-j} U_C(j+1), \tag{4.21}$$

where $\binom{K-1}{j} x^j (1-x)^{K-1-j}$ is the probability that $J+1$ users contributes to cooperative sensing. Similarly, the average payoff for pure strategy D is given by

$$\bar{U}_D(x) = \sum_{j=0}^{K-1} \binom{K-1}{j} x^j (1-x)^{K-1-j} U_D(j). \tag{4.22}$$

Since the average payoff $\bar{U}(x) = x\bar{U}_C + (1-x)\bar{U}_D$, then (4.17) becomes

$$\dot{x} = \epsilon x(1-x)\big[\bar{U}_C(x) - \bar{U}_D(x)\big]. \tag{4.23}$$

In equilibrium x^*, no player will deviate from the optimal strategy, indicating $\dot{x}^* = 0$, and we obtain $x^* = 0$, or 1, or the solution of $\bar{U}_C^*(x) = \bar{U}_D^*(x)$.

Subtracting $\bar{U}_D(x)$ from $\bar{U}_C(x)$ we get

$$\begin{aligned}
&\bar{U}_C(x) - \bar{U}_D(x) \\
=&\sum_{j=0}^{K-1} \binom{K-1}{j} x^j (1-x)^{K-1-j} [U_C(j+1) - U_D(j)] \\
=&\sum_{j=0}^{K-1} \binom{K-1}{j} x^j (1-x)^{K-1-j} [U_0(1 - \frac{\tau}{j+1}) - U_0] + M_t \\
=&-U_0\tau \sum_{j=1}^{K-1} \binom{K-1}{j} x^j (1-x)^{K-1-j} \frac{1}{j+1} + M_t \\
=&-\frac{\tau U_0}{xK} \sum_{j=1}^{K-1} \frac{K!}{(j+1)!(K-j-1)!} x^{j+1} (1-x)^{K-j-1} + M_t \\
=&-\frac{\tau U_0}{xK} \sum_{j=2}^{K} \binom{K}{j} x^j (1-x)^{K-j} + M_t \\
=&\frac{\tau U_0}{xK}[(1-x)^K + Kx(1-x)^{K-1} - 1] + M_t \\
=&\frac{U_0}{K}\left[\frac{\tau(1-x)^K + Kx(1-x)^{K-1} - \tau}{x}\right],
\end{aligned} \tag{4.24}$$

with $M_t = (1-x)^{K-1}U_0(1-\tau)$. By using L'Hôpital's rule, we know that $\lim_{x\to 0}\bar{U}_C(x) - \bar{U}_D(x) = \lim_{x\to 0}\frac{U_0}{K}[-K\tau(1-x)^{K-1} + K(1-x)^{K-1} - Kx(K-1)(1-x)^{K-2}] = U_0(1-\tau) > 0$. Thus, $x = 0$ is not a solution to equation $\bar{U}_C(x) - \bar{U}_D(x) = 0$, and the solution satisfies

$$\tau(1-x^*)^K + Kx^*(1-x^*)^{K-1} - \tau = 0. \tag{4.25}$$

Next we show that the dynamics defined in (4.17) converge to the above-mentioned equilibriums, which are asymptotically stable and hence the ESS. Note that the variable in (4.17) is the probability that a user chooses strategy $a_i \in \{C, D\}$, so we need to guarantee that $x_C(t) + x_D(t) = 1$ in the dynamic process. We show this in the following proposition.

Proposition 1 *The sum of the probability that a secondary user chooses strategy "C" and "D" is equal to one in the replicator dynamics of a symmetric sensing game.*

PROOF. Summing x_{a_i} in (4.17) over a_i yields

$$\dot{x}_C + \dot{x}_D = \epsilon[x_C\bar{U}(C, x_D) + x_D\bar{U}(D, x_C) - (x_C + x_D)\bar{U}(x)]. \tag{4.26}$$

Since $\bar{U}(x) = x_C\bar{U}(C, x_D) + x_D\bar{U}(D, x_C)$, and initially a user chooses $x_C + x_D = 1$, (4.26) is reduced to $\dot{x}_C + \dot{x}_D = 0$. Therefore, $x_C(t) + x_D(t) = 1$ holds at any t during the dynamic process. A similar conclusion also holds in an asymmetric game. ▲

In order to prove that the replicator dynamics converge to the equilibrium, we first show that all non-equilibria strategies of the sensing game will be eliminated

during the dynamic process. It suffices to prove that (4.17) is a *myopic adjustment dynamic* [FL98].

Definition 2 *A system is a* myopic adjustment dynamic *if*

$$\sum_{h\in\mathcal{A}} \bar{U}_{s_j}(h, x_{-s_j})\dot{x}_{h,s_j} \geq 0, \ \forall s_j \in \mathcal{S}. \tag{4.27}$$

Inequality (4.27) indicates that the average utility of a player will not decrease in a myopic adjustment dynamic system. We then prove that the dynamics (4.17) satisfy Definition 2.

Proposition 2 *The replicator dynamics (4.17) are* myopic adjustment dynamics.

Proof. Substituting (4.17) into (4.27), we get

$$\begin{aligned}
&\sum_{a_i\in\mathcal{A}} \dot{x}_{a_i}\bar{U}(a_i, x_{-a_i}) \\
&= \sum_{a_i\in\mathcal{A}} \epsilon\bar{U}(a_i, x_{-a_i})[\bar{U}(a_i, x_{-a_i}) - \bar{U}(x)]x_{a_i} \qquad (4.28)\\
&= \epsilon\sum_{a_i\in\mathcal{A}} x_{a_i}\bar{U}^2(a_i, x_{-a_i}) - \epsilon\Big[\sum_{a_i\in\mathcal{A}} x_{a_i}\bar{U}(a_i, x_{-a_i})\Big]^2.
\end{aligned}$$

According to Jensen's inequality, we know (4.28) is non-negative, which completes the proof. In addition, we can show (4.27) also holds for a game with heterogeneous players in a similar way. ▲

In the following theorem, we show that the replicator dynamics in (4.17) converge to the ESS.

Theorem 1 *Starting from any interior point $x \in (0, 1)$, the replicator dynamics defined in (4.17) converge to the ESS x^*.*

PROOF. From the simplified dynamics (4.23), we know that the sign of $\dot{x}_C(t)$ is determined by the sign of $\bar{U}_C(x) - \bar{U}_D(x)$, given $x \in (0,1)$ and $\epsilon > 0$. $\bar{U}_C(x)$ and $\bar{U}_D(x)$ are simplified as the following

$$\begin{aligned} \bar{U}_C(x) &= U_0 - U_0(1-x)^{K-1}\tau - U_0 \sum_{j=1}^{K-1} \binom{K-1}{j} x^j (1-x)^{K-j-1} \frac{\tau}{j+1}, \\ \bar{U}_D(x) &= U_0 - U_0(1-x)^{K-1}. \end{aligned} \tag{4.29}$$

Furthermore, the difference $\bar{U}_C(x) - \bar{U}_D(x)$ is calculated in Appendix **??** as

$$\bar{U}_C(x) - \bar{U}_D(x) = \frac{U_0}{K}\left[\frac{\tau(1-x)^K + Kx(1-x)^{K-1} - \tau}{x}\right]. \tag{4.30}$$

According to different values of parameter τ, we prove the theorem in three different cases.

Case I ($\tau = 1$): from (4.29) we know $\bar{U}_C(x) < \bar{U}_D(x)$, $\frac{dx}{dt} < 0$, and the replicator dynamics converge to $x^* = 0$.

Case II ($\tau = 0$): from (4.29) we have $\bar{U}_C(x) > \bar{U}_D(x)$, $\frac{dx}{dt} > 0$, and the replicator dynamics converge to $x^* = 1$.

Case III ($0 < \tau < 1$): Define $\Phi(x) = \bar{U}_C(x) - \bar{U}_D(x) = \frac{U_0}{Kx} f(x)$, with $f(x) = \tau(1-x)^K + Kx(1-x)^{K-1} - \tau$. When $x \to 0$, using L'Hôpital's rule, we know from (4.30) that $\lim_{x\to 0} \Phi(x) = (1-\tau)U_0 > 0$. When $x \to 1$, $\lim_{x\to 1} \Phi(x) = -\frac{\tau}{K} < 0$. Since $\Phi(0) > 0$, $\Phi(1) < 0$, and $\Phi(x)$ is a continuous function of x in $(0,1)$, then $\Phi(x)$ must have at least one intersection with the x-axis, i.e., $\exists \tilde{x}$, such that $\Phi(\tilde{x}) = 0$. If there is only one such $\tilde{x}$, then we can infer that $\Phi(x) > 0$ when $x < \tilde{x}$, and $\Phi(x) < 0$ when $x > \tilde{x}$. Since $\Phi(x)$ has the same sign as $f(x)$ when $0 < x < 1$, it suffices to prove that there exists only one solution in $(0,1)$ to equation $f(x) = 0$. Taking

derivative of $f(x)$ with respect to x, we get

$$\frac{df(x)}{dx} = (1-x)^{K-2}\big[-(K-\tau)x + (1-\tau)\big]. \tag{4.31}$$

When $x = \frac{1-\tau}{K-\tau}$, $\frac{df(x)}{dx} = 0$. Observing (4.31) we find that $f(x)$ is increasing when $0 < x < \frac{1-\tau}{K-\tau}$ with $f(0) = 0$, while decreasing when $\frac{1-\tau}{K-\tau} < x < 1$ with $f(1) = -\tau < 0$. This means equation $f(x) = 0$ has only one root x^* in $(0, 1)$, which is the equilibrium solved in (4.25). When $0 < x < x^*$, $f(x) > 0$; and when $x^* < x < 1$, $f(x) < 0$. Since $\Phi(x)$ has the same sign as $f(x)$, we can conclude that for $0 < x < x^*$, $\Phi(x) > 0$, i.e., $\frac{dx}{dt} > 0$; for $x^* < x < 1$, $\Phi(x) < 0$, i.e., $\frac{dx}{dt} < 0$. Thus, the replicator dynamics converge to the equilibrium x^*.

Therefore, we have proved the convergence of replicator dynamics to the ESS x^*. ▲

4.2.4 Sensing Game with Heterogeneous Players

For games with heterogeneous players, it is generally very difficult to represent $\bar{U}_{s_j}(h, x_{-s_j})$ in a compact form, and directly obtain the ESS in closed-form by solving (4.18). Therefore, we first analyze a two-user game to gain some insight, then generalize the observation to a multi-user game.

When there are two secondary users in the cognitive radio network, i.e., $\mathcal{S} = \{s_1, s_2\}$, according to equations (4.10)-(4.12) we can write the payoff matrix as in Table 4.1, where for simplicity we define $A \triangleq 1 - P_F^{\mathcal{S}_c}$, with $\mathcal{S}_c = \{s_1, s_2\}$, $B_i \triangleq 1 - P_{F,s_i}$, $D_i \triangleq P_{H_0} C_i$, and $\tau = \frac{\delta(N)}{T}$.

Let us denote x_1 and x_2 as the probability that user 1 and user 2 take action

Table 4.1: Payoff table of a two-user sensing game

	C	D
C	$D_1A(1-\frac{\tau}{2})$,$D_2A(1-\frac{\tau}{2})$	$D_1B_1(1-\tau)$,D_2B_1
D	D_1B_2,$D_2B_2(1-\tau)$	0,0

"C", respectively, then we have the expected payoff $\bar{U}_{s_1}(C, x_2)$ when user 1 chooses to contribute to sensing as

$$\bar{U}_{s_1}(C, x_2) = D_1A(1-\frac{\tau}{2})x_2 + D_1B_1(1-\tau)(1-x_2), \tag{4.32}$$

and the expected payoff $\bar{U}_{s_1}(x)$ as

$$\bar{U}_{s_1}(x) = D_1A(1-\frac{\tau}{2})x_1x_2 + D_1B_1(1-\tau)x_1(1-x_2) + D_1B_2(1-x_1)x_2. \tag{4.33}$$

Thus we get the replicator dynamics equation of user 1 according to (4.18) as

$$\dot{x}_1 = x_1(1-x_1)D_1\Big[B_1(1-\tau) - E_1x_2\Big], \tag{4.34}$$

where $E_1 = B_2 + B_1(1-\tau) - A(1-\frac{\tau}{2})$. Similarly the replicator dynamics equation of user 2 is written as

$$\dot{x}_2 = x_2(1-x_2)D_2\Big[B_2(1-\tau) - E_2x_1\Big], \tag{4.35}$$

where $E_2 = B_1 + B_2(1-\tau) - A(1-\frac{\tau}{2})$.

At equilibrium we know $\dot{x}_1 = 0$ and $\dot{x}_2 = 0$, then from (4.34) and (4.35) we get five equilibria: $(0,0)$, $(0,1)$, $(1,0)$, $(1,1)$, and the mixed strategy equilibrium $\Big(\frac{B_2(1-\tau)}{E_2}, \frac{B_1(1-\tau)}{E_1}\Big)$.

According to [Cre03], if an equilibrium of the replicator dynamics equations is a locally asymptotically stable point in a dynamic system, it is an ESS. So we can view (4.34) and (4.35) as a nonlinear dynamic system and judge whether the five equilibria are ESSs by analyzing the Jacobian matrix. By taking partial derivatives of (4.34) and (4.35), we obtain the Jacobian matrix as

$$J_m = \begin{bmatrix} D_1(1-2x_1)E_{11} & -x_1(1-x_1)D_1E_1 \\ -x_2(1-x_2)D_2E_2 & (1-2x_2)D_2E_{22} \end{bmatrix}, \tag{4.36}$$

where $E_{11} = B_1(1-\tau) - E_1x_2$, and $E_{22} = B_2(1-\tau) - E_2x_1$.

The asymptotical stability requires that $\det(J_m) > 0$ and $\mathrm{tr}(J_m) < 0$. Substituting the five equilibria mentioned above to (4.36), we can conclude that

1. When $A(1-\frac{\tau}{2}) < B_1$, there is one ESS $(1,0)$, and the strategy profile user 1 and user 2 adopt converges to (C,D);

2. When $A(1-\frac{\tau}{2}) < B_2$, there is one ESS $(0,1)$, and the strategy profile converges to (D,C);

3. When $A(1-\frac{\tau}{2}) > B_2$ and $A(1-\frac{\tau}{2}) > B_1$, there is one ESS $(1,1)$, and the strategy profiles converges to (C,C);

4. When $A(1-\frac{\tau}{2}) < B_1$ and $A(1-\frac{\tau}{2}) < B_2$, there are two ESSs $(1,0)$ and $(0,1)$, and the strategy profile converges to (C,D) or (D,C) depending on different initial strategy profiles.

In order to explain the above-mentioned conclusions and generalize them to a multi-player game, we next analyze the properties of the mixed strategy equilibrium,

although it is not an ESS. Let us take the derivative of $x_1^* = \frac{B_2(1-\tau)}{E_2}$ with respect to the performance of a detector (A, B_2) and the sensing cost τ, then we get

$$\frac{\partial x_1^*}{\partial A} = \frac{B_2(1-\tau/2)(1-\tau)}{E_2^2} > 0, \tag{4.37}$$

$$\frac{\partial x_1^*}{\partial B_2} = \frac{[A(1-\tau/2) - B_1](1-\tau)}{E_2^2} < 0, \tag{4.38}$$

and

$$\frac{\partial x_1^*}{\partial \tau} = \frac{(A/2 - B_1)B_2}{E_2^2} < 0. \tag{4.39}$$

Inequality (4.38) holds because $A(1-\tau/2) - B_1 < 0$; otherwise $x_1^* = \frac{B_2(1-\tau)}{E_2} > 1$, which is impractical. Inequality (4.39) holds because in practical applications, we have $P_{F,s_i} < 0.5$, $B_i = 1 - P_{F,s_i} > 0.5$, and $A < 1$; therefore, $\frac{A}{2} < B_i$, and $\frac{\partial x_1^*}{\partial \tau} < 0$.

From (4.37) we know that when cooperative sensing brings a greater gain, i.e., as A increases, x_1^* (and x_2^*) increases. This is why when $A(1-\frac{\tau}{2}) > B_i$, $i = 1, 2$, the strategy profile converges to (C,C). From (4.38) we find that the incentive of a secondary user s_i contributing to cooperative sensing decreases as the other user s_j's detection performance increases. This is because when user s_i learns through repeated interactions that s_j has a better B_j, s_i tends not to sense the spectrum and enjoys a free-ride. Then s_j has to sense the spectrum; otherwise, he is at the risk of having no one sense and receiving a very low expected payoff. That is why when $A(1-\frac{\tau}{2}) < B_1$ (or $A(1-\frac{\tau}{2}) < B_2$), the strategy profile converges to (C,D) (or (D,C)). When the sensing cost (τ) becomes larger, the secondary users will be more reluctant to contribute to cooperative sensing and x_1^* decreases, as shown in (4.39).

From the above-mentioned observation, we can infer that if some user s_i has a better detection performance B_i, the other users tend to take advantage of s_i. If

there are more than two users in the sensing game, the strategy of the users with worse B_i's (and γ_i's) will converge to "D". Using replicator dynamics, users with better detection performance tend to contribute to spectrum sensing, because they are aware of the low throughput if no one senses the spectrum. Similarly, if the secondary users have different data rates, the user with a lower rate C_{s_j} tends to take advantage of those with higher rates, since the latter suffer relatively heavier losses if no one contributes to sensing and they have to become more active in sensing.

The work in [PL07] discussed how to select a proper subset of secondary users in cooperative sensing so as to optimize detection performance. However, their approach assumes that the information about the received SNR's (γ_i's) is available at the secondary base station. In our evolutionary game framework, the secondary users can learn the ESS by using replicator dynamics only with their own payoff history. Therefore, it is suitable for distributed implementation when there exists no secondary base station and the secondary users behave selfishly. In the next section we propose a distributed learning algorithm and further justify the convergence with computer simulations.

4.2.5 Learning Algorithm for ESS

In the above cooperative sensing games with multiple players, we have shown that the ESS is solvable. However, solving the equilibrium requires the knowledge of utility function as well as exchange of private information (e.g., γ_{s_j} and C_{s_j})

and strategies adopted by the other users. This results in a lot of communication overhead. Therefore, a distributed learning algorithm that gradually converges to the ESS without too much information exchange is preferred.

From (4.18), we can derive the strategy adjustment for the secondary user as follows. Denote the pure strategy taken by user s_j at time t by $A_{s_j}(t)$. Define an indicator function $\mathbf{1}_{s_j}^h(t)$ as

$$\mathbf{1}_{s_j}^h(t) = \begin{cases} 1, & \text{if } A_{s_j}(t) = h; \\ 0, & \text{if } A_{s_j}(t) \neq h. \end{cases} \tag{4.40}$$

At some interval mT, we can approximate $\bar{U}_{s_j}(h, x_{-s_j})$ by

$$\bar{U}_{s_j}(h, x_{-s_j}) \doteq \frac{\sum_{0 \leq t \leq mT} \tilde{U}_{s_j}(A_{s_j}(t), A_{-s_j}(t)) \mathbf{1}_{s_j}^h(t)}{\sum_{0 \leq t \leq mT} \mathbf{1}_{s_j}^h(t)}, \tag{4.41}$$

where $\tilde{U}_{s_j}(A_{s_j}(t), A_{-s_j}(t))$ is the payoff value for s_j as determined by (4.10)-(4.12). Similarly, $\bar{U}_{s_j}(x)$ can be approximated by

$$\bar{U}_{s_j}(x) \doteq \frac{1}{m} \sum_{0 \leq t \leq mT} \tilde{U}_{s_j}(A_{s_j}(t), A_{-s_j}(t)). \tag{4.42}$$

Then, the derivative $\dot{x}_{h,s_j}(mT)$ can be approximated by substituting the estimations (4.41) and (4.42) into (4.18). Therefore, the probability of user s_j taking action h can be adjusted by

$$x_{h,s_j}((m+1)T) = x_{h,s_j}(mT) + \eta_{s_j} \dot{x}_{h,s_j}(mT), \tag{4.43}$$

with η_{s_j} being the step size of adjustment chosen by s_j.

Eq. (4.43) can be viewed as a discrete-time replicator dynamic system. It has been shown in [HS74] that if a steady state is hyperbolic and asymptotically

stable under the continuous-time dynamics, then it is asymptotically stable for sufficiently small time periods in corresponding discrete-time dynamics. Since the ESS is the asymptotically stable point in the continuous-time replicator dynamics and also hyperbolic [FL98], if a player knows precise information about $\dot{x}_{h,s_j}$, adapting strategies according to (4.43) can converge to an ESS. With the learning algorithm, users will try different strategies in every time slot, accumulate information about the average payoff values based on (4.41) and (4.42), calculate the probability change of some strategy using (4.18), and adapt their actions to an equilibrium.

By summarizing the above learning algorithm and analysis in this section, we can arrive at the following cooperation strategy in the de-centralized cooperative spectrum sensing:

Cooperation Strategy in Cooperative Spectrum Sensing:

Denote the probability of contributing to sensing for user $s_i \in \mathcal{S}$ by x_{c,s_i}, then the following strategy will be used by s_i:

- if starting with a high x_{c,s_i}, s_i will rely more on the others and reduce x_{c,s_i} until further reduction of x_{c,s_i} decreases his throughput or x_{c,s_i} approaches 0.
- if starting with a low x_{c,s_i}, s_i will gradually increase x_{c,s_i} until further increase of x_{c,s_i} decreases his throughput or x_{c,s_i} approaches 1.
- s_i shall reduce x_{c,s_i} by taking advantage of those users with better detection performance or higher data rates.
- s_i shall increase x_{c,s_i} if cooperation with more users can bring a better detection performance than the case of single-user sensing without cooperation.

4.3 Simulation Studies

The parameters used in the simulation are as follows. We assume that the primary signal is a baseband QPSK modulated signal, the sampling frequency is $f_s = 1$MHz, and the frame duration is $T = 20$ ms. The probability that the primary user is inactive is set as $P_{H_0} = 0.9$, and the required target detection probability $\bar{P}_D$ is 0.95. The noise is assumed to be a zero-mean CSCG process. The distance between the cognitive radio network and the primary base station is very large, so the received γ_{s_j}'s are in the low SNR regime, with an average value of -12 dB.

4.3.1 Sensing Game with Homogeneous Players

We first illustrate the ESS of the secondary users in a homogeneous K-user sensing game as in Section 4.2.3, where the data rate is $C = 1$ Mbps. In Figure 4.3(a), we show the equilibrium probability of being a contributor x^*. The x-axis represents $\tau = \frac{\delta(N)}{T}$, the ratio of sensing time duration over the frame duration. From Figure 4.3(a), we can see that x^* decreases as τ increases. For the same τ, x^* decreases as the number of secondary users increases. This indicates that the incentive of contributing to cooperative sensing drops as the cost of sensing increases and more users exist in the network. This is because the players tend to wait for someone else to sense the spectrum and can then enjoy a free ride, when they are faced with a high sensing cost and more counterpart players. In Figure 4.3(b), we show the average throughput per user when all users adopt the equilibrium strategy. We see that there is a tradeoff between the cost of sensing and the throughput for an

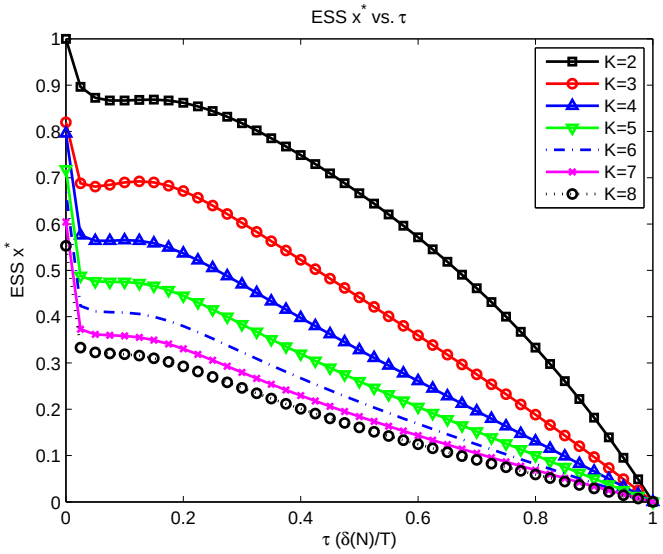

(a) Probability of being a contributor

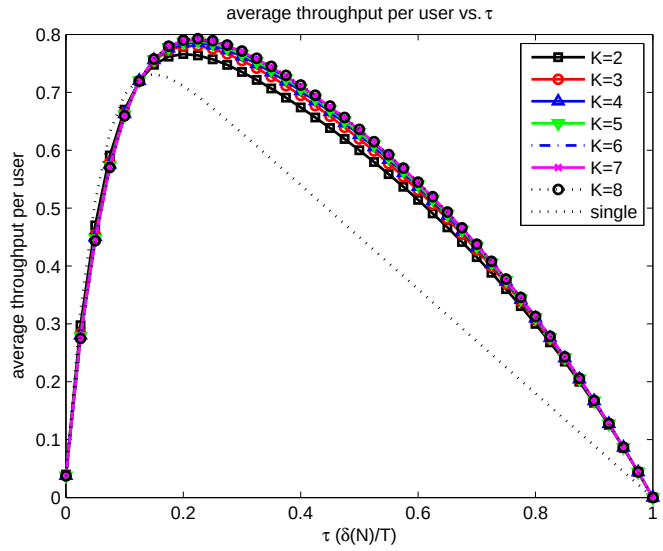

(b) Average throughput per user

Figure 4.3: ESS and average throughput vs. τ.

arbitrary number of users, and the optimal value of τ is around 0.25. For comparison, we also plot the throughput for a single-user sensing (dotted line "single"), where the optimal value of τ is around 0.15. Although the cost of sensing increases, we see that as more users share the sensing cost, the average throughput per user still increases, and the average throughput values for the cooperative sensing game are higher than that of the single-user sensing case.

4.3.2 Convergence of the Dynamics

In Figure 4.4, we show the replicator dynamics of the game with homogeneous users, where $\tau = 0.5$. We observe in Figure 4.4(a) that starting from a high initial probability of cooperation, all users gradually reduce their degree of cooperation, because being a free-rider more often saves more time for one's own data transmission and brings a higher throughput. However, too low a degree of cooperation greatly increases the chance of having no user contribute to sensing, so the users become more cooperative starting from a low initial probability of cooperation as shown in Figure 4.4(b). It takes less than 20 iterations to attain the equilibrium by choosing a proper step size $\eta_{s_i} = 3$.

In Figure 4.5, we show the replicator dynamics for the game with three heterogeneous players, using the learning algorithm discussed in Section 4.2.5. We choose $\tau = 0.5$, $\gamma_1 = -14$ dB, $\gamma_2 = -10$ dB, and $\gamma_3 = -10$ dB. As expected, starting from a low initial probability of cooperation, the users tend to increase the degree of cooperation. During the iterations, the users with a worse γ_i (user 1) learn

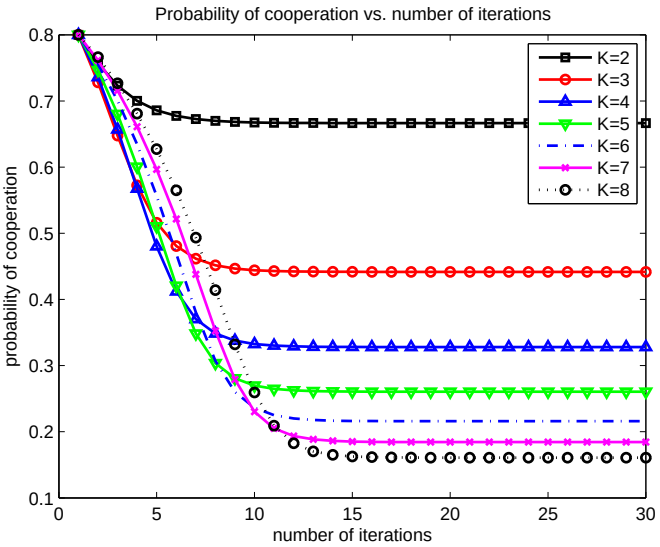

(a) initial $x = 0.8$

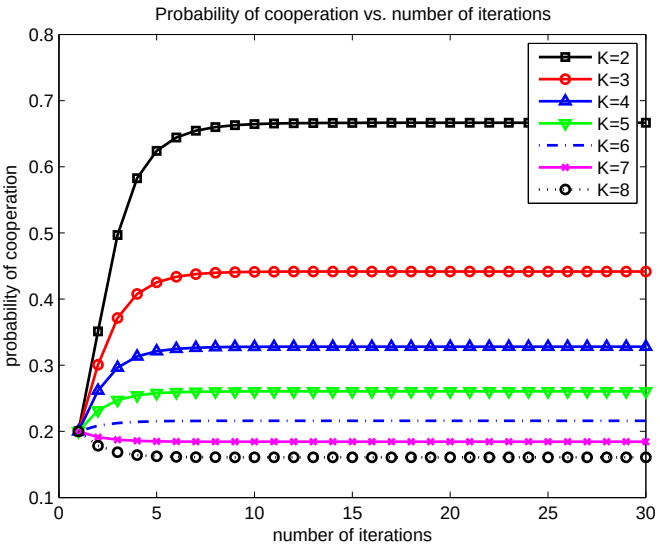

(b) initial $x = 0.2$

Figure 4.4: Behavior dynamics of a homogeneous K-user sensing game

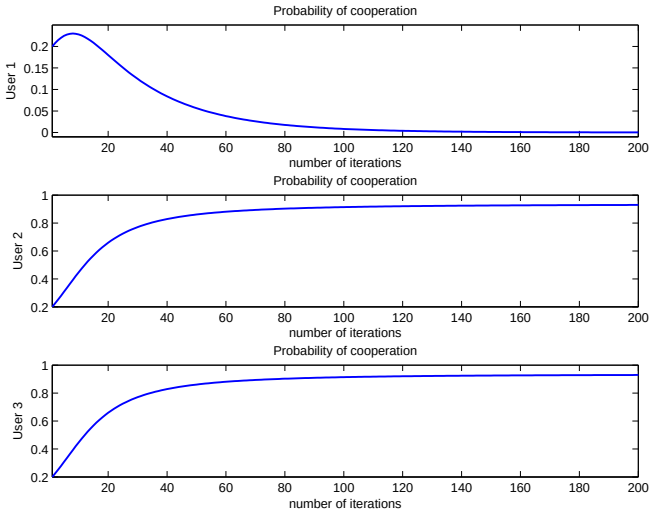

Figure 4.5: Behavior dynamics of a heterogeneous 3-user sensing game

that listening to the detection results from the users with a better γ_i can bring a higher throughput. Hence, user 1's strategy converges to "D" in the long run, while the users with better detection performance (user 2 and user 3) have to sense the spectrum to guarantee their own throughput.

4.3.3 Comparison of ESS and Full Cooperation

In Figure 4.6, we compare the total throughput of a 3-user sensing game using their ESS and the total throughput when the users always participate in cooperative sensing and share the sensing cost, i.e., $x_{s_i} = 1$. In the first four groups of comparison we assume a homogeneous setting, where γ_i of each user takes value from $\{-13, -14, -15, -16\}$ dB, respectively. In the last four groups, a heterogeneous setting is assumed, where γ_1 equals to $\{-12, -13, -14, -15\}$ dB, respectively, and γ_2 and γ_3 are kept the same as in the homogeneous setting. We find in the figure that

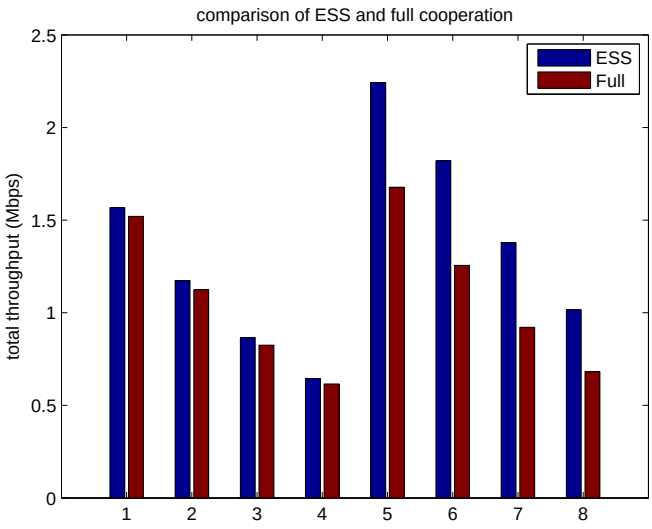

Figure 4.6: Comparison of ESS and full cooperation

using ESS has better performance than all secondary users cooperating in sensing at every time slot. This is because under ESS, the users can take turns to jointly complete the common task, and on average contribute less time to sensing and enjoy a higher throughput. This indicates that in order to guarantee a certain detection performance, it is not necessary to force all users to contribute in every time slot, and ESS can achieve a satisfying system performance even when there exist selfish users.

4.4 Summary

Cooperative spectrum sensing with multiple secondary users has been shown to achieve a better detection performance than single-user sensing without cooperation. However, how to collaborate in cooperative spectrum sensing over decentralized cognitive radio networks is still an open problem, as selfish users are

not willing to contribute their energy/time to sensing. In this chapter, we propose an evolutionary game-theoretic framework to develop the best cooperation strategy for cooperative sensing with selfish users. Using replicator dynamics, users can try different strategies and learn a better strategy through strategic interactions. We study the behavior dynamics of secondary users, derive and analyze the property of the ESSs, and further propose a distributed learning algorithm that aids the secondary users approach the ESSs only with their own payoff history. From simulation results we find that the proposed game has a better performance than having all secondary users sense at every time slot, in terms of total throughput. Moreover, the average throughput per user in the sensing game is higher than in the single-user sensing case without user cooperation.

Chapter 5

Stackelberg Game for Distributed Resource Allocation in Cooperative Networks

Recently, cooperative communications [LTW04] have gained much attention as an emerging transmit strategy for future wireless networks. The basic idea is that relay nodes can act as a virtual antenna array to help the source node forward its information to the destination. In this way, cooperative communication efficiently takes advantage of the broadcasting nature of wireless networks. Besides, it exploits the inherent spatial and multiuser diversities.

In order to improve the performance of cooperative transmissions, it is very important to design efficient resource allocation, such as relay selection, power control, and reply deployment. However, most existing works described in Chapter 2

solve resource allocation problems in cooperative communications by means of a centralized fashion. Such schemes require that complete and precise channel state information (CSI) should be available in order to optimize the system performance, which are generally neither scalable nor robust to channel estimation errors. This fact motivates the research on distributed resource allocation without requiring CSI. For distributed resource allocation, there are two main questions over multiuser cooperative wireless networks: First, among all the distributed nodes, who can help relay and improve the source node's link quality better; Second, for the selected relay nodes, how much power they need to transmit. Moreover, in multiuser cooperative wireless networks with selfish nodes, different nodes may belong to a different authorities. Therefore, a mechanism of reimbursement to relay nodes is needed such that relay nodes can earn benefits from spending their own transmission power in helping the source node forward its information. On the other hand, if the source node reimburses relay nodes for their help, it needs to choose the most beneficial relay nodes.

According to such characteristics, in this chapter, we employ a Stackelberg game [FT93] to jointly consider the benefits of the source node and relay nodes in cooperative communications. The game is divided into two levels. The source node plays the *buyer-level* game, since it aims to achieve the best performance with the relay nodes' help with the least reimbursements to them. We analyze how many and which relay nodes are selected by the source node to participate in relaying after they announce their optimal prices. In addition, we optimize how much service (such as power) the source node will buy from each relay node. On the other hand, each

relay node plays the *seller-level* game, in which it aims to earn the payment that not only covers its forwarding cost but also gains as many extra profits as possible. Therefore, the relay node needs to set the optimal price per unit for the service, so as to maximize its own benefit. To study the game outcomes, we analyze several properties of the proposed game. Then, we develop a distributed algorithm that can converge to the optimal game equilibrium.

The remainder of the chapter is organized as follows: In Section 5.1, we describe the system model, and formulate the cooperative optimization as a Stackelberg game. We construct the distributed implementation of multiuser cooperation transmissions and provide the solutions in Section 5.2. Simulation results are shown in Section 5.3. Finally, we present the summary in Section 5.4.

5.1 System Description

In this section, we first derive the expression of the maximal achievable rate in cooperative transmission with relay nodes' help. Then, we formulate the optimization problem of relay selection and power control using a Stackelberg game.

5.1.1 System Model

In the sequel, we employ the amplify-and-forward (AF) cooperation protocol [LTW04] as our system model; other cooperation protocols [LTW04] can be considered in a similar way. The system diagrams are shown in Figure 5.1, in which there are in total N relay nodes, one source node s and one destination node d. The

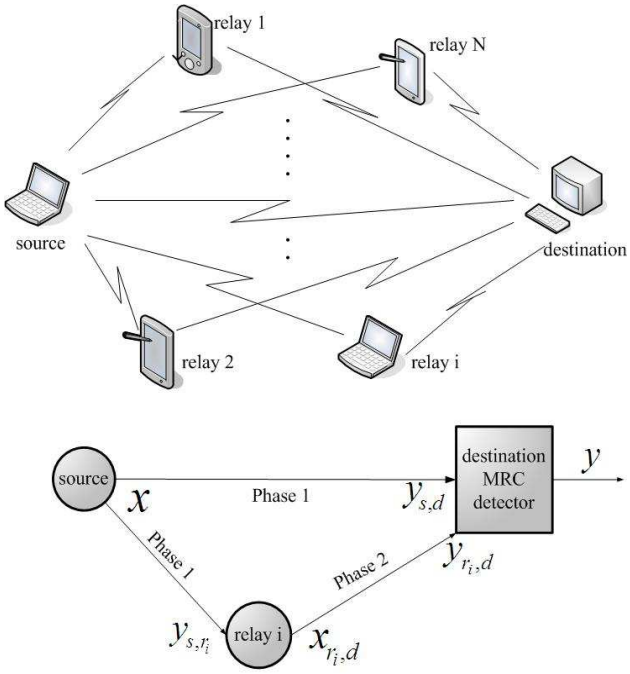

Figure 5.1: System diagrams.

cooperative transmission consists of two phases.

In Phase 1, source node s broadcasts its information to both destination node d and each relay node r_i. The received signals $y_{s,d}$ and y_{s,r_i} at node d and node r_i can be expressed as

$$y_{s,d} = \sqrt{P_s G_{s,d}} x + \eta_{s,d}, \tag{5.1}$$

and

$$y_{s,r_i} = \sqrt{P_s G_{s,r_i}} x + \eta_{s,r_i}, \tag{5.2}$$

where P_s represents the transmit power at node s, x is the broadcast information symbol with unit energy from node s to node d and node r_i, $G_{s,d}$ and G_{s,r_i} are the channel gains from node s to node d and node r_i respectively, and $\eta_{s,d}$ and η_{s,r_i} are the additive white Gaussian noises (AWGN). Without loss of generality, we assume that the noise power is the same for all the links, denoted by σ^2. We also assume the channels are stable over each transmission frame.

Without the relay nodes' help, the signal-to-noise ratio (SNR) that results from the direct transmission from node s to node d can be expressed by

$$\Gamma_{s,d} = \frac{P_s G_{s,d}}{\sigma^2}, \tag{5.3}$$

and the rate of the direct transmission is

$$R_{s,d} = W \log_2 \left(1 + \frac{\Gamma_{s,d}}{\Gamma} \right), \tag{5.4}$$

where W is the bandwidth for transmission, and Γ is a constant representing the capacity gap.

In Phase 2, relay node r_i amplifies y_{s,r_i} and forwards it to destination d with transmitted power P_{r_i}. The received signal at destination node d is

$$y_{r_i,d} = \sqrt{P_{r_i} G_{r_i,d}} x_{r_i,d} + \eta_{r_i,d}, \tag{5.5}$$

where

$$x_{r_i,d} = \frac{y_{s,r_i}}{|y_{s,r_i}|} \tag{5.6}$$

is the transmitted signal from node r_i to node d that is normalized to have unit energy, $G_{r_i,d}$ is the channel gain from node r_i to node d, and $\eta_{r_i,d}$ is the received noise. Substituting (5.2) into (5.6), we can rewrite (5.5) as

$$Y_{r_i,d} = \frac{\sqrt{P_{r_i} G_{r_i,d}}(\sqrt{P_s G_{s,r_i}} X + \eta_{s,r_i})}{\sqrt{P_s G_{s,r_i} + \sigma^2}} + \eta_{r_i,d}. \tag{5.7}$$

Using (5.7), the relayed SNR for source node s, which is helped by relay node r_i, is given by:

$$\Gamma_{s,r_i,d} = \frac{P_{r_i} P_s G_{r_i,d} G_{s,r_i}}{\sigma^2 (P_{r_i} G_{r_i,d} + P_s G_{s,r_i} + \sigma^2)}. \tag{5.8}$$

Therefore, by (5.4) and (5.8), we have the rate at the output of the maximal-ratio combining (MRC) detector with one relay node r_i helping as

$$R_{s,r_i,d} = \frac{W}{2} \log_2 \left(1 + \frac{\Gamma_{s,d} + \Gamma_{s,r_i,d}}{\Gamma} \right). \tag{5.9}$$

If the relay nodes available to help source node s at a certain time constitute a set, denoted by $L = \{r_1, \ldots, r_N\}$, then we have

$$R_{s,r,d} = \gamma_L W \log_2 \left(1 + \frac{\Gamma_{s,d} + \sum\limits_{r_i \in L} \Gamma_{s,r_i,d}}{\Gamma} \right), \tag{5.10}$$

where γ_L denotes a bandwidth factor.

According to different network applications, γ_L can have different definitions. For the energy-constrained networks, γ_L is set to 1. For the network with a limited bandwidth, the bandwidth should be divided for the source node and relay nodes, and γ_L depends on the number of relay nodes that actually help forwarding, since not all the relay nodes will contribute to a better performance for the source node. If N' out of N relay nodes are selected by the source node, $N' \leq N$, then $\gamma_L = \frac{1}{N'+1}$.[1]We will study the energy constrained scenario first, then we show the effects of the varying γ_L in the simulation part.

5.1.2 Problem Formulation

To exploit the cooperative diversity for multiuser systems, from (5.10), two fundamental questions on resource allocation need to be answered: First, which relay nodes will be included; Second, what is the optimal power P_{r_i}. However, solving these issues in a centralized manner requires accurate and complete channel-state information (CSI), bringing considerable overheads and signaling of information about channel estimations. In contrast, the distributed resource allocation only needs local knowledge about channel information. Moreover, in general, nodes in multiuser cooperative wireless networks may belong to different authorities and act selfishly. Incentives need to be provided by the source node to the relay nodes for relaying the information. Consequently, the source node needs to choose the most beneficial relay nodes. According to the behaviors of the source node and the relay

[1]The source node can know the number of available relay nodes by broadcasting its signal and listening to the relay nodes' feedback on whether to help forward the source node's information.

nodes, we employ a distributed resource allocation using a Stackelberg-game based scheme as the following formulated problem.

(1) Source Node/Buyer: The source node s can be modeled as a buyer and aims to obtain most benefits at least possible payments. The utility function of source node s can be defined as

$$U_s = aR_{s,r,d} - M, \tag{5.11}$$

where $R_{s,r,d}$ denotes the achievable rate with the relay nodes' help, a denotes the gain per unit of rate at the MRC output, and

$$M = \sum_{r_i \in L} p_i P_{r_i} = p_1 P_{r_1} + p_2 P_{r_2} + \cdots + p_N P_{r_N} \tag{5.12}$$

represents the total payments paid by source node s to the relay nodes. In (5.12), p_i represents the price per unit of power selling from relay node r_i to source node s, and P_{r_i} denotes how much power node s will buy from node r_i.

The relay nodes helping source node s constitute a set, still denoted by L, then the optimization problem for source node s, or the *buyer-level* game can be formulated as:

$$\max_{\{P_{r_i}\}} U_s = aR_{s,r,d} - M, \text{ s.t. } P_{r_i} \geq 0, r_i \in L. \tag{5.13}$$

(2) Relay Node/Seller: Each relay node r_i can be seen as a seller and aims to not only earn the payment which covers its forwarding cost but also gain as many extra profits as possible. We introduce a parameter c_i, the cost of power for relaying data, in our formulation. Then, relay node r_i's utility function can be defined as

$$U_{r_i} = p_i P_{r_i} - c_i P_{r_i} = (p_i - c_i) P_{r_i}, \tag{5.14}$$

where P_{r_i} is the source node's power consumption by optimizing U_s described in (5.13). The optimization problem for relay node r_i, or the *seller-level* game is:

$$\max_{p_i>0} \; U_{r_i} = (p_i - c_i)P_{r_i}, \quad \forall i. \tag{5.15}$$

The choice of the optimal price p_i is not only affected by each relay node's own channel conditions to the source node and the destination node, but also by the other relay nodes' prices. This is because the seller-level game is non-cooperative, and the relay nodes compete to get selected by source node s. If a certain relay node r_j asks such a high price that makes it less beneficial than the other relay nodes to source node s, then source node s will buy less from relay node r_j or even discard it. On the other hand, if the price is too low, the profit obtained by (5.14) will be unnecessarily low. Overall, there is a tradeoff for setting the price. If under the optimal price, denoted by p_i^*, the resulting utility of relay node r_i is negative, i.e., $U_{r_i}^* \leq 0$, then node r_i will quit the *seller-level* game since it can not cover the basic cost by selling power to the source node.

It is worth noticing that the only signaling required to exchange between the source node and the relay nodes are the price p_i and the information about how much power P_{r_i} to buy. Consequently, the proposed two-level game-theoretic approach can be implemented in a distributed way. The outcome of the proposed games will be shown in detail in the following section.

5.2 Analysis of the Proposed Games

In this section, we first obtain closed-form solutions to the outcomes of the proposed games. Then, we prove that these solutions are the global optima, and further show that the set of solutions is a unique fixed point and the proposed game converges to that point. Finally, we compare the performance of the proposed distributed scheme to that of a centralized scheme.

5.2.1 Buyer-Level Game for the Source Node

Relay Selection

As relay nodes are located in different places and ask different prices for helping the source node, it may not be good for source node s to choose all relay nodes, especially those with bad channel conditions but asking a high price. Moreover, if the source node will exclude the less beneficial relay nodes sooner or later during the buyer-level game, it is better to reject them at the beginning so as to reduce the signaling overhead. Because source node s aims at maximizing utility U_s through buying an optimal amount of power P_{r_i}, then a natural way of relay selection for source node s is to observe how U_s varies with P_{r_i}, i.e., observe the sign of $\frac{\partial U_s}{\partial P_{r_i}}$. Since source node s gradually increases the amount of power bought from the relay nodes to approach the optimum, by observing the sign of $\frac{\partial U_s}{\partial P_{r_i}}$ when $P_{r_i} = 0$, node s can exclude (or select) those less (or more) beneficial relay nodes.

From the definition in (5.11), we know

$$\frac{\partial U_s}{\partial P_{r_i}} = a\frac{\partial R_{s,r,d}}{\partial P_{r_i}} - p_i, \quad i = 1, \cdots, N. \tag{5.16}$$

When $P_{r_j} = 0,\ j = 1, \cdots, N$, if p_i satisfies $p_i < a\,\frac{\partial R_{s,r,d}}{\partial P_{r_i}}$ for relay node r_i, then we have $\frac{\partial U_s}{\partial P_{r_i}} > 0$, meaning the source node will obtain a larger U_s by increasing P_{r_i}. Otherwise, relay node r_i should be excluded.

Then a question is how each relay node r_i asks its price p_i at the beginning. Since in a distributed implementation, each relay node does not know the other relay nodes' prices, it is natural to first tentatively set $p_i = c_i$. If the initial price p_i is lower than c_i, utility U_{r_i} will be negative and hence impractical; on the other hand, if the initial price is greater than c_i, relay node r_i may be at the risk of being excluded by the source node. If under these lowest initial prices, the source node would choose not to buy any power from some relay node r_i, then r_i will not participate in the *seller-level* game because $U_{r_i} = 0$.

To summarize the analysis above, the *relay rejection criteria* of the source node are as follows. Assume the total number of the relay nodes is N. At first the source node tentatively chooses $P_{r_i} = 0$, $i = 1, \cdots, N$, and all the relay nodes set their initial prices as $p_i = c_i, \forall i$. For relay node r_j, if $c_j \geq (a\,\frac{\partial R_{s,r,d}}{\partial P_{r_j}})$, then r_j is rejected by the source node with correspondingly $P_{r_j} = 0$. It will be shown later that this rejection is fixed and will not change after the game is played.

With the proposed *relay rejection criteria*, source node s can exclude the least beneficial relay nodes at the very beginning. In this way, the signaling overhead can be further reduced, because the source node and the rejected relay nodes no longer need to exchange their information about the purchased power and prices.

Optimal Power Allocation for the Selected Relay Nodes

After the selection, for the selected relay nodes that constitute a set $L_h =$

$\{r_1, \cdots, r_{N'}\}$, we can solve the optimal power P_{r_i} by taking derivative of U_s in (5.11) with respect to P_{r_i} as

$$\frac{\partial U_s}{\partial P_{r_i}} = a\frac{\partial R_{s,r,d}}{\partial P_{r_i}} - p_i = 0, \quad r_i \in L_h. \tag{5.17}$$

For simplicity, define $C = 1 + \frac{\Gamma_{s,d}}{\Gamma}$, $W' = \frac{aW}{\ln 2}$. By (5.10), we get the first term of U_s as

$$aR_{s,r,d} = aW \log_2 \left(C + \frac{1}{\Gamma} \sum_{r_i \in L_h} \Gamma_{s,r_i,d} \right) = W' \ln \left(1 + \Delta SNR'_{tot} \right) + W' \ln C, \tag{5.18}$$

where

$$\Delta SNR'_{tot} = \sum_{r_i \in L_h} \Gamma'_{s,r_i,d} = \frac{1}{\Gamma C} \sum_{r_i \in L_h} \Gamma_{s,r_i,d}, \tag{5.19}$$

and

$$\Gamma'_{s,r_i,d} = \frac{\Gamma_{s,r_i,d}}{\Gamma C} = \frac{A_i}{1 + \frac{B_i}{P_{r_i}}} = \frac{A_i P_{r_i}}{P_{r_i} + B_i}, \tag{5.20}$$

with $A_i = \frac{P_s G_{s,r_i}}{\left(\Gamma \sigma^2 + P_s G_{s,d}\right)}$ and $B_i = \frac{P_s G_{s,r_i} + \sigma^2}{G_{r_i,d}}$.

Substituting (5.12) and (5.18) into (5.17), we have

$$\frac{W'}{\left(1 + \sum_{r_k \in L_h} \frac{A_k P_{r_k}}{P_{r_k} + B_k} \right)} = \frac{p_i}{A_i B_i} \left(P_{r_i} + B_i \right)^2. \tag{5.21}$$

Since the left-hand side (LHS) of (5.21) is the same for any relay node on the right-hand side (RHS), by equating the RHS of (5.21) for relay nodes r_i and r_j, we get

$$P_{r_j} = \sqrt{\frac{p_i A_j B_j}{p_j A_i B_i}} \left(P_{r_i} + B_i \right) - B_j. \tag{5.22}$$

Substituting the above P_{r_j} into (5.20) and simplifying, we have

$$\Gamma'_{s,r_j,d} = \frac{A_j}{1 + \frac{B_j}{P_{r_j}}} = A_j - \sqrt{\frac{p_j A_i B_i}{p_i A_j B_j}} \frac{A_j B_j}{(P_{r_i} + B_i)}, \tag{5.23}$$

then (5.19) can be reorganized as

$$\Delta SNR'_{tot} = \left[A_1 - \sqrt{\frac{p_1 A_i B_i}{p_i A_1 B_1}} \frac{A_1 B_1}{(P_{r_i} + B_i)}\right] + \cdots + \left[A_i - \frac{A_i B_i}{P_{r_i} + B_i}\right] + \cdots$$
$$+ \left[A_{N'} - \sqrt{\frac{p_{N'} A_i B_i}{p_i A_{N'} B_{N'}}} \frac{A_{N'} B_{N'}}{(P_{r_i} + B_i)}\right] = \sum_{r_j \in L_h} A_j - \sqrt{\frac{A_i B_i}{p_i}} \frac{1}{P_{r_i} + B_i} \sum_{r_j \in L_h} \sqrt{p_j A_j B_j}. \tag{5.24}$$

Substituting (5.24) into (5.21), after some manipulations, we can have a quadratic equation of P_{r_i}. The optimal power consumption is

$$P^*_{r_i} = \sqrt{\frac{A_i B_i}{p_i}} \frac{Y + \sqrt{Y^2 + 4XW'}}{2X} - B_i, \tag{5.25}$$

where $X = 1 + \sum_{r_j \in L_h} A_j$ and $Y = \sum_{r_j \in L_h} \sqrt{p_j A_j B_j}$.

The solution in (5.25) can also be verified by the Karush-Kuhn-Tucker (KKT) condition [Bar93] to be the global optimum to problem (5.13), since the U_s function is concave in $\{P_{r_i}\}_{i=1}^N$ and the supporting set $\{P_{r_i} | P_{r_i} \geq 0, i = 1, \cdots, N\}$ is convex.

5.2.2 Seller-Level Game for the Relay Nodes

Substituting (5.25) into (5.15), we have

$$\max_{\{p_i\}>0} U_{r_i} = (p_i - c_i) P^*_{r_i}(p_1, \ldots, p_i, \ldots, p_{N'}). \tag{5.26}$$

We can note that (5.26) is a noncooperative game by the relay nodes, and there exists a tradeoff between the price p_i and the relay node's utility U_{r_i}. If relay node r_i in good channel conditions asks for a relatively low price p_i at first, source node s will buy more power from relay node r_i and U_{r_i} will increase as p_i grows. When p_i keeps growing and exceeds a certain value, it is no longer beneficial for source s to buy power from relay r_i, even though relay r_i may be in very good channel conditions. In this way, P_{r_i} will shrink and hence results in a decrement of U_{r_i}.

Therefore, there is an optimal price for each relay node to ask for, depending on the relay node's channel conditions. Besides, the optimal price is also affected by the other relay nodes' prices since the source node only chooses the most beneficial relay nodes.

From the analysis above, by taking derivative of U_{r_i} to p_i and equating it to zero, we have

$$\frac{\partial U_{r_i}}{\partial p_i} = P^*_{r_i} + (p_i - c_i)\frac{\partial P^*_{r_i}}{\partial p_i} = 0, \quad r_i \in L_h. \tag{5.27}$$

Solving the above equations of p_i, we denote the optimal prices as

$$p^*_i = p^*_i(\sigma^2, \{G_{s,r_i}\}, \{G_{r_i,d}\}), \quad r_i \in L_h. \tag{5.28}$$

In Section 5.2.1 we assume that the source node transmits with a constant power. However, if the source node has a lower transmission power, it is willing to buy more power from the relay nodes in order to obtain a high data rate, and hence the relay nodes can ask higher prices for helping the source node. On the other hand, if the source has a higher transmission power, it will buy less power from the relay nodes and also pay less to them.

5.2.3 Existence of the Equilibrium

In this subsection, we prove that the solution $P^*_{r_i}$ in (5.25) and p^*_i in (5.28) is the Stackelberg Equilibrium (SE) for the proposed game, and show the conditions for the SE to be optimal by the following properties, proposition, and theorem.

We first define the SE of the proposed game as follows.

Definition 1: $P^{SE}_{r_i}$ and p^{SE}_i are the SE of the proposed game, if for every

$r_i \in L$, when p_i is fixed,

$$U_s(\{P_{r_i}^{SE}\}) = \sup_{\{P_{r_i}\} \geq \mathbf{0}} U_s(\{P_{r_i}\}), \forall r_i \in L, \tag{5.29}$$

and for every $r_i \in L_h$, when P_{r_i} is fixed,

$$U_{r_i}(p_i^{SE}) = \sup_{p_i > c_i} U_{r_i}(p_i), \quad \forall r_i \in L_h. \tag{5.30}$$

Then, we show that the optimizer $P_{r_i}^*$ of problem (5.13) can be solved by equating $\frac{\partial U_s}{\partial P_{r_i}}$ to zero by the following property.

Property 1: The utility function U_s of the source node is jointly concave in $\{P_{r_i}\}_{i=1}^N$, with $P_{r_i} \geq 0$, and p_i is fixed, $\forall i$.

PROOF. Taking the second order derivatives of the source node's utility U_s, we can get

$$\frac{\partial^2 U_s}{\partial P_{r_i}^2} = -\frac{W'}{\left(1 + \sum_{k=1}^{N} \frac{A_k P_{r_k}}{P_{r_k} + B_k}\right)^2} \left[\frac{A_i B_i}{(P_{r_i} + B_i)^2}\right]^2 - 2\frac{W'}{\left(1 + \sum_{k=1}^{N} \frac{A_k P_{r_k}}{P_{r_k} + B_k}\right)} \frac{A_i B_i}{(P_{r_i} + B_i)^3}, \tag{5.31}$$

and

$$\frac{\partial^2 U_s}{\partial P_{r_i} \partial P_{r_j}} = -\frac{W'}{\left(1 + \sum_{k=1}^{N} \frac{A_k P_{r_k}}{P_{r_k} + B_k}\right)^2} \times \frac{A_i B_i}{(P_{r_i} + B_i)^2} \frac{A_j B_j}{(P_{r_j} + B_j)^2}. \tag{5.32}$$

For each relay, by definition, $W' > 0$, $A_i > 0$, $B_i > 0$, and $P_{r_i} \geq 0$. As a result, $\frac{\partial^2 U_s}{\partial P_{r_i}^2} < 0$ and $\frac{\partial^2 U_s}{\partial P_{r_i} \partial P_{r_j}} < 0$. It is straightforward to verify that $\frac{\partial^2 U_s}{\partial P_{r_i}^2} \frac{\partial^2 U_s}{\partial P_{r_j}^2} - (\frac{\partial^2 U_s}{\partial P_{r_i} \partial P_{r_j}})^2 > 0$, $\forall i \neq j$. Moreover, U_s is continuous in P_{r_i}, so when $P_{r_i} \geq 0$, U_s is strictly concave in each P_{r_i}, $\forall i$, and jointly concave over $\{P_{r_i}\}_{i=1}^N$ as well.

▲

Due to *Property 1*, $P_{r_i}^*$ in (5.25) is the global optimum that maximizes the source node's utility U_s. Therefore, $P_{r_i}^*$ satisfies condition (5.29) and is the SE $P_{r_i}^{SE}$.

Moreover, in practical implementation of the game, the source node can find the optimal power amount by gradually increasing the purchased power from each relay node until U_s reaches its maximum without knowing CSI.

In the following two properties, we show that the relay nodes can not infinitely increase U_{r_i} by asking arbitrarily high prices.

Property 2: The optimal power consumption $P^*_{r_i}$ for relay node r_i is decreasing with its price p_i, when other relay nodes' prices are fixed.

PROOF. Taking the first order derivative of the optimal power consumption $P^*_{r_i}$, we have

$$\frac{\partial P^*_{r_i}}{\partial p_i} = \sqrt{\frac{A_i B_i}{p_i}} \frac{Y + \sqrt{Y^2 + 4XW'}}{2X} \times \left[-\frac{1}{2p_i} \left(1 - \frac{\sqrt{p_i A_i B_i}}{\sqrt{Y^2 + 4XW'}} \right) \right] < 0. \tag{5.33}$$

So $P^*_{r_i}$ is decreasing with p_i. This is because when some relay node individually increases its price while the others keep the same prices as before, the source node will buy less from that relay node. ▲

Consequently, there is a tradeoff for each relay node to ask a proper price, and we can solve the optimal price by equating $\frac{\partial U_{r_i}}{\partial p_i} = 0$, the reason of which is shown as follows.

Property 3: The utility function U_{r_i} of each relay node is concave in its own price p_i, when its power consumption is the optimized purchase amount from the source node as calculated in (5.25), and the other relay nodes' prices are fixed.

PROOF. $P^*_{r_i}$ is a continuous function of p_i, so U_{r_i} is continuous in p_i too. Taking

derivatives of the relay node's utility U_{r_i} results in

$$\frac{\partial U_{r_i}}{\partial p_i} = -B_i + \sqrt{\frac{A_i B_i}{p_i}} \frac{Y + \sqrt{Y^2 + 4XW'}}{2X} \times \left[1 - \frac{p_i - c_i}{2p_i}\left(1 - \frac{\sqrt{p_i A_i B_i}}{\sqrt{Y^2 + 4XW'}}\right)\right], \tag{5.34}$$

and further

$$\begin{aligned}\frac{\partial^2 U_{r_i}}{\partial p_i^2} = &\sqrt{\frac{A_i B_i}{p_i}} \frac{Y_i}{2X}\left(1 - \frac{\sqrt{p_i A_i B_i}}{\sqrt{Y^2 + 4XW'}}\right)\left(\frac{-p_i - 3c_i}{4p_i^2}\right) + \frac{\sqrt{\frac{A_i B_i}{p_i}}}{8Xp_i^2\left(\sqrt{Y^2 + 4XW'}\right)^3} \\ &\times \Big[\left(Y_i^2 + 2Y_i\sqrt{p_i A_i B_i} + 4XW'\right)^2(-p_i - 3c_i) + p_i A_i B_i \\ &\times \left(Y_i^2 + 2Y_i\sqrt{p_i A_i B_i}\right)(-p_i - 3c_i) + p_i A_i B_i 4XW'(-4c_i)\Big],\end{aligned} \tag{5.35}$$

where $Y_i = Y - \sqrt{p_i A_i B_i}$. Since A_i, B_i, p_i, Y_i, c_i, X, and $W' > 0$, we have $\frac{\partial^2 U_{r_i}}{\partial p_i^2} < 0$. So U_{r_i} is concave with respect to p_i. ▲

Based on *Properties 1-3*, we can show that the *relay rejection criteria* stated in Section 5.2.1 help the source node reject the least beneficial relay nodes in the following proposition.

Proposition 1: The *relay rejection criteria* described in Section 5.2.1 is *necessary* and *sufficient* to exclude the least beneficial relay nodes to the source node. By *necessary*, it means that any r_i in L_h cannot get further discarded in the following U_{r_i} maximization process; While by *sufficient*, it means that, even if we keep r_j that satisfies the rejection criteria in L_h, it is still discarded in the following U_{r_j} maximization process.

PROOF. We first prove the *sufficient* part. Assume the relay rejection criteria apply to some relay node r_j, i.e., $(\frac{\partial U_s}{\partial P_{r_j}}) < 0$, when $P_{r_i} = 0, \text{and } p_i = c_i, \forall i$. Since U_s is concave in $\{P_{r_i}\}_{i=1}^N$, r_j's optimal power allocation $P_{r_j}^* < 0$. Suppose source s does

not exclude relay r_j and in the following price update process, all remaining relay nodes gradually increase their prices to get more utilities. To prove that the new resulting $P_{r_j}^{*new} < 0$, it suffices to prove $\Delta P_{r_j}^* < 0$, where $\Delta P_{r_j}^*$ denotes the increase of $P_{r_j}^*$ when each relay node r_i increase p_i by a very small positive amount from the cost c_i. This can be verified equivalent by proving

$$\sum_{i \neq j} \frac{\partial P_{r_j}^*}{\partial p_i} + \frac{\partial P_{r_j}^*}{\partial p_j}\Big|_{\{p_i = c_i,\ \forall i\}} < 0. \tag{5.36}$$

We know

$$\frac{\partial P_{r_j}^*}{\partial p_i} = \sqrt{\frac{A_j B_j}{p_j}} \frac{Y + \sqrt{Y^2 + 4XW'}}{2X} \left(\frac{1}{2p_i} \frac{\sqrt{p_i A_i B_i}}{\sqrt{Y^2 + 4XW'}} \right) > 0, \tag{5.37}$$

and

$$\frac{\partial P_{r_j}^*}{\partial p_j} = \sqrt{\frac{A_j B_j}{p_j}} \frac{Y + \sqrt{Y^2 + 4XW'}}{2X} \left(-\frac{1}{2p_j} \right) \left(1 - \frac{\sqrt{p_j A_j B_j}}{\sqrt{Y^2 + 4XW'}} \right) < 0, \tag{5.38}$$

so it suffices to prove (5.36) by proving the following

$$\sum_{i \neq j} \left(\frac{1}{2p_i} \frac{\sqrt{p_i A_i B_i}}{\sqrt{Y^2 + 4XW'}} \right) < \left(\frac{1}{2p_j} \right) \left(1 - \frac{\sqrt{p_j A_j B_j}}{\sqrt{Y^2 + 4XW'}} \right)\Big|_{\{p_i = c_i,\ \forall i\}}. \tag{5.39}$$

Without loss of generality, assuming the selected relay nodes generally share similar properties, i.e., $c_i = c_j = c, \forall i \neq j$, then we can prove (5.39) by the following inequality

$$\begin{aligned} &\sum_{i \neq j} \frac{1}{2p_i} \frac{\sqrt{p_i A_i B_i}}{\sqrt{Y^2 + 4XW'}} < \frac{1}{2c} \sum_{i \neq j} \frac{\sqrt{p_i A_i B_i}}{Y} \\ &= \frac{1}{2p_j} \left(1 - \frac{\sqrt{p_j A_j B_j}}{Y} \right) < \frac{1}{2p_j} \left(1 - \frac{\sqrt{p_j A_j B_j}}{\sqrt{Y^2 + 4XW'}} \right). \end{aligned} \tag{5.40}$$

So in the following price increasing process, r_j is still discarded by the source node by observing $P_{r_j}^{*new} < 0$.

Next, we prove the *necessary* part. In each round, any two relay nodes r_k and r_i update their prices in two consecutive steps. First, r_k increases its price p_k^* to the new optimal p_k^{*new}, then, by (5.37), the resulting $P_{r_i}^{*new}$ is larger than $P_{r_i}^*$, where $P_{r_i}^* > 0$. Thus, $P_{r_i}^{*new} > 0$, which means r_i won't be discarded if r_k increases p_k. Second, after p_k is increased, r_i increases its own price p_i. In (5.34), assuming $\bar{p}_i$ is the price for r_i such that $P_{r_i}^* = 0$ when the other relay nodes' prices are fixed, we have

$$\frac{\partial U_{r_i}}{\partial p_i}\Big|_{p_i \to \bar{p}_i} < -B_i + \sqrt{\frac{A_i B_i}{\bar{p}_i}} \frac{Y + \sqrt{Y^2 + 4XW'}}{2X} \to 0. \tag{5.41}$$

By *Property 3*, the optimal price p_i^* such that $\frac{\partial U_{r_i}}{\partial p_i} = 0$ must satisfy $c_i < p_i^* < \bar{p}_i$. This means to maximize U_{r_i}, r_i asks a lower price than $\bar{p}_i$ to avoid being rejected by the source node. ▲

If relay node r_i gets selected by the source node, due to the concavity of U_{r_i} proved in *Property 3*, r_i can always find its optimal price $p_i^* \in (c_i, \infty)$, and thus $U_{r_i}(p_i^*) \geq U_{r_i}(p_i)$, $\forall r_i \in L_h$. Together with *Property 1*, we conclude the following theorem.

Theorem 1: The pair of $\{P_{r_i}^*\}_{i=1}^N$ in (5.25) and $\{p_i^*\}_{i=1}^{N'}$ in (5.28) are the SE for the proposed game, where the SE is defined in (5.29) and (5.30).

In the next subsection, we will show that the SE is unique, and the proposed game converges to the unique SE when each relay node updates its price according to a simple function.

5.2.4 Distributed Price Updating

From the previous subsection, one relay node needs to modify its own price, after the other relay nodes change their prices. Consequently, for every $r_i \in L_h$, relay node r_i updates p_i so that its utility U_{r_i} satisfies the following equality,

$$\frac{\partial U_{r_i}}{\partial p_i} = \frac{\partial}{\partial p_i}[(p_i - c_i)P^*_{r_i}] = P^*_{r_i} + (p_i - c_i)\frac{\partial P^*_{r_i}}{\partial p_i} = 0, \tag{5.42}$$

with equality holds if and only if p_i reaches the optimum.

After re-arranging (5.42), we have

$$p_i = I_i(\boldsymbol{p}) \stackrel{\triangle}{=} c_i - \frac{P^*_{r_i}}{\partial P^*_{r_i}/\partial p_i}. \tag{5.43}$$

In order to calculate p_i in (5.43), each relay node r_i listens to the instantaneous feedback information about $P^*_{r_i}$ and $\partial P^*_{r_i}/\partial p_i$ from the source node, which is similar to the needed information exchange in iterative power control [Yat95]. Then, the updating of the relay nodes' prices can be described by a vector equality of the form

$$\boldsymbol{p} = \boldsymbol{I}(\boldsymbol{p}), \tag{5.44}$$

where $\boldsymbol{p} = (p_1, \cdots, p_{N'})$, with p_i denoting relay node r_i's price; $\boldsymbol{I}(\boldsymbol{p}) = (I_1(\boldsymbol{p}), \cdots, I_{N'}(\boldsymbol{p}))$, with $I_i(\boldsymbol{p})$ representing the price competition constraint to r_i from the other relay nodes. Therefore, for the N' relay nodes in set L_h with competition constraints in (5.44), the iterations of the price updating can be expressed as follows,

$$\boldsymbol{p}(t+1) = \boldsymbol{I}(\boldsymbol{p}(t)). \tag{5.45}$$

Remark: If K source nodes, denoted by $\mathcal{S} = \{s_1, s_2, \cdots, s_K\}$, exist in the network, assuming that the price of relay node r_i when it helps source node s_k is

$p_i^{s_k}$ with corresponding power $P_{r_i}^{s_k}$, then the buyer-level game for each source node s_k is essentially the same as the single-buyer case. However, the seller-level game becomes more complicated, because now relay node r_i needs to choose K prices, $\{p_i^{s_k}\}_{s_k \in \mathcal{S}}$, in order to maximize its utility

$$U_{r_i} = \sum_{s_k \in \mathcal{S}} (p_i^{s_k} - c_i) P_{r_i}^{s_k}. \tag{5.46}$$

If the relay nodes treat all source nodes equally with $p_i^{s_k} = p_i$, $\forall s_k \in \mathcal{S}$, i.e., relay node r_i asks a uniform price p_i no matter which source node it helps, then utility U_{r_i} is simplified as

$$U_{r_i} = (p_i - c_i) \sum_{s_k \in \mathcal{S}} P_{r_i}^{s_k}, \tag{5.47}$$

and the proposed algorithm is still applicable, with the modified price updating function

$$p_i = I_i(\boldsymbol{p}) \stackrel{\triangle}{=} c_i - \frac{\sum_{s_k \in \mathcal{S}} P_{r_i}^{s_k^*}}{\sum_{s_k \in \mathcal{S}} \partial P_{r_i}^{s_k^*} / \partial p_i}. \tag{5.48}$$

However, if the relay nodes treat the source nodes differently, then each relay node r_i needs to update K prices, $\{p_i^{s_k}\}_{s_k \in \mathcal{S}}$, using the following updating function

$$p_i^{s_k} = I_i(\boldsymbol{p}^{s_k}) \stackrel{\triangle}{=} c_i - \frac{P_{r_i}^{s_k^*}}{\partial P_{r_i}^{s_k^*} / \partial p_i^k}. \tag{5.49}$$

Therefore, if there are multiple source nodes in the network, the propose algorithm is still applicable: the buyer-level game of each source node is essentially the same as the single-source case; the only change is in the seller-level game of the relay nodes, where the price updating function is modified as in (5.48) or (5.49).

We show next the convergence of the iterations in (5.45) by proving that the price updating function $\boldsymbol{I}(\boldsymbol{p})$ is a *standard function* [Yat95].

Definition 2: A function $\boldsymbol{I}(\boldsymbol{p})$ is *standard*, if for all $\boldsymbol{p} \geq 0$, the following properties are satisfied [Yat95]:

- *Positivity:* $\boldsymbol{I}(\boldsymbol{p}) > 0$,
- *Monotonicity:* If $\boldsymbol{p} \geq \boldsymbol{p}'$, then $\boldsymbol{I}(\boldsymbol{p}) \geq \boldsymbol{I}(\boldsymbol{p}')$,
- *Scalability:* For all $\alpha > 1$, $\alpha \boldsymbol{I}(\boldsymbol{p}) > \boldsymbol{I}(\alpha \boldsymbol{p})$.

Proposition 2: The price updating function $\boldsymbol{I}(\boldsymbol{p})$ is *standard*.

PROOF. Positivity: By *Property 2*, $\frac{\partial P_{r_i}^*}{\partial p_i} < 0$. Moreover, if $c_i > 0$ and $P_{r_i} \geq 0$, then by the definition of (5.43), $I_i(\boldsymbol{p}) \geq c_i > 0$. So in real price updating process, each relay node starts increasing its price from c_i.

Scalability: Comparing $\alpha \boldsymbol{I}(\boldsymbol{p})$ and $\boldsymbol{I}(\alpha \boldsymbol{p})$ in an element-wise manner, we have

$$\alpha I_i(\boldsymbol{p}) - I_i(\alpha \boldsymbol{p}) = (\alpha - 1) c_i + \alpha \left[\frac{P_{r_i}(\alpha \boldsymbol{p})}{\partial P_{r_i}(\alpha \boldsymbol{p}) / \partial p_i} - \frac{P_{r_i}(\boldsymbol{p})}{\partial P_{r_i}(\boldsymbol{p}) / \partial p_i} \right]. \tag{5.50}$$

Since $\alpha > 1$, $(\alpha - 1) c_i > 0$. Then the problem reduces to proving the second term in the RHS of (5.50) is positive.

If we define $F_i(W')$ as follows,

$$\begin{aligned} F_i(W') &= \frac{P_{r_i}(\boldsymbol{p})}{\partial P_{r_i}(\boldsymbol{p}) / \partial p_i} \\ &= \left(1 - \frac{B_i}{\sqrt{\frac{A_i B_i}{p_i}} \frac{Y + \sqrt{Y^2 + 4XW'}}{2X}} \right) \times \left[-\frac{1}{2p_i} \left(1 - \frac{\sqrt{p_i A_i B_i}}{\sqrt{Y^2 + 4XW'}} \right) \right]^{-1}, \end{aligned} \tag{5.51}$$

then we can get

$$\begin{aligned} \frac{P_{r_i}(\alpha \boldsymbol{p})}{\partial P_{r_i}(\alpha \boldsymbol{p}) / \partial p_i} &= \left(1 - \frac{B_i}{\sqrt{\frac{A_i B_i}{p_i}} \frac{Y + \sqrt{Y^2 + 4XW'/\alpha}}{2X}} \right) \times \left[-\frac{1}{2p_i} \left(1 - \frac{\sqrt{p_i A_i B_i}}{\sqrt{Y^2 + 4XW'/\alpha}} \right) \right]^{-1} \\ &= F_i\left(W'/\alpha\right). \end{aligned} \tag{5.52}$$

Thus, to prove the positivity of the second term of RHS of (5.50) is equivalent to prove $F_i(\frac{W'}{\alpha}) > F_i(W')$, where $\frac{W'}{\alpha} < W'$. Since $F_i(W')$ is continuous and differentiable in W', we only need to prove $\frac{\partial F_i}{\partial W'} < 0$. Expanding $\frac{\partial F_i}{\partial W'}$, we get

$$\begin{aligned}\frac{\partial F_i}{\partial W'} =& 8Xp_i \times \left(\sqrt{\frac{A_iB_i}{p_i}}\sqrt{Y^2+4XW'}\right)^{-1} \times \left(\sqrt{Y^2+4XW'} - \sqrt{p_iA_iB_i}\right)^{-2} \\ & \times \left(Y+\sqrt{Y^2+4XW'}\right)^{-2} \quad \times \Bigg[- XB_i\left(Y^2+4XW'+Y\sqrt{p_iA_iB_i}\right) \\ & + \frac{1}{2}A_iB_i\left(Y+\sqrt{Y^2+4XW'}\right)^2\Bigg].\end{aligned} \tag{5.53}$$

The first four terms of the RHS of (5.53) are all positive. After extensive numerical tests for a wide range of parameters when the nodes are randomly located, we observe that the last term in the square brackets is negative. Then, the $\frac{\partial F_i}{\partial W'}$ in (5.53) is less than zero. Therefore, we can claim that $\alpha I(\boldsymbol{p}) > I(\alpha \boldsymbol{p})$.

Monotonicity: Suppose $\boldsymbol{p}$ and $\boldsymbol{p}'$ are different price vectors, and the vector inequality $\boldsymbol{p} \geq \boldsymbol{p}'$ means $p_i \geq p_i'$, $\forall i \in \{1, \cdots, N'\}$. If $\forall i \neq j,\ i, j\ \in \{1, \cdots, N'\}$, $I_j([p_1 \cdots p_i \cdots p_j \cdots p_{N'}]) \geq I_j([p_1 \cdots p_i' \cdots p_j \cdots p_{N'}])$, and $I_i([p_1 \cdots p_i \cdots p_j \cdots p_{N'}]) \geq I_i([p_1 \cdots p_i' \cdots p_j \cdots p_{N'}])$, then monotonicity can be shown to hold. So the problem reduces to proving $\partial I_j(\boldsymbol{p})/\partial p_i \geq 0$ and $\partial I_i(\boldsymbol{p})/\partial p_i \geq 0$. Expanding and reorganizing $\partial I_j(\boldsymbol{p})/\partial p_i$ to express it as a product of a positive term and a second term, we get

$$\begin{aligned}\frac{\partial I_j(\boldsymbol{p})}{\partial p_i} =& \frac{\frac{1}{p_i}\frac{\sqrt{p_iA_iB_i}}{\sqrt{Y^2+4XW'}}}{\frac{1}{p_j}\left(1-\frac{\sqrt{p_jA_jB_j}}{\sqrt{Y^2+4XW'}}\right)} \times \Bigg[1 - \frac{\left(\sqrt{\frac{A_jB_j}{p_j}}\frac{Y+\sqrt{Y^2+4XW'}}{2X} - B_j\right)}{\left(\sqrt{\frac{A_jB_j}{p_j}}\frac{Y+\sqrt{Y^2+4XW'}}{2X}\right)} \\ & \times \frac{\left(1-\frac{\sqrt{p_jA_jB_j}}{\sqrt{Y^2+4XW'}} + \frac{Y\sqrt{p_jA_jB_j}}{Y^2+4XW'}\right)}{\left(1-\frac{\sqrt{p_jA_jB_j}}{\sqrt{Y^2+4XW'}}\right)}\Bigg].\end{aligned} \tag{5.54}$$

The first term of the RHS of (5.54) is positive, to decide the sign of the second

term, it suffices to compare the difference of the denominator and numerator of the fraction inside the square brackets, which are both positive. By using $\sqrt{\frac{A_i B_i}{p_i}} < \frac{X B_i}{Y}$ proved in the scalability property, we can finally show that

$$\begin{aligned}
&\left(\sqrt{\frac{A_j B_j}{p_j}}\frac{Y+\sqrt{Y^2+4XW'}}{2X}\right)\left(1-\frac{\sqrt{p_j A_j B_j}}{\sqrt{Y^2+4XW'}}\right) \\
&\quad-\left(\sqrt{\frac{A_j B_j}{p_j}}\frac{Y+\sqrt{Y^2+4XW'}}{2X}-B_j\right)\times\left(1-\frac{\sqrt{p_j A_j B_j}}{\sqrt{Y^2+4XW'}}+\frac{Y\sqrt{p_j A_j B_j}}{Y^2+4XW'}\right) \\
&> B_j\left(1-\frac{2\sqrt{p_j A_j B_j}}{\sqrt{Y^2+4XW'}}+\frac{\sqrt{p_j A_j B_j}\sqrt{p_j A_j B_j}}{Y^2+4XW'}\right)=B_j\left(1-\frac{\sqrt{p_j A_j B_j}}{\sqrt{Y^2+4XW'}}\right)^2>0,
\end{aligned} \tag{5.55}$$

so $\frac{\partial I_j(\boldsymbol{p})}{\partial p_i} > 0$. Similarly, we can also prove $\frac{\partial I_i(\boldsymbol{p})}{\partial p_i} > 0$, so monotonicity holds for the price updating function. Finally, from the above three parts, we prove that the price updating function is *standard*. ▲

In [Yat95], a proof has been given that starting from any feasible initial power vector $\boldsymbol{p}$, the power vector $\boldsymbol{I}^n(\boldsymbol{p})$ produced after n iterations of the standard power control algorithm gradually converges to a unique fixed point. As we have discussed in Section 5.2.1, it is natural for the relay nodes to initialize the prices as $p_i = c_i$, because lowering p_i below c_i will result in a negative utility U_{r_i}, while by setting p_i above c_i, relay node r_i may be at the risk of being excluded by the source node at the very beginning. So we assume that the initial price vector is $\boldsymbol{c} = (c_1, \cdots, c_{N'})$, where c_i is the cost per unit of power for relay node r_i, as introduced in eqn. (14). Therefore, we can conclude that starting from the feasible initial price vector $\boldsymbol{c} = (c_1, \cdots, c_{N'})$, the iteration of the *standard* price updating produces a non-decreasing sequence of price vectors $\boldsymbol{I}^n(\boldsymbol{c})$ that converges to a unique fixed point $\boldsymbol{p}^*$.

From eqn. (37), we know that, for relay node $r_i \in L_h$, its utility U_{r_i} satisfies $\frac{\partial U_{r_i}}{\partial p_i} = 0$ every time after r_i updates its price p_i given the feedback of $\frac{\partial P^*_{r_i}}{\partial p_i}$ from the source. After the vector $\boldsymbol{I}^n(\boldsymbol{p})$ converges to $\boldsymbol{p}^*$, no relay can gain a higher utility by further varying its price, meaning $\frac{\partial U_{r_i}}{\partial p_i} = 0$ for $\forall r_i \in L_h$. From eqns. (27) and (28), we know that $\boldsymbol{p}^*$ is exactly the optimal price vector. As *Property 1* shows, U_s is concave in P_{r_i}, so the source node can gradually increase the power from 0 and find the optimal $P^*_{r_i}$. Thus, if the prices of all the selected relay nodes converge to their optima, then the source node will correspondingly buy the optimal power. Therefore, once $\boldsymbol{I}^n(\boldsymbol{p})$ converges to $\boldsymbol{p}^*$, P_{r_i} and p_i converges to the SE. It is worth mentioning that although the closed-form solutions $\{P^*_{r_i}\}_{i=1}^N$ in (5.25) and $\{p_i^*\}_{i=1}^{N'}$ in (5.28) are functions of the channel-state information, in practical implementation of the game, the source node can find the optimal power amount by gradually increasing the purchased power from each relay node until U_s reaches its maximum due to *Property 1*. Actually the reason why we express the closed-form solution $\{P^*_{r_i}\}_{i=1}^N$ as a function of CSI is just to show that the relay node's utility U_{r_i} is concave in p_i (*Property 3*), and hence to prove that the relay nodes can utilize the proposed price updating algorithm and gradually converge to the optimal price $\{p_i^*\}_{i=1}^{N'}$ (*Proposition 2*). Hence, the only signallings between an individual relay node and the source node are the instant price and corresponding power, and no CSI is needed. Moreover, there is no price information exchange between the relay nodes. Therefore, the proposed game achieves its equilibrium in a distributed way with local information.

5.2.5 Comparison with the Centralized Optimal Scheme

In order to demonstrate the performance of the proposed game-theoretic scheme, we first investigate a centralized optimal power allocation problem with closed-form solutions. Then, we illustrate the numerical comparison of the performance in Section 5.3.

Suppose the system resources are shared by all available N relay nodes. From [ZAL06], we can model the centralized optimal power allocation problem as follows,

$$\max_{P_{r_i}} \quad \frac{W}{N+1}\log_2\left(1+\frac{\Gamma_{s,d}+\sum_{i=1}^{N}\Gamma_{s,r_i,d}}{\Gamma}\right) \tag{5.56}$$

$$\text{s.t.} \quad \sum_{i=1}^{N} P_{r_i} \le P_r^{tot},\ 0 \le P_{r_i} \le P_{r_i}^{max} \quad \forall i,$$

where $\Gamma_{s,d}$ and $\Gamma_{s,r_i,d}$ are defined in (5.3) and (5.8) respectively.

Because $\log_2(1+x)$ is a strictly increasing function of x, reorganizing the objective function of (5.56), we can get an equivalent optimization problem as in [ZAL06],

$$\min \quad \sum_{i=1}^{N} \frac{P_s^2 a_i^2 + P_s a_i}{P_s a_i + P_{r_i} b_i + 1} \tag{5.57}$$

$$\text{s.t.} \quad \sum_{i=1}^{N} P_{r_i} \le P_r^{tot},\ 0 \le P_{r_i} \le P_{r_i}^{max} \quad \forall i,$$

where $a_i = \frac{G_{s,r_i}}{\sigma^2}$ and $b_i = \frac{G_{r_i,d}}{\sigma^2}$.

The solution of (5.57) can be solved as

$$P_{r_i} = \left(\sqrt{\frac{P_s^2 a_i^2 + P_s a_i}{b_i}}\lambda - \frac{P_s a_i + 1}{b_i}\right)_0^{P_{r_i}^{max}}, \tag{5.58}$$

where λ is a constant chosen to meet the total power constraint and $(x)_l^u$ is defined

as

$$(x)_l^u = \begin{cases} l, & x < l; \\ x, & l \leq x \leq u; \\ u, & u < x. \end{cases} \tag{5.59}$$

In order to make a fair comparison, in the proposed scheme, we can change a, the gain per unit of the rate, to equivalently reflect different P_r^{tot} constraints as in the centralized scheme. The reason is explained as follows. When a is so large that the total payment M in U_s is negligible, $U_s \approx aR_{s,r,d}$, then the optimal power consumption of the problem in (5.13) will be $P_{r_i}^* \to \infty$. It is equivalent to have $P_r^{tot} \to \infty$ in the centralized scheme. On the contrary, when a is so small that the total gain of the rate $aR_{s,r,d}$ in U_s is negligible, $U_s \approx -M = -\sum_i p_i P_{r_i}$, then in this case we get $P_{r_i}^* = 0$. It is equivalent to have $P_r^{tot} = 0$ in the centralized scheme. Therefore, by varying a in a large range, we can get the optimal achievable rates corresponding to different total power consumptions and fairly compare the performance with that of the centralized scheme[2].

In the following, we sketch the analytical comparison between the centralized optimization scheme and the proposed distributed game. First, according to (5.56), we can represent the Lagrangian of the centralized optimal scheme as follows,

$$\begin{aligned} L_{cen}(\mathbf{P_r}, \lambda, \nu) =& R_{s,r,d} + \sum_{i=1}^{N} \nu_i(-P_{r_i}) + \sum_{i=1}^{N} \lambda_i(P_{r_i} - P_{r_i}^{max}) \\ &+ \lambda_{N+1}(\sum_{i=1}^{N} P_{r_i} - P_r^{tot}), \end{aligned} \tag{5.60}$$

where the Lagrangian multipliers are $\lambda = (\lambda_1, \cdots, \lambda_{N+1})$, and $\nu = (\nu_1, \cdots, \nu_N)$, with $\lambda_i, \nu_i \geq 0$. In the proposed game, each node maximizes its own utility defined in eq. (5.13) and (5.15), so we can equivalently view the objective as a vector

optimization, and the scalarization can be represented in the following

$$\max \quad U_s + \sum_{i=1}^{N} w_i U_{r_i} \tag{5.61}$$

$$\text{s.t} \quad 0 \le P_{r_i} \le P_{r_i}^{max}, \quad i = 1, \cdots, N, \tag{5.62}$$

$$p_i \ge 0, \quad i = 1, \cdots, N, \tag{5.63}$$

where $\mathbf{w} = (w_1, \cdots, w_N)$ is any weight vector, and $w_i > 0$, $\forall i$. Similarly, we can express the Lagrangian for the scalarized optimization as

$$\begin{aligned} \tilde{L}_{game}(\mathbf{Pr}, \mathbf{p}, \tilde{\lambda}, \tilde{\nu}, \tilde{\mu}) =& U_s + \sum_{i=1}^{N} w_i U_{r_i} + \sum_{i=1}^{N} \tilde{\mu}_i(-p_i) \\ &+ \sum_{i=1}^{N} \tilde{\nu}_i(-P_{r_i}) + \sum_{i=1}^{N} \tilde{\lambda}_i(P_{r_i} - P_{r_i}^{max}), \end{aligned} \tag{5.64}$$

where the Lagrangian multipliers are $\tilde{\lambda} = (\tilde{\lambda}_1, \cdots, \tilde{\lambda}_N)$, $\tilde{\mu} = (\tilde{\mu}_1, \cdots, \tilde{\mu}_N)$, and $\tilde{\nu} = (\tilde{\nu}_1, \cdots, \tilde{\nu}_N)$, with $\tilde{\lambda}_i, \tilde{\mu}_i, \tilde{\nu}_i \ge 0$, $\forall i$.

Substituting (5.13) and (5.15) into (5.64), after some manipulation, $\tilde{L}_{game}(\mathbf{Pr}, \mathbf{p}, \tilde{\lambda}, \tilde{\nu}, \tilde{\mu})$ becomes

$$\begin{aligned} \tilde{L}_{game}(\mathbf{Pr}, \mathbf{p}, \tilde{\lambda}, \tilde{\nu}, \tilde{\mu}) =& aR_{s,r,d} + \sum_{i=1}^{N} [w_i(p_i - c_i) - p_i] P_{r_i} - \sum_{i=1}^{N} \tilde{\mu}_i p_i \\ &+ \sum_{i=1}^{N} \tilde{\nu}_i(-P_{r_i}) + \sum_{i=1}^{N} \tilde{\lambda}_i(P_{r_i} - P_{r_i}^{max}). \end{aligned} \tag{5.65}$$

Since $a > 0$ and for simplicity, the above Lagrangian can be further converted to

$$\begin{aligned} \tilde{L'}_{game}(\mathbf{Pr}, \mathbf{p}, \lambda, \nu, \mu) =& R_{s,r,d} + \sum_{i=1}^{N} \frac{[w_i(p_i - c_i) - p_i]}{a} P_{r_i} - \sum_{i=1}^{N} \frac{\tilde{\mu}_i}{a} p_i \\ &+ \sum_{i=1}^{N} \frac{\tilde{\nu}_i}{a}(-P_{r_i}) + \sum_{i=1}^{N} \frac{\tilde{\lambda}_i}{a}(P_{r_i} - P_{r_i}^{max}). \end{aligned} \tag{5.66}$$

Comparing eq. (5.60) and (5.66), we can find they have similar terms, which can be viewed as one-to-one mappings, i.e., $\lambda_i \leftrightarrow \frac{\tilde{\lambda}_i}{a}$, $\nu_i \leftrightarrow \frac{\tilde{\nu}_i}{a}$, and $\lambda_{N+1}(\sum_{i=1}^{N} P_{r_i} - P_r^{tot}) \leftrightarrow$

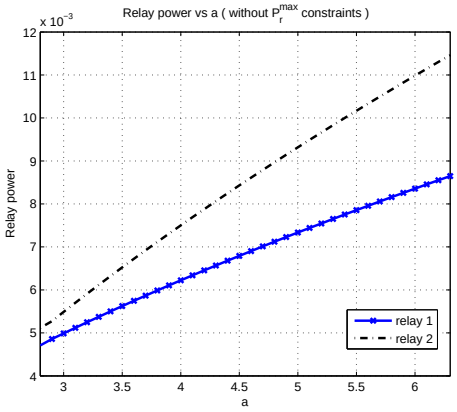

(a) Optimal power in game

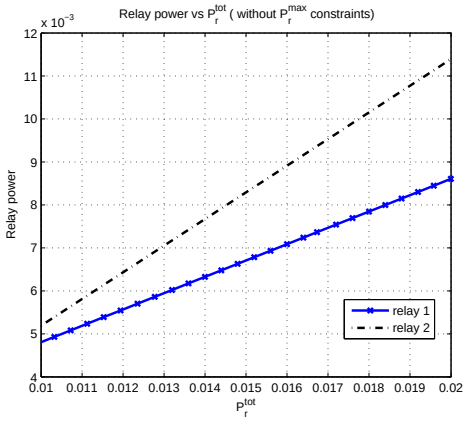

(b) Optimal power in centralized scheme

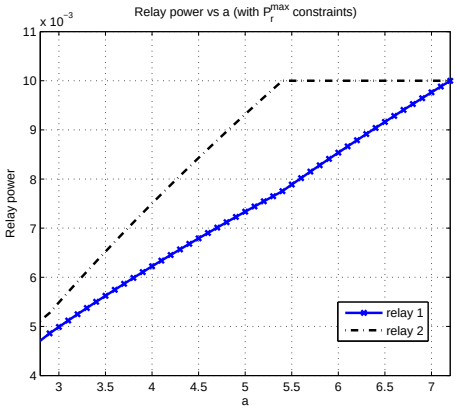

(c) Optimal power in game ($P_{r_i} \leq P_{r_i}^{max}$)

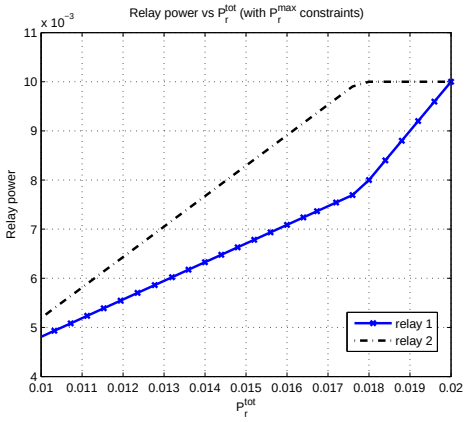

(d) Optimal power in centralized scheme($P_{r_i} \leq P_{r_i}^{max}$)

Figure 5.2: Comparison of optimal relay power of the game and the centralized scheme.

$\frac{1}{a}\left(\sum_{i=1}^{N}[w_i(p_i-c_i)-p_i]P_{r_i}-\sum_{i=1}^{N}\tilde{\mu}_i p_i\right)$. Without loss of generality, let us view a as a parameter in the proposed game, and correspondingly P_r^{tot} a parameter in the centralized optimal scheme. When a increases, $\frac{1}{a}\left(\sum_{i=1}^{N}[w_i(p_i-c_i)-p_i]P_{r_i}-\sum_{i=1}^{N}\tilde{\mu}_i p_i\right)$ decreases. In order to map $\lambda_{N+1}(\sum_{i=1}^{N}P_{r_i}-P_r^{tot})$ to it, P_r^{tot} should increase. That is the reason why varying the parameter a in the proposed game is equivalent to varying P_r^{tot} in the centralized optimization. To justify our claim, we show the opti-

mal powers versus P_r^{tot} and a of the two schemes in Figure 5.2, with or without the $P_{r_i}^{max}$ constraints, respectively. From both the simulation and the above analysis, we can see that due to the equivalence of the Lagrangian in the two approaches, the proposed game can achieve comparable performance to that in the centralized optimal scheme.

However, the centralized optimal power allocation scheme needs considerable overheads and signaling, because it requires that the complete channel-state information (CSI), i.e., $G_{s,d}$, G_{s,r_i} and $G_{r_i,d}$ available. In Section 5.3, we show that our proposed distributed scheme can achieve comparable performance while the needed signaling between the source node and the relay nodes is only the information about the prices and the power consumptions.

5.3 Simulation Studies

To evaluate the performance of the proposed scheme, in what follows, the simulation results for a one-relay case, for a two-relay case, and for a multiple-relay case are to be shown. Then we provide the performance comparisons of the proposed approach with the centralized optimal scheme. Finally, we discuss the effect of the bandwidth factor.

[2]We do not include explicitly the constraints on the relay nodes' power in the proposed game for ease of analysis. From the simulation in the next section and analytical proof in Appendix **??**, it will be shown that the game will achieve comparable performance when we consider the constraints on relay nodes' power.

5.3.1 One-Relay Case

There are one source-destination node pair (s, d) and one relay node r in the network. Destination node d is located at coordinate $(0\text{m}, 0\text{m})$, and source node s is located at coordinate $(100\text{m}, 0\text{m})$. We fix the y-coordinate of relay node r at 25m and its x-coordinate varies within the range of $[-250\text{m}, 300\text{m}]$. The propagation loss factor is set to 2. The transmit power $P_s = 10\text{mW}$, the noise level is $\sigma^2 = 10^{-8}\text{W}$, and we select the capacity gap $\Gamma = 1$, $W = 1\text{MHz}$, the gain per unit of rate $a = 0.01$ and the cost per unit of power $c = 0.2$.

In Figure 5.3(a), we show the optimal price for relay node r and the optimal power bought by source node s, respectively. In this simulation, relay node r moves along a line. We observe that when relay node r is close to source node s at $(100\text{m}, 0\text{m})$, the source can gain a higher U_s in the game, so the relay can more efficiently help source node s. However, the relay cannot arbitrarily select its price in order to improve its utility. As we have shown in *Property 2* and *Property 3*, the optimal power P_r^* the source buys from relay node r is decreasing with p, and node r_i's utility U_{r_i} is concave in p. Since the objective of the relay node is to maximize its utility U_r, the price p should be carefully selected instead of an arbitrarily large value. As decreasing price p can attract more buying from the source, relay node r reduces its price to enhance its utility U_r. When relay node r moves close to destination node d at $(0\text{m}, 0\text{m})$, relay node r can use very small amount of power to relay source node s's data, so relay node r sets a very high price in order to get more profits by selling this small amount of power. However, even the price is higher

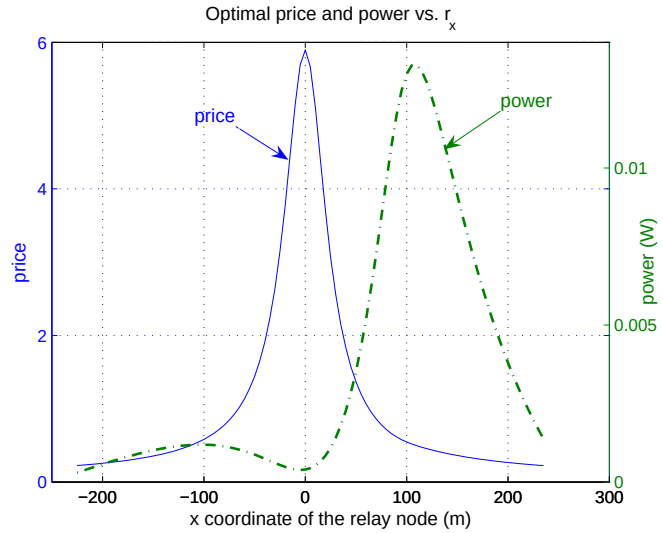

(a) Optimal price and power of the relay node

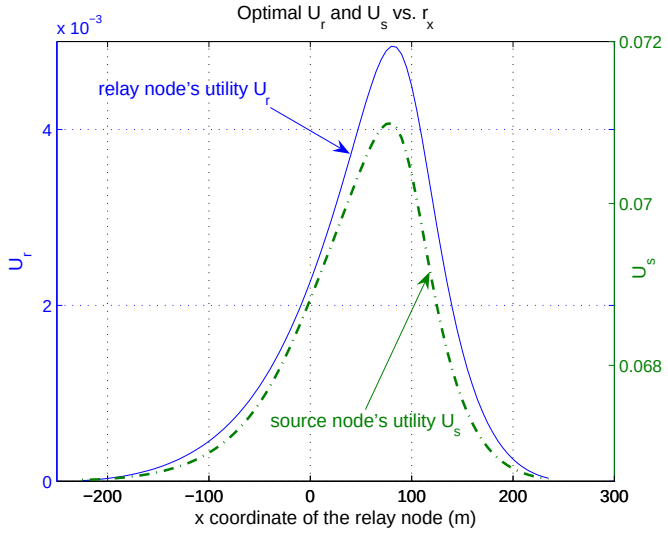

(b) Optimal utility of the relay and the source node

Figure 5.3: 1-relay case with the relay node at different locations.

than that when r is closer to the source, the utility U_r is still lower when the relay is close to the destination. When relay node r keeps moving away from destination node d, source node s stops buying services because asking for relay node r's help is no longer beneficial to source node s. Similarly, when relay node r moves in the opposite direction and locates far away from source node s, s would not buy services either.

In Figure 5.3(b), we show, respectively, the optimal utilities relay node r and source node s can obtain using the proposed game. When relay node r is close to source node s, both r and s can get their maximal utilities. The reason is that around this location, relay node r can most efficiently help source node s increase its utility, and the optimal price of relay node r is lower than that when r is at other locations. So source node s buys more power, resulting in a higher utility to relay node r.

5.3.2 Two-Relay Case

We also set up two-relay simulations to test the proposed game. In the simulations, the coordinates of s and d are $(100\text{m}, 0\text{m})$ and $(0\text{m}, 0\text{m})$, respectively. Relay node r_1 is fixed at the coordinate $(50\text{m}, 25\text{m})$ and relay node r_2 moves along the line from $(-250\text{m}, 25\text{m})$ to $(300\text{m}, 25\text{m})$. For each r_i, we set $c_i = 0.1$. Other settings are the same as those of the one-relay case.

In Figure 5.4, we can observe that even though only r_2 moves, the prices of both the relay nodes change accordingly, and s buys different amounts of power

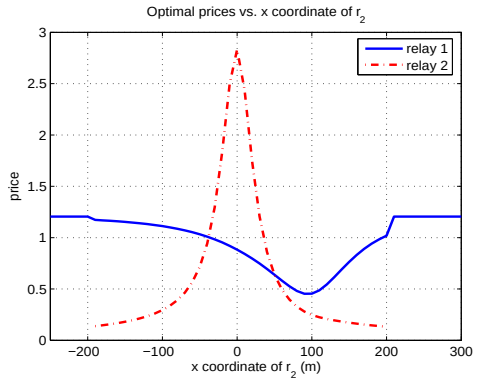

(a) Optimal prices of the relay nodes

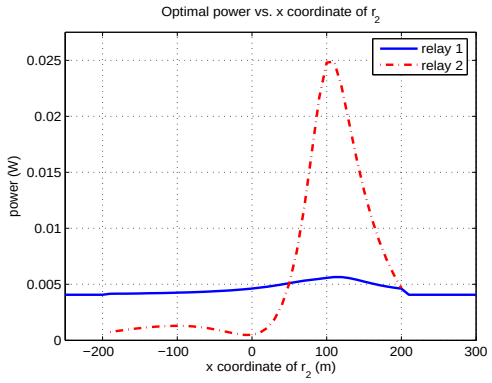

(b) Optimal power consumptions of the relay nodes

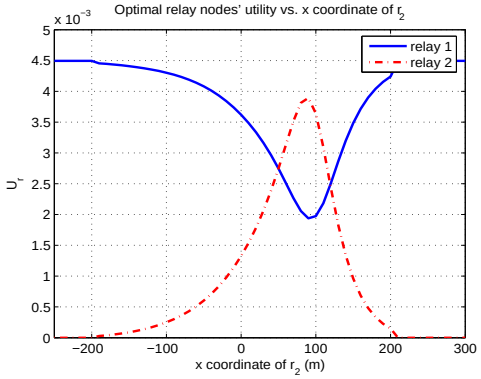

(c) Optimal utilities of the relay nodes

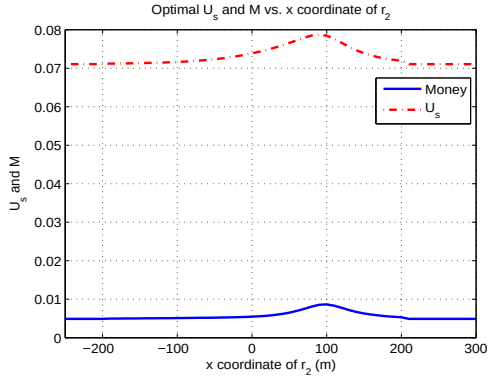

(d) U_s and M of the source node

Figure 5.4: 2-relay case with relay node r_2 at different locations.

from them. This fact is because the relay nodes influence and compete with each other in the proposed game. When relay node r_2 is close to d at $(0\text{m}, 0\text{m})$, it sets a very high price as explained in the one-relay case. Accordingly, r_1 increases its price and $P^*_{r_1}$ slightly decreases. When r_2 is close to s at $(100\text{m}, 0\text{m})$, r_2 is more suitable to help s than r_1, and $U^*_{r_2}$ is very high. Hence, in order to attract source s to buy its service, r_1 reduces its price a lot, but $U^*_{r_1}$ still drops. Because r_2 close to s results in the most efficient help to s from the relay nodes, both U_s and M reach their maxima around this location. As r_2 moves far away from s or d, r_2's price drops because r_2 is less competitive than r_1. When its utility is less than 0, r_2 quits the competition and $P^*_{r_2} = 0\text{mW}$. At that moment, r_1 can slightly increase its price since there is no competition. However, source node s will buy slightly less power from r_1. This fact suppresses the incentive of r_1 to ask arbitrarily high price in the absence of competition, otherwise r_2 will rejoin the competition. At the transition point when r_2 quits, U_{r_1} is smooth. Note that when r_2 moves to $(50\text{m}, 25\text{m})$, the same location as r_1, the power consumptions, the prices and the utilities of both the relay nodes are the same. This is because the source node is indifferent for the two relay nodes locating together and treats them equally.

5.3.3 Multiple-Relay Case

We then set up multiple-relay simulations to test the proposed game. The coordinates of the source node and the destination node are $(100\text{m}, 0\text{m})$ and $(0\text{m}, 0\text{m})$, respectively, and the relay nodes are uniformly located within the range of $[-50\text{m}, 150\text{m}]$

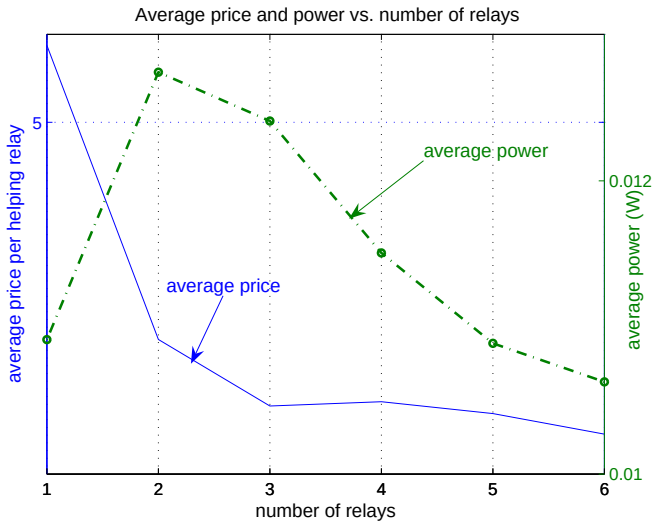

(a) Average price and power vs. number of relay nodes

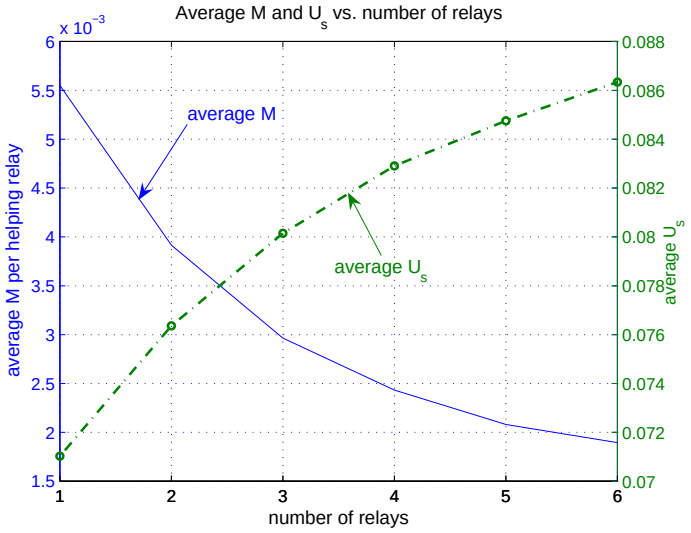

(b) Average U_s and M vs. number of relay nodes

Figure 5.5: Multiple-relay case with different number of relay nodes.

in x-axis and $[0\text{m}, 20\text{m}]$ in y-axis. From Figure 5.5, we can observe that as the total number of the available relay nodes increases, the competitions among the relay nodes become more severe, so the average price per relay node decreases. The source node increases the amount of average power purchase when the number of the relay nodes is not so large (less than 3), because the average price is decreased. When the number of the relay nodes becomes larger (greater than 3), the source node decreases the amount of average power purchase, because it buys power from more relay nodes. Correspondingly, the total payments are shared by more relay nodes, which leads to less average payment from the source node. Thus, the source node obtains an increasing utility.

5.3.4 Convergence Speed of the Game

As described in Section 5.2.4, the relay nodes start increasing their price p_i from c_i after the N' more beneficial relay nodes have been selected by the source node. Denote the price vector at time t as $\mathbf{p}(t) = (p_1(t), p_2(t), \cdots, p_{N'}(t))$. From (5.25), the optimal power purchased by the source node at time t can be denoted as

$$P^*_{r_i}(t) := P^*_{r_i}(\mathbf{p}(t)) = P^*_{r_i}(p_1(t), p_2(t), \cdots, p_{N'}(t)). \tag{5.67}$$

In order to obtain $\partial P^*_{r_i}/\partial p_i$ and update their prices by (5.43), the selected relay nodes will simultaneously increase each $p_i(t)$ by a small amount δ_i. The source node receives this price updating, and calculates $\partial P^*_{r_i}/\partial p_i$ using the following approximation

$$\frac{\partial P^*_{r_i}}{\partial p_i} \simeq \frac{P^*_{r_i}(p_1(t), \cdots, p_i(t) + \delta_i, \cdots, p_{N'}(t)) - P^*_{r_i}(\mathbf{p}(t))}{\delta_i}. \tag{5.68}$$

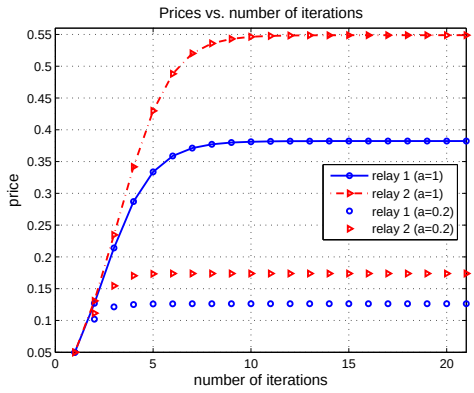

(a) Prices of relay nodes vs. iteration index

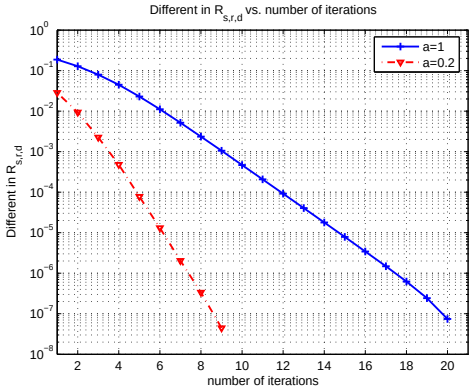

(b) Difference in $R_{s,r,d}$ vs. iteration index

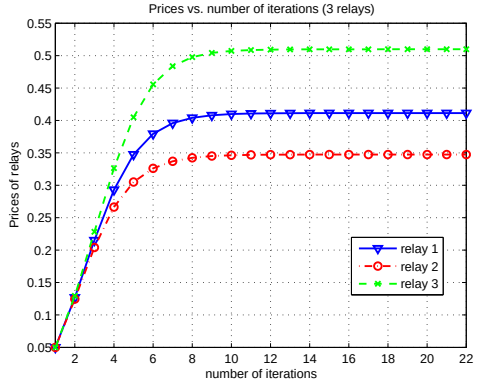

(c) Prices of relay nodes vs. iteration index (3 relays)

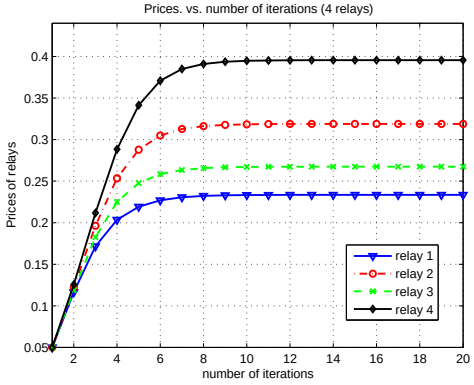

(d) Prices of relay nodes vs. iteration index (4 relays)

Figure 5.6: Observation of convergence speed.

Substituting the above approximation signalled from the source node into (5.43), where the numerator $P^*_{r_i}(t)$ is as defined in (5.67), the relay nodes can obtain $\mathbf{p}(t+1) = \mathbf{I}(\mathbf{p}(t))$. In the above updating process, the source node can signal the approximated derivatives calculated by (5.68) to all the relay nodes at one time, and need not interact with them one by one. So this process can be viewed as one iteration, and does not depend on the number of relay nodes. Then we conducted simulations when 2 to 4 relay nodes are available to help the source node, and observe the convergence behavior of the proposed game. In Figure 5.6(a), it is seen

that the proposed scheme has fast convergence to the Stackelberg Equilibria $\mathbf{p}^*$. It takes less than 15 iterations until the price vector $\mathbf{p}$ converges to the optimum when there are 2 relay nodes in the system for $a = 1$, where a denotes the gain per unit of rate as defined in (5.11), and less than 10 iterations for $a = 0.2$. In addition, in Figure 5.6(b), the convergence behavior of $R_{s,r,d}$ to the optimized transmission rate using $\mathbf{P_r}^*$ and $\mathbf{p}^*$ appears to be exponentially fast. Finally, we keep $a = 1$, increase the number of relay nodes to 3 and 4, and show the convergence behavior of the prices in Figure 5.6(c) and 5.6(d), respectively. We can see the number of iterations until convergence happens almost keeps the same as there are more relay nodes existing in the system.

5.3.5 Comparison with the Centralized Optimal Scheme

To compare the performance of the proposed game with the centralized scheme, we set up two simulations as follows. There are two relay nodes and one (s, d) pair. One of the relay nodes is fixed at coordinate $(50\text{m}, 25\text{m})$ and the other node is fixed at $(60\text{m}, 25\text{m})$ and $(40\text{m}, 25\text{m})$ in the two simulations, respectively. For the centralized scheme defined in (5.56), we set $P_{r_i}^{max} = 10\text{mW}$, and let P_r^{tot} vary within the range of $[10, 20]\text{mW}$. Then, we can obtain a curve of the maximal rates versus different total power consumption constraints. For the distributed scheme, as explained in Section 5.2.5, by varying a and including the same constraint $P_{r_i}^{max} = 10\text{mW}$ on P_{r_i}, we can also get different total power consumptions and corresponding maximal rates. From Figure 5.7(a) and 5.7(b), we observe that the proposed game achieves almost equal

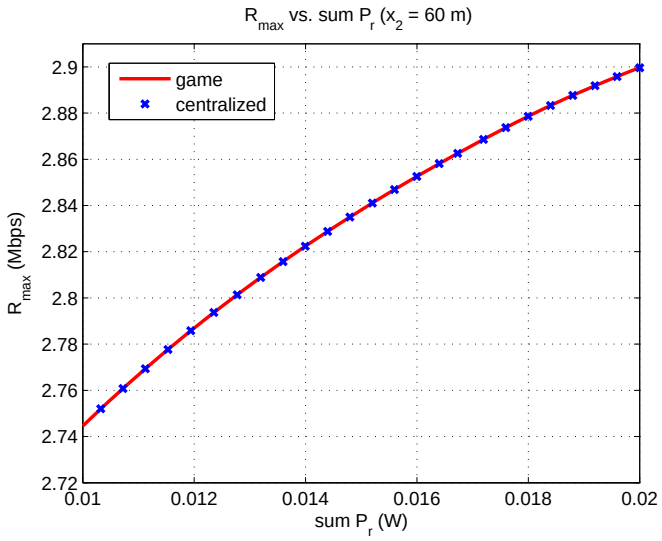

(a) x-coordinate of $r_2 = 60$m

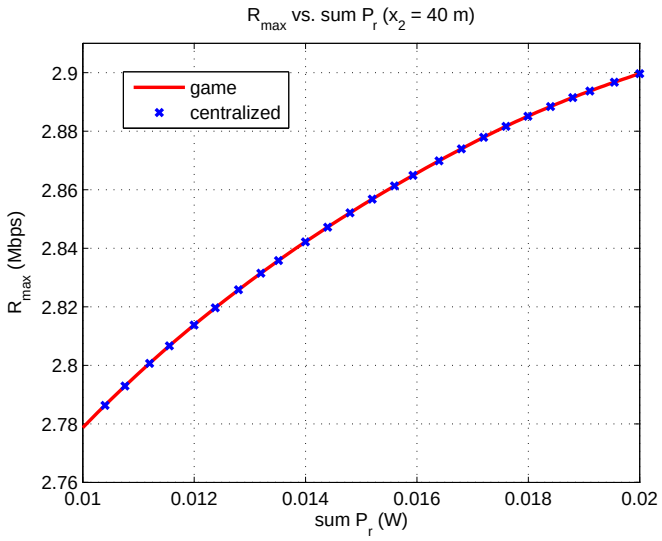

(b) x-coordinate of $r_2 = 40$m

Figure 5.7: Optimal rate in distributed and centralized schemes.

rates as the centralized scheme under the same total power consumptions.

5.3.6 Effect of the Bandwidth Factor

As explained in Section 5.1.1, for the network with a limited bandwidth, the bandwidth should be divided for the source node and the relay nodes. If N' out of the total N available relay nodes are selected by the source node, where $N' \leq N$, then $\gamma_L = \frac{1}{N'+1}$ in (5.10), indicating the bandwidth factor decreases as more relay nodes help the source node. Thus, using less relay nodes among the selected N' relay nodes may further increase U_s for the source node. Therefore, for the networks with a limited bandwidth, it is not sufficient for the source node to implement only one round of relay selection. Instead, after source node s selects N' relay nodes using the *relay rejection criteria*, s continues to try different subsets of the N' selected relay nodes, get the corresponding optimal utility U_s^* for each trial, and choose the subset of relay nodes that results in the largest U_s^*. In this subsection, we set up simulations to observe the effect of the varying bandwidth factor.

We set $a = 0.85$, relay node r_1 is at $(100\text{m}, 5\text{m})$, and r_2 moves along the line between points $(-250\text{m}, 5\text{m})$ and $(300\text{m}, 5\text{m})$. In Figure 5.8, we show the optimal U_s^* obtained by the source node under four scenarios, i.e., when no relay node, only r_1, only r_2, and both relay nodes are available to help, respectively. We see that when r_2 moves close to r_1 and the source node s, i.e., the x-coordinate of r_2 lies in the interval of $(85\text{m}, 115\text{m})$, both r_2 and r_1 are beneficial to node s. Moreover, as explained in the multiple-relay case in Section 5.3.3, since there is competition between two relay

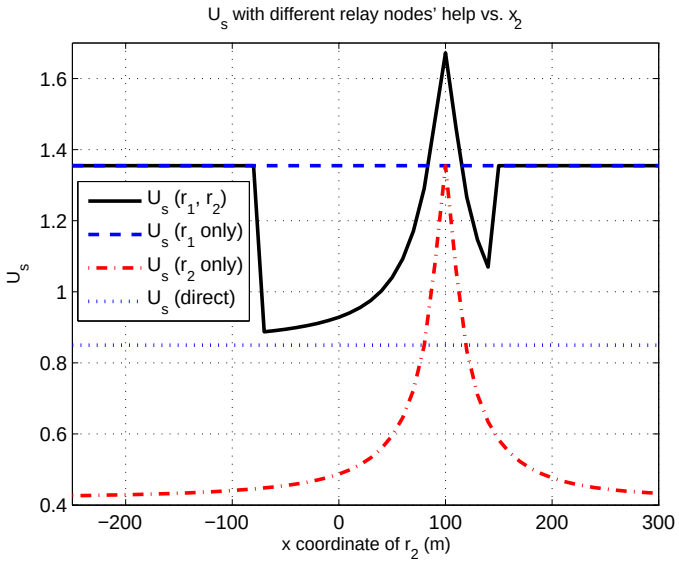

Figure 5.8: Optimal U_s including the bandwidth-factor effect, with different relay nodes' help, $a = 0.85$.

nodes, the average power bought from the relay node is much greater, while the average payment is lower, compared with the 1-relay case. Hence, although γ_L is only $1/3$, $U_s(r_1, r_2)$ is still greater than $U_s(r_i\text{only})$, for $i = 1, 2$, and both relay nodes are selected. When r_2 moves farther away from s, r_2 is less beneficial, asks a higher price, and r_1 is also influenced to ask a higher price. So $U_s(r_1, r_2)$ decreases, and becomes smaller than $U_s(r_1\text{only})$ where γ_L is $1/2$. So choosing r_1 only is better than choosing both relay nodes. When r_2 keeps moving away from s, it is no longer beneficial for the source node s to select it to help. So r_2 will be rejected, and the bandwidth factor jumps from $1/3$ to $1/2$. So there are two bumps of $U_s(r_1, r_2)$ when the x-coordinate of r_2 is about -70m and 140m.

5.4 Summary

In this chapter, we propose a game-theoretic approach for distributed resource allocation over multiuser cooperative communication networks. We target for answering two questions: who will be the relays and how much power for the relays to transmit for the cooperative transmission. We employ a Stackelberg (buyer/seller) game to jointly consider the benefits of the source node and the relay nodes. The proposed scheme not only helps the source node optimally choose the relay nodes at better locations but also helps the competing relay nodes ask optimal prices to maximize their utilities. From the simulation results, relay nodes closer to the source node can play a more important role in increasing the source node's utility, so the source node buys more power from these preferred relay nodes. If the total number of the available relay nodes increases, the source node can obtain a greater utility value and the average payment to the relay nodes shrinks, due to more severe competitions among the relay nodes. It is also shown that the distributed resource allocation can achieve comparable performance to that of the centralized scheme, without requiring knowledge of CSI. The proposed Stackelberg-game based framework can be extended as a building block in large-scale wireless ad hoc networks to stimulate cooperation among distributed nodes.

Chapter 6

Attacks in Spectrum Sensing

In the Chapter 4, we have analyzed the spectrum sensing game assuming that all secondary users are selfish by pursuing as high a throughput as possible. But we assume they will not cause damage to each other. However, it is highly possible that the secondary users are operating in a hostile environment, where malicious users intend to attack the legitimate secondary system by interrupting spectrum sensing. In this chapter, we investigate possible attacks on cooperative spectrum sensing, analyze their damages, and compare the throughput performance of the spectrum sensing game with that of individual sensing without cooperation.

6.1 Mask Primary User Signal

As we have discussed in Chapter 3, in dynamic spectrum access, it is usually required that secondary users' operation should not conflict or interfere with primary users. Otherwise, a primary user will prohibit secondary users from utilizing

the primary band if the detection probability falls below a predetermined threshold $\bar{P}_D$. This requirement poses vulnerabilities in spectrum sensing if the legitimate secondary users are induced to cause interference with the primary user [BS08]. From the malicious attackers' viewpoint, if they can reduce the received primary signal strength of the legitimate secondary users, or raise the noise level, the legitimate users will have greater difficulty in distinguishing between the primary user signal and noise. This in turn increases the probability of false alarm, and thus the average throughput of the legitimate secondary users will get reduced according to the definition in (4.9).

Specifically, if the malicious users increase the noise power on every detection of the legitimate secondary user from σ_w^2 to $\tilde{\sigma}_w^2$, in order to guarantee the same detection probability $\bar{P}_D$, the threshold of the energy detector will be increased to

$$\tilde{\lambda} = \left[\mathcal{Q}^{-1}(\bar{P}_D)\sqrt{\frac{2\tilde{\gamma}+1}{N}} + \tilde{\gamma} + 1 \right] \tilde{\sigma}_w^2, \tag{6.1}$$

with $\tilde{\gamma} = \frac{|h|^2\sigma_s^2}{\tilde{\sigma}_w^2}$ being the received SNR of the primary user under attack. Substituting this threshold to (4.3), we get the false alarm probability when the primary signal is masked as

$$\tilde{P}_F(\bar{P}_D, N, \tilde{\gamma}) = \mathcal{Q}\left(\sqrt{2\tilde{\gamma}+1}\,\mathcal{Q}^{-1}(\bar{P}_D) + \sqrt{N}\tilde{\gamma}\right). \tag{6.2}$$

We can see from (6.2) that when the malicious users induce the legitimate secondary users to interfere with the primary users, the false alarm probability becomes higher, and the damage to the legitimate users will depend on the noise power. However, even when the primary signal is masked by the malicious users, the legitimate users who join in the cooperative sensing game still have a greater chance

of achieving a higher throughput than those sensing the primary user individually, because more users are available to share the time spent in sensing. We will show the comparison via simulations in the next section.

6.2 Report Faulty Sensory Data

Since the cooperative spectrum sensing requires local detection reports from all contributing secondary users and a certain decision fusion rule to make a final judgement, another effective attack is to distort sensory data, especially when the legitimate secondary users only have limited information about the primary users' activity/operation pattern. Although in a centralized cognitive radio network, public-key authentication and digital signature mechanism [BS08] can validate the source and integrity of the reported information, verifying distributed cooperative users would be much more difficult. The malicious users can report by themselves, or compromise the legitimate secondary users to report, faulty sensory data, which can lead to belief manipulation [CG08]. Since the legitimate secondary users will adjust their strategies through strategic interactions, the manipulated beliefs will be distributed throughout the cognitive radio network, resulting in suboptimal performance. In the following, we analyze the damage to the legitimate secondary users of this attack.

Without loss of generality, we assume K_a malicious users share the total K sub-bands with another $K-K_a$ legitimate secondary users. Majority rule is adopted as the decision fusion rule. To degrade the throughput by increasing the false alarm

probability of the legitimate secondary users, the K_a malicious user pretend to be very active in contributing to sensing while always report the presence of the primary user (H_1) in every detection without taking any real samples of the primary signal. Denote the set formed by the legitimate secondary users who contribute to sensing as $\mathcal{S}_c^g$. By assuming each contributor takes equal responsibility in making the final decision, i.e., P_{D,s_i} is identical for any user s_i, we obtain the detection probability under this attack as follows,

$$\bar{P}_D = \sum_{j=\lceil \frac{1+K_a+|\mathcal{S}_c^g|}{2} \rceil}^{K_a+|\mathcal{S}_c^g|} \binom{K_a+|\mathcal{S}_c^g|}{j} P_{D,s_i}^j (1-P_{D,s_i})^{K_a+|\mathcal{S}_c^g|-j}, \tag{6.3}$$

because the legitimate users are made to believe K_a users would always contribute to sensing. From (6.3) we can solve the required $\bar{P}_{D,s_i}$, and get the false alarm probability for any user s_i as

$$P_{F,s_i} = \mathcal{Q}\left(\sqrt{2\gamma_{s_i}+1}\mathcal{Q}^{-1}(\bar{P}_{D,s_i}) + \sqrt{N/(|\mathcal{S}_c^g|+K_a)}\gamma_{s_i}\right), \tag{6.4}$$

With majority rule, the false alarm probability after decision fusion is given by

$$P_F(S_c^g) = P\left[\text{at least } \lceil \frac{1+K_a+|\mathcal{S}_c^g|}{2} \rceil \text{ out of } K_a+|\mathcal{S}_c^g| \text{ users report } H_1 \middle| H_0\right]. \tag{6.5}$$

Since the K_a malicious users always report H_1 in every detection to increase the false alarm of the legitimate secondary users, the above equation is further reduced to

$$P_F(S_c^g) = P\left[\text{at least } \lceil \frac{1+|\mathcal{S}_c^g|-K_a}{2} \rceil \text{ out of } |\mathcal{S}_c^g| \text{ good users report } H_1 \middle| H_0\right]. \tag{6.6}$$

If the legitimate secondary users are clustering together, we can assume they have similar γ_{s_i}'s and P_{F,s_i}'s, and write the false alarm probability as

$$P_F(S_c^g) = \sum_{j=\lceil \frac{1+|\mathcal{S}_c^g|-K_a}{2} \rceil}^{|\mathcal{S}_c^g|} \binom{|\mathcal{S}_c^g|}{j} P_{F,s_i}^j (1-P_{F,s_i})^{|\mathcal{S}_c^g|-j}. \tag{6.7}$$

Similar to the analysis in Section 4.2.3, the payoff functions for the legitimate secondary users defined in (4.10)-(4.12) for a symmetric game setting become

$$U_C^g(|S_c^g|) = U_0(S_c^g)(1 - \frac{\tau}{K_a + |S_c^g|}), \tag{6.8}$$

and

$$U_D^g(|S_c^g|) = U_0(S_c^g), \tag{6.9}$$

where $U_0(S_c^g)$ is defined as

$$U_0(S_c^g) = \begin{cases} P_{H_0}[1 - P_F(S_c^g)]C, & \text{if } |S_c^g| \in [K_a + 1, K - K_a]; \\ 0, & \text{if } |S_c^g| \in [0, K_a + 1]. \end{cases} \tag{6.10}$$

Then, the average payoff for a legitimate user taking pure strategy C under attack can be obtained as

$$\bar{U}_C^g(x_g) = \sum_{j=0}^{K-K_a-1} x_g^j (1-x_g)^{K-K_a-1-j} U_C^g(j+1), \tag{6.11}$$

where x_g denotes the probability that a legitimate secondary user contributes to spectrum sensing when there exist malicious users reporting faulty sensory information. Similarly, the average payoff for a legitimate user taking pure strategy D is given by

$$\bar{U}_D^g(x_g) = \sum_{j=0}^{K-K_a-1} x_g^j (1-x_g)^{K-K_a-1-j} U_D^g(j). \tag{6.12}$$

We can solve the ESS by equating (6.11) and (6.12). Since the payoff functions share similar form to those without malicious users, it can be expected that the dynamics defined in (4.17) converge to the ESS in this case as well. We will show the ESS after convergence and the resulting average throughput for the legitimate secondary users in the following section.

6.3 Simulation Studies

In this section, we illustrate the ESS and the average throughput performance for each legitimate secondary user in a homogeneous sensing game with malicious users.

Figure 6.1 shows the case when the primary signal is masked by the malicious user, where the average received SNR is reduced from -12 dB to -19 dB. We see from the figure that the ESS probability of cooperation is almost the same as that with no malicious users. However, as the received SNR of the primary user is reduced, the legitimate users have greater difficulty in correctly detecting the primary user's activity, and the average throughput gets heavily reduced. In order to obtain more precise detection and reduce false alarm, the legitimate users have to collect more samples, so the optimal value of τ increases from around 0.25 to around 0.55. As more users are available to share the sensing cost, the average throughput per user in the sensing game is still higher than the single-user sensing under attack.

In Figure 6.2, we show the case where 2 malicious users share a total of K sub-bands with $K-2$ legitimate secondary users. We vary K in the range of [5,11]

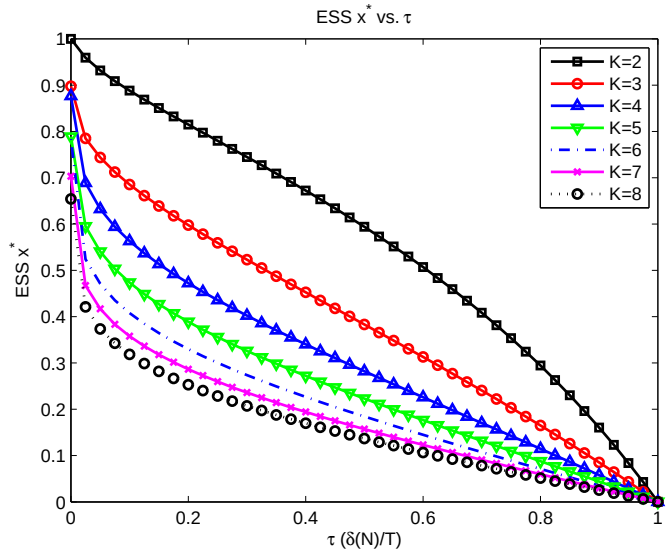

(a) Probability of being a contributor

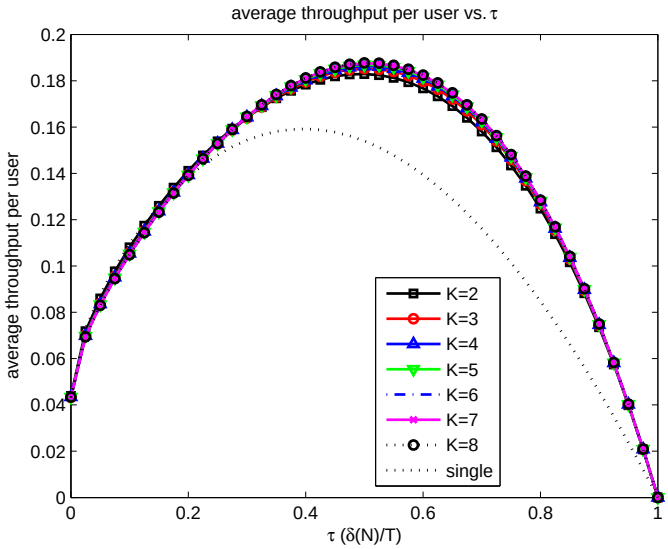

(b) Average throughput per legitimate user

Figure 6.1: ESS and average throughput vs. τ when the primary signal is masked.

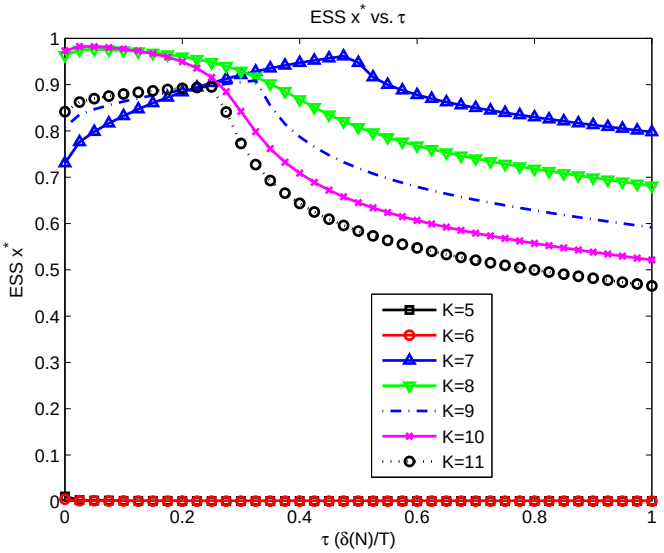

(a) Probability of being a contributor

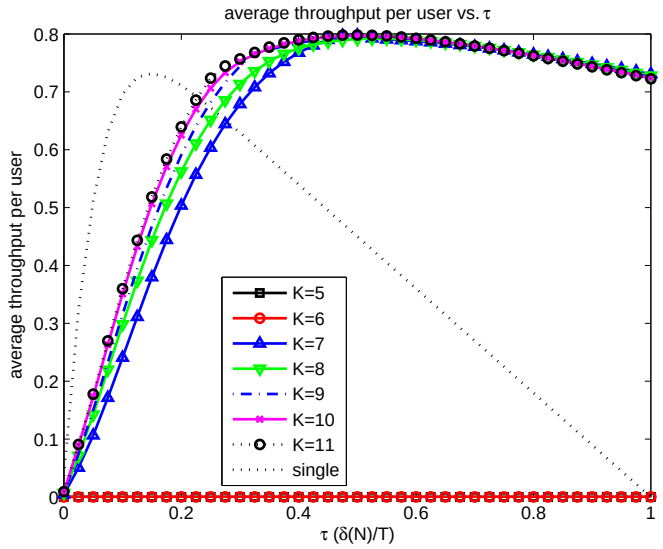

(b) Average throughput per legitimate user

Figure 6.2: ESS and average throughput vs. τ when 2 malicious users report faulty sensory data.

and observe the ESS probability of cooperation in Figure 6.2(a) and the average throughput in Figure 6.2(b). We find that when there are only a few (3 or 4) legitimate users, the faulty sensory data from the malicious users overwhelms the correct information from the legitimate users, which makes the legitimate users believe the primary user is always present and the degree of cooperation of the legitimate users become 0. Since the belief of the legitimate users are manipulated, the false alarm probability approaches 1, and the average throughput is 0. However, when there are more than 4 legitimate users (i.e., $K \geq 7$), the faulty sensory data cannot dominate the decision fusion, and the legitimate users obtain an average throughput greater than 0. It is interesting that due to the high false alarm created by the malicious users, the legitimate users will become more cooperative than the case with no malicious users, because only by more cooperation can the legitimate users collect more precise sensory data, maintain a lower false alarm probability, and efficiently utilize the spectrum opportunity.

We illustrate in Figure 6.3 the scenario where 3 malicious users share a total of K sub-bands with $K-3$ legitimate secondary users, with K varying in the range of [7,13]. We find that as more malicious users exist in the sensing game, more legitimate users (greater than 8, or $K \geq 12$) are needed to combat the damage of the malicious users, and their probability of cooperation is also higher than that when there exist no malicious users. In both Figure 6.2 and Figure 6.3, we also compare the average throughput of the legitimate users in the sensing game under attack to that of the single-user sensing where his/her decision is not affected by the malicious users. We find that as long as there are a plenty of legitimate users who

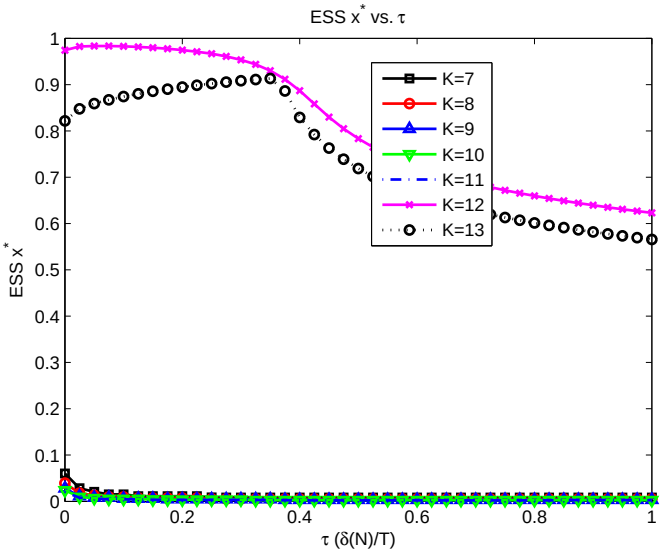

(a) Probability of being a contributor

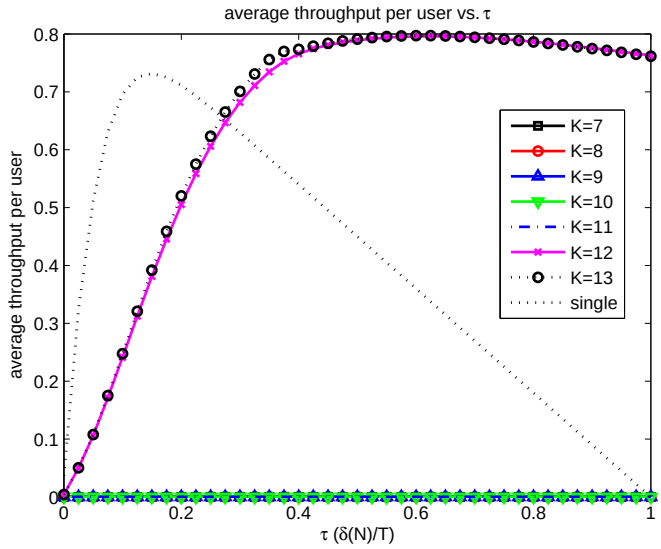

(b) Average throughput per legitimate user

Figure 6.3: ESS and average throughput vs. τ when 3 malicious users report faulty sensory data.

collectively collect enough samples of the primary signal (about $\tau > 0.4$), joining in the sensing game is still a better choice for the legitimate users than the single-user sensing, because each user can spend less time in sensing while not badly affected by the malicious users' faulty sensory data.

6.4 Summary

In order to avoid conflict with primary users, spectrum sensing has become an essential functionality of cognitive radios. However, malicious attacks can severely deteriorates the performance of spectrum sensing.In this chapter, we investigate possible attacks on cooperative spectrum sensing under the evolutionary sensing game framework, and analyze their damage both theoretically and by simulations. Simulation results show that if the primary signal is masked by the malicious users, the legitimate secondary users need to collectively take more samples to obtain a better throughput; if malicious users exchange false sensory data to interrupt decision fusion, more legitimate users are required and they should behave more cooperatively so as to dominate the false sensory data. It is also shown that the evolutionary sensing game can still achieve better throughput than that of individual sensing without cooperation under malicious attacks.

Chapter 7

Conclusions and Future Work

7.1 Conclusions

In this dissertation, we have studied how to design efficient spectrum allocation scheme in cognitive cooperative wireless networks. We focus on studying the optimal collaboration strategy of selfish users in forwarding information and cooperative spectrum sensing for detecting primary users using a game-theoretic framework, and dynamic spectrum access with statistical modeling that can predict future traffic patterns and optimize system throughput.

First, we have developed a statistical modeling approach that characterizes the traffic dynamics for opportunistic spectrum access in licensed spectrum. In order to improve the spectrum utilization efficiency, secondary users are allowed to access the spectrum white space in a licensed band. However, if they access the licensed spectrum too greedily, their throughput will be heavily reduced due to interference or collisions. Further, dynamics caused by different user activities, e.g., primary

user re-occupying/vacating the licensed band and secondary users starting/ceasing a communication session, make it more challenging to optimize spectrum efficiency in real-time. In this dissertation, we model the traffic variations of the radio environment as CTMC that can predict future traffic patterns in the share spectrum. By optimizing spectrum access probabilities, throughput degradation due to interference is compensated.

Second, we have investigated how to collaborate in cooperative spectrum sensing for primary user detection. In cooperative spectrum sensing, it may not be optimal to have all secondary users cooperate in every sensing effort. Moreover, sensing takes energy/time which may be used for data transmission. In self-organizing networks, where different secondary users belong to different network controllers and exchange their local sensory data to make a final decision, the selfish users tend to overhear the other's sensing outcomes to reserve more time for their own data transmission. In this dissertation, we study the time evolution of selfish users' cooperation behavior and propose an evolutionary cooperative sensing game that converges to the ESS. With the proposed game, we can obtain the optimal number of cooperating users only based on users' own observation of their past throughput. Moreover, the performance of ESS is better than that having all users always cooperate.

Third, we have studied how to enforce cooperation between source nodes and relay nodes in cooperative wireless networks. Most existing works on resource allocation in cooperative networks assume all users belong to the same central authority that can collect precise CSI of different channels and allocate network resources to different users. In this dissertation we present a distributed relay selection and

power control scheme using Stackelberg game, without requiring a central authority. In the proposed game-theoretic framework, source nodes can find relay nodes that can better improve the source nodes' throughput with less cost, and relay nodes can maximize their revenues from forwarding source nodes' information as well. In addition, there is no need to measure and exchange CSI, since relay nodes can adapt their prices according to the proposed price updating function, which is easy to implement and guaranteed to converge to the optimal operating point. Therefore, the proposed Stackelberg game reduces communication overhead greatly that is usually involved in conventional cooperative wireless networking. Moreover, the proposed scheme is a good candidate for cooperation stimulation in large-scale wireless ad hoc networks, where users controlled by different operators only aim at maximizing their own performance.

Finally, we have investigated possible attacks on cooperative spectrum sensing. Since it is highly possible that the secondary users are operating in a hostile environment, malicious users intend to attack the legitimate secondary system by interrupting spectrum sensing. In this dissertation, we studied possible attacks on cooperative spectrum sensing under the evolutionary game framework, analyze their damages, and compare the throughput performance of the spectrum sensing game with that of individual sensing without cooperation. It is shown that the evolutionary sensing game can still achieve better throughput than that of individual sensing without cooperation under malicious attacks.

7.2 Future Work

In this dissertation, we have addressed several critical issues in efficient spectrum allocation design for cognitive cooperative networks, where we mainly assume that users will not do harm to others. However, in practical wireless networks, not all users will behave well and there exist malicious users who may cause damage to other users and even ruin the network. Therefore, efficient spectrum allocation cannot be made possible without considering security enforcement. In this section, we will list some of the security issues that we would like to address in our future research.

We plan to continue investigating various security enforcement schemes in spectrum sensing. Since primary user detection is very sensitive to noise uncertainty, malicious users in the vicinity of legitimate users may inject jamming pulses to make primary user detection more difficult. In cooperative spectrum sensing, secondary users exchange their local sensing outcomes and make a final decision using some decision fusion rule. Thus, besides always reporting a primary user's existence, malicious users can adaptively manipulate their sensory data so that legitimate users can hardly detect the re-appearance of a primary user, conflict with it and have difficulty in recognizing the malicious users. In addition, during a sensing period, all users should stop their transmission and listen to the licensed spectrum. Malicious users can mimic the primary user signal in the sensing periods so as to waste the spectrum opportunity. Therefore, we would like to investigate possible attacks in spectrum sensing, characterize the symptoms when spectrum sensing is

disturbed by malicious users, locate the malicious users, and exclude them from the network.

We will also be interested in studying how to secure spectrum allocation and sharing in different network layers. As secondary users may occupy multiple under-used licensed bands, whenever the current channel conditions become worse or a primary user re-appears, they need to re-select a proper spectrum band (i.e., spectrum handoff) to resume transmission and guarantee reliable and seamless communication. If a legitimate user is compromised by malicious users and distorts the signaling when exchanging information for spectrum handoff, not only may packet error rate and latency increase, but the other transmitting users may also get impaired during the frequency change. Therefore, we plan to systematically investigate how to design optimal spectrum allocation when there exist inside malicious attackers. In addition, in order to perform spectrum allocation and spectrum handoff within a network, certain control information should be broadcast to all network users through a dedicated channel. If control channels are jammed by malicious users that transmit junk packets using very high power, all information about spectrum allocation will be lost, and the entire secondary network will not function normally. Hence, we plan to design robust spectrum allocation where the channel control information is broadcast with a proper redundancy and in a randomized pattern.

BIBLIOGRAPHY

[ACM07] R. Annavajjala, P. C. Cosman, and L. B. Milstein. Statistical channel knowledge-based optimum power allocation for relaying protocols in the high SNR regime. *IEEE Journal on Selected Areas in Communications*, 25(2):292–305, Feb. 2007.

[AH07] E. Altman and Y. Hayel. An evolutionary game model of resources-sharing mechanism in P2P networks. In *Workshop on Intelligent Information Technology Application (IITA) 2007*, pages 282–285, Dec. 2007.

[Bar93] M. S. Barzaraa. *Nonlinear programming: theory and algorithms, 2nd ed.* John Wiley & Sons, 1993.

[BLR05] A. Bletsas, A. Lippman, and D. P. Reed. A simple distributed method for relay selection in cooperative diversity wireless networks, based on reciprocity and channel measurements. In *IEEE Vehicular Technology Conference*, volume 3, pages 1484–1488, Stockholm, Sweden, May 2005.

[BS02] T. Basar and R. Srikant. Revenue-maximizing pricing and capacity expansion in a many-users regime. In *IEEE INFOCOM*, pages 294–301, New York, Jun. 2002.

[BS08] T. X. Brown and A. Sethi. Potential cognitive radio denial-of-service vulnerabilities and protection countermeasures: a multi-dimensional analysis and assessment. *Mobile Networks and Applications*, 13(5):516–532, Oct. 2008.

[CG08] T. C. Clancy and N. Goergen. Security in cognitive radio networks: threats and mitigation. In *3rd International Conference on Cognitive Radio Oriented Wireless Networks and Communications (CrownCom)*, pages 1–8, May 2008.

[Cla07a] T. Clancy. Achievable capacity under the interference temperature model. In *26th IEEE International Conference on Computer Communications (INFOCOM)*, pages 794–802, Anchorage, AK, May 2007.

[Cla07b] T. Clancy. Formalizing the interference temperature model. *Wiley Journal on Wireless Communications and Mobile Computing*, 7(9):1077–1086, Nov. 2007.

[Cre03] R. Cressman. *Evolutionary dynamics and extensive form games*. MIT Press, Cambridge, MA, 2003.

[CT90] T. M. Cover and J. A. Thomas. *Elements of information theory*. New York: Wiley-Interscience, 1990.

[CV86] Z. Chair and P. K. Varshney. Optimal data fusion in multiple sensor detection systems. *IEEE Trans. on Aerospace and Elect. Syst.*, 22:98–101, Jan. 1986.

[CZ05] L. Cao and H. Zheng. Distributed spectrum allocation via local bargaining. In *IEEE Communications Society Conference on Sensor, Mesh and Ad Hoc Communications and Networks (SECON)*, pages 475–486, Santa Clara, CA, Sep. 2005.

[DPA00] L. A. DaSilva, D. W. Petr, and N. Akar. Static pricing and quality of service in multiple service networks. In *5th Joint Conference on Information Sciences*, volume 1, pages 355–358, Atlantic City, MD, Feb. 2000.

[EPT07] R. Etkin, A. Parekh, and D. Tse. Spectrum sharing for unlicensed bands. *IEEE Journal on Selected Areas in Communications*, 25(3):517–528, Apr. 2007.

[FCC02] FCC. Spectrum policy task force report. FCC Document ET Docket No. 02-135, Nov. 2002.

[FCC03a] FCC. Establishement of interference temperature metric to quantify and manage interference and to expand available unlicensed operation in certain fixed mobile and satellite frequency bands. FCC Document ET Docket 03-289, 2003.

[FCC03b] FCC. Facilitating opportunities for flexible, efficient and reliable spectrum use employing cognitive radio technologies: notice of proposed rule making and order. FCC Document ET Docket No. 03-108, Dec. 2003.

[FGR05] A. Fehske, J. D. Gaeddert, and J. H. Reed. A new approach to signal classification using spectral correlation and neural networks. In *IEEE Symposia on New Frontiers in Dynamic Spectrum Access Networks (DySPAN)*, pages 144–150, Baltimore, MD, Nov. 2005.

[FL91] D. Fudenberg and D. K. Levine. *Game theory*. MIT Press, Cambridge, MA, 1991.

[FL98] D. Fudenberg and D. K. Levine. *The theory of learning in games*. MIT Press, Cambridge, MA, 1998.

[FT93] D. Fudenberg and J. Tirole. *Game theory*. MIT Press, Cambridge, MA, 1993.

[GL07] G. Ganesan and Y. Li. Cooperative spectrum sensing in cognitive radio. *IEEE Transactions on Wireless Communications*, 6(6):2204–2222, Jun. 2007.

[GLBL08] G. Ganesan, Y. Li, B. Bing, and S. Li. Spatiotemporal sensing in cognitive radio networks. *IEEE Journal on Selected Areas in Communications*, 26(1):5–12, Jan. 2008.

[GS05] A. Ghasemi and E. S. Sousa. Collaborative spectrum sensing in cognitive radio networks. In *IEEE Symposia on New Frontiers in Dynamic Spectrum Access Networks (DySPAN)*, pages 131–136, Baltimore, MD, Nov. 2005.

[HA03] M. O. Hasna and M.-S. Alouini. Optimal power allocation for relayed transmissions over Rayleigh fading channels. In *IEEE Vehicular Technology Conference*, volume 4, pages 2461–2465, Jeju, Korea, Apr. 2003.

[HBH06] J. Huang, R. A. Berry, and M. L. Honig. Auction-based spectrum sharing. *ACM/Springer Mobile Networks and Applications Journal (MONET)*, 11(3):405–418, Jun. 2006.

[HHLW00] Z. Haas, J. Halpern, L. Li, and S. B. Wicker. A decision-theoretic approach to resource allocation in wireless multimedia networks. In *Dial M for Mobility*, pages 86–95, 2000.

[HHSL05] Z. Han, T. Himsoon, W. Siriwongpairat, and K. J. R. Liu. Energy efficient cooperative transmission over multiuser OFDM networks: who helps whom and how to cooperate. In *IEEE Wireless Communications and Networking Conference*, volume 2, pages 1030–1035, New Orleans, LA, Mar. 2005.

[HJL05] Z. Han, Z. Ji, and K. J. R. Liu. Fair multiuser channel allocation for OFDMA networks using Nash bargaining and coalitions. *IEEE Transactions on Communications*, 53(8):1366–1376, Aug. 2005.

[HL08] Z. Han and K. J. R. Liu. *Resource allocation for wireless networks: basics, techniques, and applications*. Cambridge University Press, Cambridge, UK, 2008.

[HS74] M. Hirsch and S. Smale. *Differential equations, dynamical systems, and linear algebra*. New York: Academic Press, 1974.

[HSHL07] T. Himsoon, W. Siriwongpairat, Z. Han, and K. J. R. Liu. Lifetime maximization framework by cooperative nodes and relay deployment in wireless networks. *IEEE Journal on Selected Areas in Communications*, 25(2):306–317, Feb. 2007.

[IEE] IEEE 802.22 working group on wireless regional area networks. http://www.ieee802.org/22/.

[IEE99] IEEE Standard. IEEE Std 802.11a-1999, Part 11: wireless LAN medium access control (MAC) and physical layer (PHY) specifications, 1999.

[III00] J. Mitola III. *Cognitive radio: an integrated agent architecture for software defined radio*. PhD thesis, KTH Royal Institute of Technology, Stockholm, Sweden, 2000.

[ISSL08] A. Ibrahim, A. K. Sadek, W. Su, and K. J. R. Liu. Cooperative communications with relay selection: when to cooperate and whom to cooperate with? *IEEE Trans. on Wireless Communications*, 7(7):2814–2827, Jul. 2008.

[JL06] Z. Ji and K. J. R. Liu. Belief-assisted pricing for dynamic spectrum allocation in wireless networks with selfish users. In *IEEE Communications Society Conference on Sensor, Mesh and Ad Hoc Communications and Networks (SECON)*, pages 119–127, Reston, VA, Sep. 2006.

[JL07] Z. Ji and K. J. R. Liu. Dynamic spectrum sharing: a game theoretical overview. *IEEE Communications Magazine*, pages 88–94, May 2007.

[KC06] S. Keshavamurthy and K. Chandra. Multiplexing analysis for spectrum sharing. In *IEEE MILCOMM*, pages 1–7, Washington, D.C., Oct. 2006.

[Kel97] F. Kelly. Charging and rate control for elastic traffic. *European Transactions on Telecommunications*, 8(1):33–37, Jan. 1997.

[KLO97] Y. A. Korilis, A. A. Lazar, and A. Orda. Achieving network optima using Stackelberg routing strategies. *IEEE/ACM Trans. on Networking*, 5(1):161–173, Feb. 1997.

[KT75] L. Kleinrock and F. Tobagi. Packet switching in radio channels: Part I-carrier sense multiple-access modes and their throughput-delay characteristics. *IEEE Transactions on Communications*, com-23(12):1400–1416, Dec. 1975.

[Kul95] V. G. Kulkarni. *Modeling and Analysis of Stochastic Systems*. CRC Press, 1995.

[LBG+04] J. Luo, R. S. Blum, L. J. Greenstein, L. J. Cimini, and A. M. Haimovich. New approaches for cooperative use of multiple antennas in ad hoc wireless neworks. In *IEEE Vehicular Technology Conference*, volume 4, pages 2769–2773, Los Angeles, CA, Sep. 2004.

[LHXS07] B. Lin, P. Ho, L. Xie, and X. Shen. Optimal relay station placement in IEEE 802.16j networks. In *International Conference on Communications and Mobile Computing*, pages 25–30, Hawaii, Aug. 2007.

[LTW04] J. N. Laneman, D. N. C. Tse, and G. W. Wornell. Cooperative diversity in wireless networks: efficient protocols and outage behavior. *IEEE Transactions on Information Theory*, 50(12):3062–3080, Dec. 2004.

[LYZH07] Y.-C. Liang, E. Peh Y. Zeng, and A. T. Hoang. Sensing-throughput tradeoff for cognitive radio networks. In *IEEE International Conference on Communications (ICC)*, pages 5330–5335, Glasgow, Scotland, Jun. 2007.

[M. 05] M. A. McHenry. NSF spectrum occupancy measurements project summary, Aug. 2005.

[MSB06] S. M. Mishra, A. Sahai, and R. W. Brodensen. Cooperative sensing among cognitive radios. In *IEEE International Conference on Communications (ICC)*, pages 1658–1663, Istanbul, Turkey, Jun. 2006.

[MW01] A. B. MacKenzie and S. B. Wicker. Game theory and the design of self-configuring, adaptive wireless networks. *IEEE Communications Magazine*, 39(11):126–131, Nov. 2001.

[MY04] I. Maric and R. D. Yates. Cooperative multihop broadcast for wireless networks. *IEEE Journal on Selected Areas in Communications*, 22(6):1080–1088, Aug. 2004.

[NY07] T. Ng and W. Yu. Joint optimization of relay strategies and resource allocations in cooperative cellular networks. *IEEE Journal on Selected Areas in Communications*, 25(2):328–339, Feb. 2007.

[Ofc] Ofcom. Improving the sharing of the radio spectrum: final report. http://www.ofcom.org.uk/research/technology/overview/ese/share/.

[PL07] E. Peh and Y.-C. Liang. Optimization for cooperative sensing in cognitive radio networks. In *IEEE Wireless Communications and Networking Conference (WCNC)*, pages 27–32, Hongkong, Mar. 2007.

[Poo94] H. V. Poor. *An introduction to signal detection and estimation.* Springer-Verlag, New York, second edition, 1994.

[PPM+08] P. Paruchuri, J. P. Pearce, J. Marecki, M. Tambe, F. Ordonez, and S. Kraus. Playing games for security: an efficient exact algorithm for solving bayesian Stackelberg games. In *Int. Conf. on Autonomous Agents and Multiagent Systems (AAMAS)*, pages 895–902, Estoril, Portugal, May 2008.

[Rou01] T. Roughgarden. Stackelberg scheduling strategies. In *Annual ACM Symposium on Theory of Computing*, pages 104 – 113, Hersonissos, Greece, 2001.

[RYM05] C. Raman, R. D. Yates, and N. B. Mandayam. Scheduling variable rate links via a spectrum server. In *IEEE Symposia on New Frontiers in Dynamic Spectrum Access Networks (DySPAN)*, pages 110–118, Baltimore, MD, Nov. 2005.

[SA06] N. Shastry and R. S. Adve. Stimulating cooperative diversity in wireless ad hoc networks through pricing. In *IEEE International Conference on Communications*, pages 3747–3752, Istanbul, Turkey, Jun. 2006.

[Sam98] L. Samuelson. *Evolutionary games and equilibrium selection.* MIT Press, Cambridge, MA, 1998.

[SC05] A. Sahai and D. Cabric. A tutorial on spectrum sensing: fundamental limits and practical challenges. In *IEEE Symposia on New Frontiers in Dynamic Spectrum Access Networks (DySPAN)*, Baltimore, MD, Nov. 2005.

[SHL06] A. K. Sadek, Z. Han, and K. J. R. Liu. An efficient cooperation protocol to extend coverage area in cellular networks. In *IEEE Wireless Communications and Networking Conference*, volume 3, pages 1687–1692, Las Vegas, NV, Apr. 2006.

[SMG02] C. U. Saraydar, N. B. Mandayam, and D. J. Goodman. Efficient power control via pricing in wireless data networks. *IEEE Transactions on Communications*, 50(2):291–303, Feb. 2002.

[Smi82] J. Maynard Smith. *Evolution and the theory of games.* Cambridege University Press, Cambridge, UK, 1982.

[SS07] S. Savazzi and U. Spagnolini. Energy aware power allocation strategies for multihop-cooperative transmission schemes. *IEEE Journal on Selected Areas in Communications*, 25(2):318–327, Feb. 2007.

[SSL08] W. Su, A. K. Sadek, and K. J. R. Liu. Cooperative communications in wireless networks: performance analysis and optimum power allocation. *Wireless Personal Communications*, 44(2):181–217, Jan. 2008.

[VJP08] F. E. Visser, G. J. Janssen, and P. Pawelczak. Multinode spectrum sensing based on energy detection for dynamic spectrum access. In *IEEE Vehicular Technology Conference (VTC)*, Singapore, May 2008.

[Wei95] J. W. Weibull. *Evolutionary game theory*. MIT Press, Cambridge, MA, 1995.

[WHL07] B. Wang, Z. Han, and K. J. R. Liu. Distributed relay selection and power control for multiuser cooperative communication networks using buyer/seller game. In *26th IEEE International Conference on Computer Communications (INFOCOM)*, pages 544–552, Anchorage, AK, May 2007.

[WHL09] B. Wang, Z. Han, and K. J. R. Liu. Distributed relay selection and power Control for multiuser cooperative communication networks using stackelberg game. *IEEE Trans. on Mobile Computing*, Aug. 2009.

[WJL07] B. Wang, Z. Ji, and K. J. R. Liu. Primary-prioritized markov approach for dynamic spectrum access. In *IEEE Symposia on New Frontiers in Dynamic Spectrum Access Networks (DySPAN)*, pages 507–515, Dublin, Ireland, Apr. 2007.

[WJLC09] B. Wang, Z. Ji, K. J. R. Liu, and T. C. Clancy. Primary-prioritized Markov approach for dynamic spectrum allocation. *IEEE Trans. on Wireless Communications*, Apr. 2009.

[WLC09] B. Wang, K. J. R. Liu, and T. C. Clancy. Evolutionary cooperative spectrum sensing game: how to cooperate? *submitted to IEEE Trans. on Communications*, 2009.

[WMdSeSa08] E. H. Watanabe, D. S. Menasché, E. de Souza e Silva, and R. M. Le ao. Modelling resource sharing dynamics of VoIP users over a WLAN using a game-theoretic approach. In *IEEE INFOCOM*, pages 915–923, Phoenix, AZ, Apr. 2008.

[WWJ+08] B. Wang, Y. Wu, Z. Ji, K. J. R. Liu, and T. C. Clancy. Game theoretical mechanism design for cognitive radio networks with selfish users. *IEEE Signal Processing Magazine*, 25(6):74–84, Nov. 2008.

[WWLC09] Y. Wu, B. Wang, K. J. R. Liu, and T. C. Clancy. Repeated open spectrum sharing game with cheat-proof strategies. *IEEE Trans. on Wireless Communications*, Apr. 2009.

[XCMS06] Y. Xing, R. Chandramouli, S. Mangold, and S. N. Shankar. Dynamic spectrum access in open spectrum wireless networks. *IEEE Journal on Selected Areas in Communications*, 24(3):626–637, Mar. 2006.

[Y. 09] Y. Wu and B. Wang and K. J. R. Liu and T. C. Clancy. A scalable collusion-resistant multi-winner cognitive spectrum auction game. *IEEE Trans. on Communications*, 2009.

[Yat95] R. Yates. A framework for uplink power control in cellular radio systems. *IEEE Journal on Selected Areas in Communications*, 13(7):1341–1348, Sep. 1995.

[ZAL06] Y. Zhao, R. S. Adve, and T. J. Lim. Improving amplify-and-forward relay networks: optimal power allocation versus selection. In *IEEE International Symposium on Information Theory*, pages 1234–1238, Seattle, WA, Jul. 2006.

[ZC05] H. Zheng and L. Cao. Device-centric spectrum management. In *IEEE Symposia on New Frontiers in Dynamic Spectrum Access Networks (DySPAN)*, pages 56–65, Baltimore, MD, Nov. 2005.